Role of Neuroinflammation in Parkinson's Disease and Related Disorders

Brandi, Edoardo

2022

Document Version:
Publisher's PDF, also known as Version of record

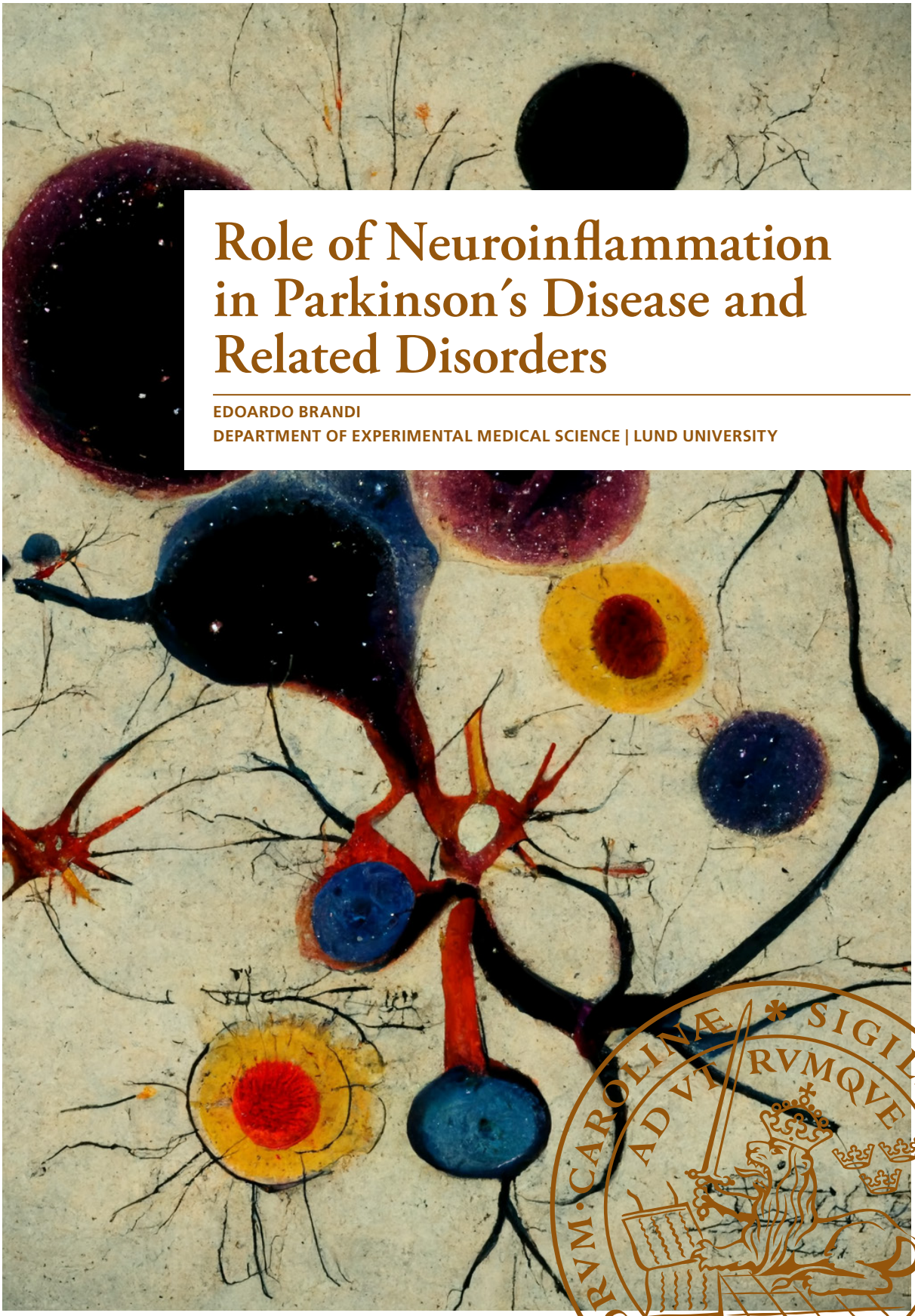

Role of Neuroinflammation in Parkinson´s Disease and Related Disorders

EDOARDO BRANDI
DEPARTMENT OF EXPERIMENTAL MEDICAL SCIENCE | LUND UNIVERSITY

Role of Neuroinflammation in Parkinson´s Disease and Related Disorders

Edoardo Brandi

LUND
UNIVERSITY

DOCTORAL DISSERTATION
by due permission of the Faculty of Medicine at Lund University, Sweden.
To be defended in Segerfalksalen, BMC A10
on November 11th, 2022 at 13:30

Faculty opponent
Marina Romero-Ramos
Associate Professor at Department of Biomedicine,
Faculty of Health Science, Aarhus University, Denmark

Organization	Document name
LUND UNIVERSITY Department of Experimental Medical Science	Doctoral Dissertation
	Date of issue November 11th, 2022
Author(s) Edoardo Brandi	**Sponsoring organization**

Title and subtitle
Role of Neuroinflammation in Parkinson´s Disease and Related Disorders

Abstract

Synucleinopathies are neurodegenerative disorders characterized by intracellular protein aggregates, progressive neurodegeneration, and neuroinflammation. Alpha-synuclein (α-syn) is the principal component of intracellular aggregates and can be modified by several mutations and post-translational modifications (PTMs), which can alter the protein structure affecting its aggregation, toxicity, and ability to spread.

Microglia and astrocyte cells are important cells for the immuno-defense within the brain. Although these cell populations are distributed in all brain parenchyma, their density, morphology, and transcriptomes are variable. Whether and how these differences could lead to different inflammatory responses in several brain regions are not well understood.

Studies demonstrated that α-syn oligomers or aggregates could trigger microglial and astrocytic activation. In contrast, other authors showed that some α-syn PTMs could derive from an inflammatory condition. These findings suggest the presence of mutual relations between α-syn and the inflammatory system, which could affect the course of these pathologies. While several studies concentrated on the ability of α-syn species to induce an inflammatory response, a few were dedicated to the impact of neuroinflammation on α-syn pathology.

This thesis aimed to explore the role of neuroinflammation in synucleinopathies in relation to α-syn pathology and dopaminergic synaptic loss and neurodegeneration. Firstly, we generated a microglial-like cell model that stably expressed α-syn. Using this model, we investigated α-syn PTMs induced by these cells, their ability to develop aggregates, and their toxicity. Then, we performed a high-throughput screening using a FRET-based system. We identified three compounds that interfere with the α-syn aggregation process in HEK 293T cell line over-expressing α-syn. Subsequently, we investigated whether the inflammatory response within the brain was different in several brain regions. We observed heterogeneity for several parameters and a peculiar inflammatory activation in the substantia nigra (SN). In the end, we investigated α-syn conformations in different human brain regions and synucleinopathies. We found different conformations and identified an α-syn truncation that is more common in Parkinson´s disease than dementia with Lewy bodies and multiple system atrophy. Our studies indicated that inflammation could have an impact on neurodegeneration in SN and on α-syn processing.

Key words α-Synuclein, pre-formed fibrills, microglia, astrocyte, neuroinflammation, lipopolysaccharides, Parkinson´s disease, Lewy body dementia, multiple system atrophy, synucleinopathies

Classification system and/or index terms (if any)

Supplementary bibliographical information		**Language English**
ISSN and key title 1652-8220		**ISBN** 978-91-8021-310-3
Recipient's notes	**Number of pages** 108	Price
	Security classification	

Signature  Date 2022-09-30

Role of Neuroinflammation in Parkinson´s Disease and Related Disorders

Edoardo Brandi

LUND
UNIVERSITY

Coverphoto by Edoardo Brandi using https://www.midjourney.com/

Faculty of Medicine
Department of Experimental Medical Science
ISBN 978-91-8021-310-3
ISSN 1652-8220
Lund University, Faculty of Medicine Doctoral Dissertation Series
2022:148

Printed in Sweden by Media-Tryck, Lund University
Lund 2020

To my family…

To my friends…

and to my little Sonny…

Table of Contents

Original papers and manuscripts

Included in the thesis

I. **Brandi E**, Svanbergsson A, Torres-Garcia L, and Li JY. Generation and characterization of α-synuclein expressing BV2 cells for studying α-synuclein aggregation and neuroinflammatory responses. (Manuscript in preparation)

II. Svanbergsson A, Ek F, Martinsson I, Rodo J, Liu D, **Brandi E**, Haikal C, Torres-Garcia L, Li W, Gouras G, Olsson R, Björklund T, Li JY. FRET-Based Screening Identifies p38 MAPK and PKC Inhibition as Targets for Prevention of Seeded α-Synuclein Aggregation. Neurotherapeutics. 2021 Jul;18(3):1692-1709.

III. **Brandi E**, Torres-Garcia L, Svanbergsson A, Haikal C, Liu D, Li W, Li JY. Brain region-specific microglial and astrocytic activation in response to systemic lipopolysaccharides exposure. Front Aging Neurosci. 2022 Aug; 14:910988

IV. Haikal C, Liu D, **Brandi E**, Melek Altay F, Li W, Englund E, Lashuel HA, and Li JY. Epitope-specific alpha-synuclein pathology in different synucleinopathies (Manuscript in preparation)

Outside of the thesis

V. Torres-Garcia L, P Domingues JM, **Brandi E**, Haikal C, Mudannayake JM, Brás IC, Gerhardt E, Li W, Svanbergsson A, Outeiro TF, Gouras GK, and Li JY. Monitoring the interactions between alpha-synuclein and Tau in vitro and in vivo using bimolecular fluorescence complementation. Sci Rep. 2022 Feb 22;12(1):2987.

Popular science summary

Synucleinopathies are a group of progressive neurodegenerative disorders, including Parkinson's disease (PD), Lewy bodies dementia, and multiple system atrophy. These pathologies primarily affect older people, and their incidence increase with aging, which is considered the main risk factor. Synucleinopathies are characterized by motor and non-motor symptoms that highly decrease the quality of life for patients and their families. These pathologies affect around 24 million people worldwide, and their number is meant to raise due to the increase in life expectancy. Although our knowledge about these pathologies has increased, we still have no cure available, and we only could partially treat some symptoms.
Recently, several studies suggested a fundamental role of inflammation in PD and related disorders. Previously, neuroinflammation was considered only a consequence induced by an abnormal accumulation of α-synuclein protein inside neurons. Currently, this vision partially changed, and inflammation seems to actively co-participate in the pathology progress.

This Ph.D. thesis aimed to explore the neuroinflammatory role in synucleinopathies. We first investigated whether the brain's most important immune cell population, known as microglial cells, can process α-synuclein. We found that these cells could generate aggregates and observed that the presence of intracellular aggregates could be toxic to microglial cells. Then, we created a cell model useful to screen several molecules able to interfere with the generation of intracellular inclusion, we identified three different inhibitors, and we investigated their mechanisms.
Subsequently, we explored whether inflammation affects the mouse brain uniformly or if it hits specific regions. We found differential inflammatory responses in several brain regions. Interestingly, most regions where we observed more robust, sensitive, or extended inflammatory reactions, are involved in neurodegenerative diseases such as PD and Alzheimer's disease. We also explored the role of CX3C receptor-1 as a possible pharmacological target and we found that mice that present a partial ablation of this receptor decreased their inflammatory response respect the control.
Lastly, we investigated whether α-synuclein inclusion presents different conformations within several human brain regions, observing that this is indeed the case. Further, studies need to be performed to investigate the correlation between inflammation and α-synuclein conformations in these samples.
Complessively, our results suggest that inflammation could influence the progression of synucleinopathies.

Populärvetenskaplig sammanfattning

Synukleinopatier är en grupp av progressiva neurodegenerativa sjukdomar som bland annat inkluderar Parkinsons sjukdom (PS), Lewy-body demens och multipel systematrofi. Dessa patologier drabbar främst äldre människor och förekomsten ökar med åldrande, vilket anses vara den främsta riskfaktorn. Synukleinopatier kännetecknas av motoriska och icke-motoriska symtom som kraftigt minskar livskvaliteten hos patienterna och deras närstående. Synukleinopatier påverkar cirka 24 miljoner människor och denna siffra väntas öka på grund av förväntad ökad livslängd. Även om vår kunskap om dessa patologier har ökat finns idag inget botemedel tillgängligt och nuvarande läkemedel behandlar endast symtom.

Människor som drabbas av synukleinopatier har också en pågående neuroinflammation. Tidigare ansågs neuroinflammationen endast vara en konsekvens av en onormal ackumulering av proteinet α-synuklein inuti nervceller. På senare tid har flera studier visat på en grundläggande roll för neuroinflammation vid sjukdomsförloppet av PS och relaterade sjukdomar. Denna doktorsavhandling syftar till att utforska den neuroinflammatoriska rollen i synukleinopatier. Vi undersökte först om hjärnans främsta immuncellspopulation, mikrogliaceller, kan bearbeta α-synuklein. Vi fann att dessa mikrogliaceller kunde generera intracellulära ansamlingar av α-synuklein och observerade att dessa ansamlingar kunde vara toxiska för cellerna. Sedan skapade vi en cellmodell för att screena flera molekyler för att undersöka om dessa kan störa ansamlingen av α-synuklein, vi identifierade tre olika molekyler som minskade ansamlingen och vi undersökte deras mekanism. Därefter undersökte vi om generell inflammation påverkar hela hjärnan eller endast specifika regioner. Vi hittade distinkta inflammatoriska svar i flera olika hjärnregioner. Vi fann bland annat att de flesta regioner där vi observerade skillnader i det inflammatoriska svaret också är involverade i neurodegenerativa sjukdomar som PS och Alzheimers sjukdom. Slutligen undersökte vi om ansamlingarna av α-synuklein har olika strukturer i olika hjärnregioner hos människor, och observerade att detta verkligen är fallet.

Sammanfattningsvis antyder våra resultat att inflammation kan påverka förloppet av synukleinopatier.

Abbreviations

6-OHDA	6-hydroxydopamine
α-syn	α-synuclein
AAV	Adeno-Associated Viruses
BBB	Blood-brain barrier
CD	Cluster of Differentiation
CNS	Central Nervous System
CSF1r	Colony-Stimulating factor 1 receptor
CVO	Circumventricular Organ
DJ1	Parkinson-associated deglycase 1
DLB	Lewy Bodies Dementia
EFI	Extended Focus Imaging
eIF1α	Eukaryotic Translation Initiation factor 1
CNS	Central Nervous System
FRET	Fluorescent Resonance Energy Transfer
GABA	Gamma-Aminobutyric Acid
GFAP	Glial Fibrillary Acid Protein
HSP	Heat Shock Protein
HTS	High-Throughput Screening
i.p.	Intraperitoneally
IL1β	Interleukin 1- β
iNOs	Inducible Nitric Oxide synthase
IRE	Iron-Responsive Element
LBs	Lewy Bodies
LNs	Lewy's Neurites
LPS	Lipopolysaccharide
LRRK2	Leucine-rich repeat kinase 2
MHC	Major Histocompatibility Complex
MPPP	1-methyl-4-phenyl-4-propionoxypiperidine

MPTP	1-methyl-4-phenyl-1,2,3,6-tetrahydropyridine
MS	Mass Spectrometry
MSA	Multiple System Atrophy
NAC	Non-Amyloid beta Component
NAc	Nucleus Accumbens
NADPH	Nicotinamide Adenine Dinucleotide Phosphate
NLRP3	Neuroinflammasome-3
p38 MAPK	p38 Mitogen-Activated Protein Kinase
PBS	Phosphate Buffered Saline
PCC	Pearson's Correlation Coefficient
PD	Parkinson's Disease
PET	Positron Emission Tomography
PFA	Paraformaldehyde
PFFs	Pre-Formed Fibrils
PINK1	PTEN-induced putative kinase 1
PKC	Protein Kinase C
PKR, EIF2AK2	Inflammation-associated serine-threonine kinase
PPA cortex	Posterior Parietal Association Areas
pS129 α-syn	Phosphorylated α-syn
PSM cortex	Primary Motor and Somatosensory cortex
PTM	Post-Translational Modifications
ROS	Reactive oxygen species
SNpc	Substantia Nigra pars compacta
SNpr	Substantia Nigra pars reticulata
TFEB	Transcription Factor EB
TH	Tyrosine Hydroxylase
TLR	Toll-like receptors
TNFα	Tumor Necrosis Factor-α
Trunc-119	Truncated Asp 119
VTA	Ventral Tegmental Area
WT	Wild-Type

Introduction

General Introduction

Synucleinopathies are progressive neurodegenerative disorders that include Parkinson's disease (PD), Lewy bodies dementia (DLB), and multiple system atrophy (MSA). These diseases are characterized by intracellular inclusions, neuroinflammation, iron accumulation, and, in most cases, dopaminergic neurodegeneration in the substantia nigra pars compacta (SNpc). Synucleinopathies affect around 24 million people worldwide (0,3%), and their incidence increases with aging, from 1% of 60 years old people to 3% of 80 years old people [1, 2]. For this reason, aging is considered the leading risk factor for synucleinopathies [3]. Interestingly, males are generally more affected than females, and smokers and coffee users seem partially protected [4, 5].

Clinical features and diagnosis

The diagnosis of synucleinopathies represents a complex issue due to clinical heterogeneity. This variability could depend on an overlap with other neuropathological conditions and cognitive decline due to natural aging [6-9]. Although several biomarkers have been suggested to increase the success in diagnostic rate, the diagnosis still needs to be confirmed by post-mortem histological analyses.
The cardinal features of PD are unilateral tremors at rest, rigidity, bradykinesia (slowness of movement), and postural instability. Moreover, flexed posture and freezing (motor blocks) are also included among classic features of parkinsonism and PD [10]. Other non-motor symptoms include sleep behaviour disorder, loss of smell, constipation, global cognitive decline that consists of depression, executive dysfunction, and working memory deficits. These non-motor symptoms can precede motor disorders or may arise later in the disease [11]. DLB and PD have common clinical characteristics such as progressive cognitive impairment associated with parkinsonism, sleep behaviour disorder, hallucinations, altered attention, and wakefulness. The timing of dementia relative to parkinsonism is the primary clinical distinction between PD and DLB. Dementia arises after motor alterations in PD, while these symptoms precede movement disorders in DLB [12]. MSA is clinically characterized by autonomic failure, parkinsonism, ataxia, and sleep behaviour

disorder and present two main phenotypes, termed either parkinsonism or cerebellar depending on the area of the brain that are affected by the pathology [13, 14].

Genetic and environmental risk factors

As mentioned, aging is considered the main risk factor of synucleinopathies. However, genetic mutations have been identified and linked with 5-10% of PD cases, involving genes decoding for proteins such as α-synuclein (α-syn), Parkinson-associated deglycase 1 (DJ1), leucine-rich repeat kinase 2 (LRRK2), Parkin, PTEN-induced putative kinase 1 (PINK1), and others. The familial cases generally have an earlier onset than the sporadic ones.

Moreover, different environmental factors have been identified, such as the exposure to environmental toxins and pesticides. The link between parkinsonism and toxins was first identified in 1976. Barry Kidston, a 23 year old chemistry student, independently tried to produce the opioid analgesic drug 1-methyl-4-phenyl-4-propionoxypiperidine (MPPP) and self-injected the result. Three days later, he started to develop parkinsonism symptoms. During MPPP production, 1-methyl-4-phenyl-1,2,3,6-tetrahydropyridine (MPTP) can be obtained as an impurity. This compound can penetrate the brain through the blood-brain barrier (BBB), which is oxidized into the toxic species MPP^+ by monoamine oxidase [15, 16]. This compound induces the neurodegeneration of dopaminergic neurons in SNpc and the development of parkinsonism. After this discovery, other toxins were identified to induce similar effects on the dopaminergic system, such as 6-hydroxydopamine (6-OHDA) and the pesticides paraquat, rotenone, DDT, and others [17-19].

The discovery of these toxins led to the generation of several animal models, which resemble some features of parkinsonism and PD, such as the dopaminergic degeneration in SNpc with consequent motor deficits and iron accumulation [20, 21]. These models were particularly useful for investigating the neuronal circuitry involved in these pathologies and several pharmacological treatments. Additionally, they allowed the identification of some milestone discoveries, such as the involvement of mitochondria, the higher susceptibility of dopaminergic neurons to reactive oxygen species (ROS), and the dopamine ability to self-oxidized. However, most of these models present limits, such as the absence of intraneuronal inclusions. The only exceptions seem to be rotenone and MPTP. In fact, the administration of these toxins was able to reproduce dopaminergic neurodegeneration and the formation of intracellular inclusions in animal models [22-29].

Since all these toxins have mitochondria as the primary target and induce an increase of ROS, these findings suggested a prominent role of these reactive species in PD and related disorders [30]. However, ROS alone do not explain why the midbrain's dopaminergic neurodegeneration affects the SNpc and leaves almost intact the same neurons in the neighbouring region, the ventral tegmental area (VTA).

Dopaminergic neurodegeneration and basal ganglia circuitry

Although several brain regions are affected in synucleinopathies, the most robust and common neurodegeneration observed is the one in substantia nigra (SN) (Figure 1). This region is a small midbrain nucleus histologically divided into pars compacta and reticulata (SNpr). SNpc consists mainly of highly compacted dopaminergic neurons that project their axons to basal ganglia (BG). SNpr presents a lower neuronal density but is enriched by fibers and glial cells [31-34]. Most of these neuronal fibers come from BG nuclei and are known as striatonigral bundles [33]. SNpr is also enriched by dopaminergic dendrites from neurons located in SNpr. Interestingly, these dendrites can release dopamine in SNpr, and some authors suggested that this dendritic release could be related to a modulatory activity on the gamma aminobutyric acid (GABA) neuronal population in SNpr [35-38].

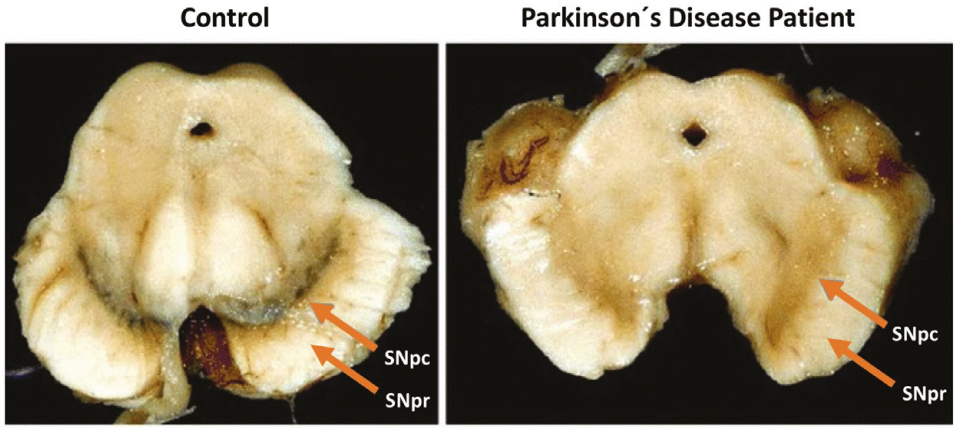

Fig. 1. Midbrains from PD patient and control subject. Images adapted from https://neuropathology-web.org/

BG consists of interconnected nuclei located between the basal forebrain and midbrain (Fig. 2). These nuclei receive projections from the motor cortex and are crucial for movement selection and control. Cortical fibers project to the caudate and putamen in the basal forebrain, making synapses with local neurons. Then, from these neuronal populations depart two different main projections known as direct and indirect bundles. The first one project directly to internal globus pallidus and SNpr, that represent the two main circuitry output of BG. The indirect bundle project to external globus pallidus before reaching the two output nuclei. Other nuclei take a role in BG modulation, such as SNpc and subthalamus [33]. The well-functioning of this neuronal circuitry depends on the activity of each of its components.

The studies performed on subject affected by parkinsonism and animal models based on toxins, showed that the dopaminergic degeneration in SNpc alone can modify this circuitry and induce the onset of motor deficits that characterize parkinsonism and PD.

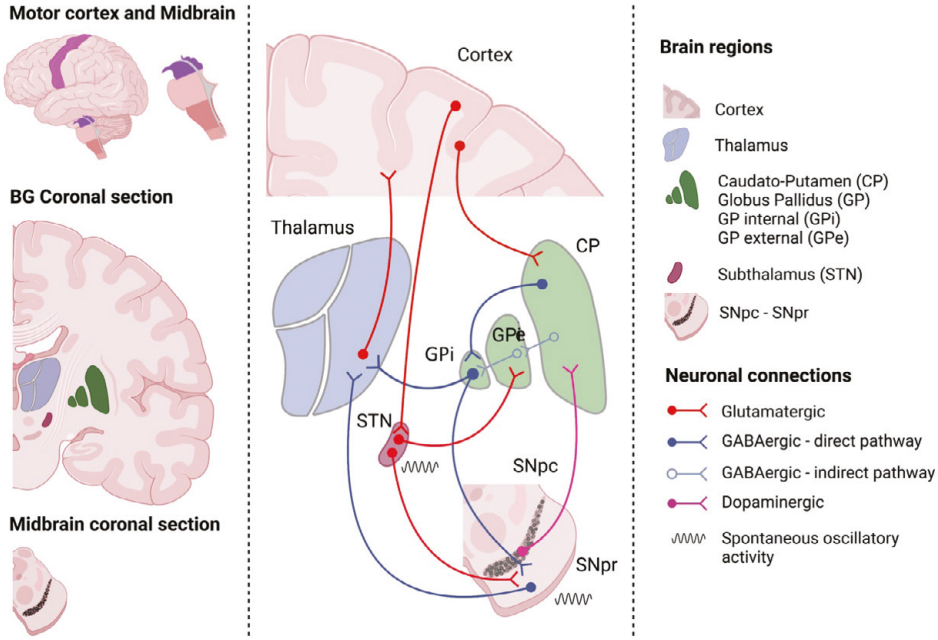

Fig. 2. Schematic BG circuitry. Figure created with https://biorender.com/

Lewy Bodies

In 1910, Fritz Heinrich Lewy described for the first time the intraneuronal inclusions that are currently considered one of the hallmarks of synucleinopathies. Some of these inclusions appeared as eosinophilic spherical masses with a dense core localized within the cytoplasm of neuronal cells and were defined as Lewy bodies (LBs) (Fig. 3). Others were localized in neurites and identified as Lewy's neurites (LNs) (Fig. 3). In MSA cases, intracellular inclusions were also observed in oligodendrocytes, representing one of the main characteristics that distinguishes this synucleinopathy from the others.

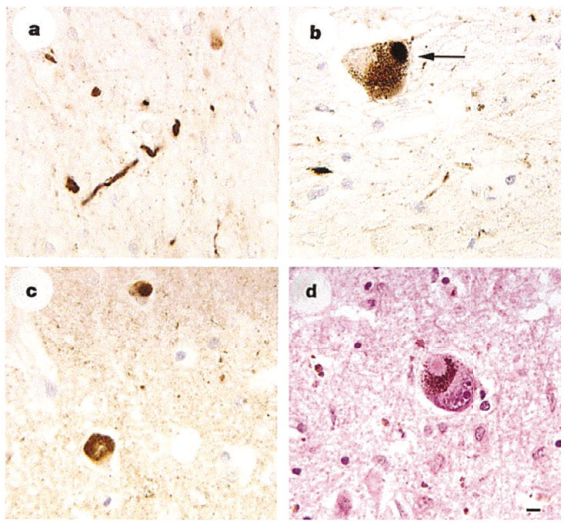

Figure 3. Lewy bodies (B, C and D) and neurites (A) [39]

Proteome analyses showed that the intracellular inclusions consist of 300 proteins mainly related to mitochondria, the ubiquitin-proteasome system, and the autophagy apparatus [40, 41]. Some of the proteins identified are related to familial forms of PD, such as α-syn, DJ1, LRRK2, Parkin, and Pink-1, strongly linking these proteins to synucleinopathies [39, 40, 42]. Furthermore, a study based on electron microscopy revealed the presence of lipid organelles and mitochondria, confirming the involvement of these organelles in the pathological process [43].

α-Synuclein: structure, expression, and function

α-Syn is the most abundant component of LBs, which is found in an insoluble fibrillar form [39, 40]. This protein consists of 140 amino acids (a.a.) and three main

domains: 1) the N-terminal domain (1-60 a.a.) with an alpha helix structure and a positive charge conferring to this region the ability to bind lipid membranes; 2) the non-amyloid beta component (NAC) domain (61-95 a.a.) that could form cross beta-structures; 3) the C-terminal acid tail (96-140 a.a.) that possess a low hydrophobicity and high negative charges leading to the formation of random coil structures [44] (Fig. 4).

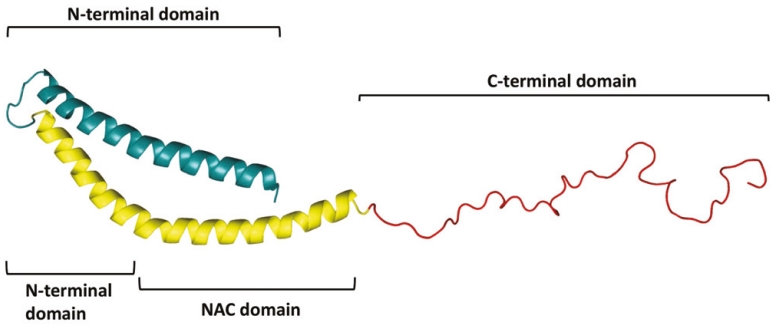

Fig. 4. **α-Syn protein and domains.** (Image adapted from [45]).

α-Syn is mainly expressed in the central nervous system (CNS), but it can be found in low amounts also in others tissues. In the brain, α-syn protein is expressed in neurons and localized mainly in the pre-synaptic terminals. α-Syn can be found free and soluble in the cytosol or bound to membranous organelles, and it has a particular affinity for membranes that present high curvatures and lipid rafts [46-49].
Although many authors have made several hypotheses about the α-syn function, this is still unknown. The most accredited hypothesis suggests that α-syn interacts with SNARE proteins, which are crucial for the pre-synaptic system for neurotransmitters' vesicle release [50-54] (Fig. 2). Liu and colleagues proposed that α-syn regulates mitochondria activity, as it has been detected in this organelle and seems to be able to modulate the complex I of the respiratory chain [55]. Other scientists indicated that the α-syn C-terminal is homologous to small heat shock proteins (HSPs) and suggested that it exerts a protective role in maintaining proteins away from the degradation process [56]. Mice knocked out for α-syn showed a few alterations, leaving this question open [57]. However, these mice were more resistant than control mice to dopaminergic degeneration when treated with MPTP, indicating a crucial role of α-syn in the neurodegeneration observed [58, 59].

α-Synuclein aggregations

α-Syn can polymerize, form tetramers, oligomers, and fibrils. Some of these polymers could represent physiological species or could be toxic. α-Syn

multimerization process, known as amyloidosis (Fig. 5), seems to be intrinsically determined by the amino acid sequence of this protein. In particular, the NAC domain seems to be involved in this process due to its ability to form beta-sheet structures. These structures are typical of proteins that form insoluble aggregates, such as amyloid proteins.

Amyloidosis is a process that consists of several steps (Fig. 5). "Primary nucleation" is the first stage and can be homogeneous or heterogeneous. In the homogeneous primary nucleation, the initial seed involves α-syn monomers only. It is a slow process and it requires high energy demand when reproduced *in vitro* (in cell-free conditions). In the heterogeneous primary nucleation, a different molecule is added to α-syn monomers, acting as a catalyst for the seeding. The second step of amyloidosis is known as "elongation." In this stage, α-syn monomers bind to the seed formed during the nucleation process and rapidly increase their mass, forming large fibers. The last stage is “secondary nucleation”, where new seeds originate from previously formed aggregates. This last step amplifies the formation of aggregates, restarting the cycle till the equilibrium between all α-syn species is reached.

Currently, different laboratories in the field developed different cell-free *in vitro* protocols to generate α-syn pre-formed fibrils (PFFs) [60, 61]. Altering pH, temperature, salt concentrations, and other factors, it is possible to obtain several fibril strains presenting differences between each other. These α-syn PFFs and/or oligomers are routinely used for research purposes to investigate their toxicity and ability to induce aggregation in cells or animal models that overexpress α-syn [62-65]. Studies investigating the toxicity of α-syn PFFs and/or oligomers, revealed that these species are harmful to neurons *in vitro*, while contradictory results were obtained *in vivo* [64-68].

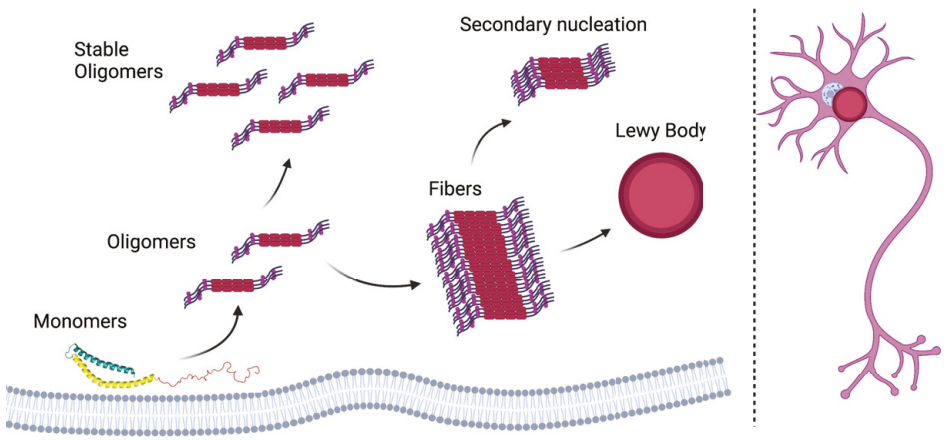

Fig. 5. Schematic α-Syn amyloidosis. Figure created with https://biorender.com/

α-Synuclein mutations and transgenic animal models

α-Syn structure and its chemical characteristics could be altered by different mutations, post-translational modifications (PTMs), and interactions with some metals. These modifications or interactions could modify α-syn ability to bind lipid membranes, translocate in other cell regions, be more or less prone to form oligomeric or aggregates species, and may be toxic.

Different autosomal point mutations were identified on the α-syn gene and linked with familial forms of PD pathology. These mutations are mainly localized in the N-terminal domain (Fig. 6) and seem to modify the α-syn ability to aggregate. Alterations in α-syn aggregation kinetics were observed stimulating the aggregation process via PFFs in cells overexpressing WT and different α-syn mutations [69, 70]. Furthermore, different transgenic mice overexpressing α-syn were created. Contradictory data were obtained in models overexpressing WT α-syn about forming Lewy-like inclusions. The models developed some motor deficits, but no dopaminergic degeneration [71, 72]. Similar results were observed when mutated forms of α-syn were overexpressed in mice and combined with α-syn PFFs injections [73]. However, different results were obtained when α-syn PFFs were used in combinations with α-syn overexpression induced by adeno-associated viruses (AAVs). In this case, intracellular inclusions, dopaminergic degeneration, and motor deficits were observed [74]. However, we must to be aware of the high α-syn concentrations expressed in these models, far away from the human physiological condition.

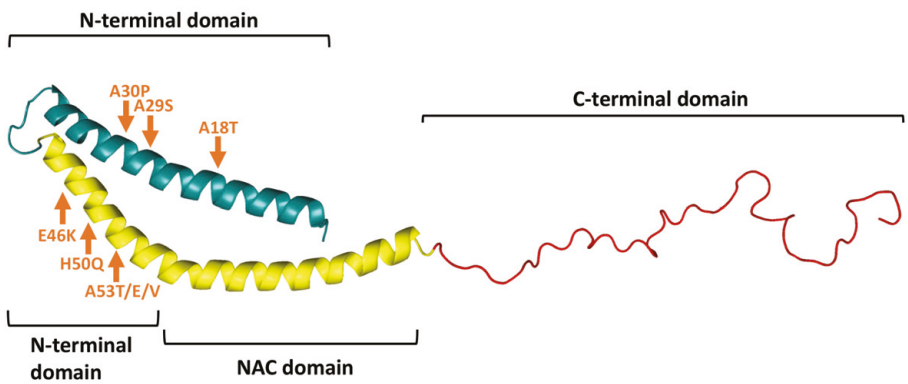

Fig. 6. α-Syn protein and mutations. (Image adapted from [45]).

α-Synuclein interaction with metals

As previously mentioned, the primary nucleation is the step limiting the formation of α-syn aggregates both *in vitro* and *in vivo*. Although α-syn can form aggregates, this process needs high energy demand, and how the first nucleation happens *in vivo* is still unknown. *In vivo*, this issue could be overcome through α-syn binding with some catalyst or structural changing mediated by enzymes.
It has been shown that the α-syn amino acidic sequence contains sites for binding divalent metals such as iron, copper, calcium and manganese [75-77]. The interactions with these ions seem to increase the tendency of α-syn to aggregate [78, 79]. Surprisingly, α-syn also possesses an iron-responsive element (IRE) in its 5'-untranslated region, and its expression increases when iron binds this region [75]. Interestingly, the IRE element is a characteristic shared with few other proteins, including ferritin [80]. Moreover, α-syn is able to reduce ferric iron into ferrous iron in the presence of nicotinamide adenine dinucleotide phosphate (NADPH), suggesting a possible physiological role concerning mitochondrial activity [81]. The link between α-syn and iron seems to be strong. However, an increase in metal levels has been observed for many neurodegenerative diseases and seems to be a common characteristic of aging [82].

α-Synuclein post-translational modifications

Several α-syn PTMs were described, such as phosphorylation, nitration, oxidation, methylation, glycation, and truncations. These PTMs have been observed in soluble and/or insoluble fractions. Anderson and colleagues found phosphorylation of serine 129, ubiquitination at Lys residues 12, 21, and 23, and truncation at Asp-119 in all LBs they examined [83]. Other PTMs commonly found were nitration at Tyr 39, 125, 132, and 135, truncations at Asp-115, Asn-122, Tyr-133, and Asp-135. A small amount of phosphorylated α-syn (pS129 α-syn) and truncated Asp 119 α-syn (trunc-119 α-syn) have also been found in the soluble fraction. At the same time, ubiquitination seems to be only present in aggregated form and primarily associated with pS129 α-syn [83-85].
Among these α-syn PTMs, pS129 is prominent in LBs and the most studied. In physiological conditions, a small amount (>4%) of α-syn present pS129, while it increases up to 90% in the brain of patients affected by synucleinopathies [83, 86, 87] and animal models [71, 88]. These findings suggested that pS129 could play a role in α-syn aggregation, while controversial observations were obtained about its toxicity [89-92]. It has been observed that the inhibition of the ubiquitin-proteasome system led to an increase in α-syn phosphorylation, suggesting a possible function of these PTMs in regulating α-syn turnover [93, 94]. Moreover, pS129 seems to alter the α-syn ability to bind metals and lipid membranes and induce nuclear translocation [95-99]. Additionally, WT α-syn interacts with mitochondrial proteins

such as complex I, II, and IV of the electron transport chain, while pS129 has higher affinity for cytoskeletal and pre-synaptic proteins [100].

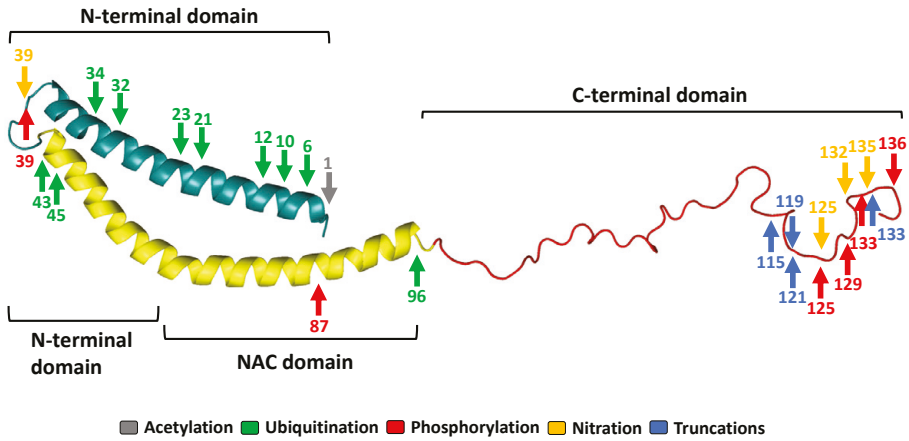

Fig. 7. α-Syn protein and PTMs. (Image adapted from [45]).

Another α-syn PTM commonly observed in patients and animal models is nitration. This PTM seems to increase with aging in humans and primates [84, 85, 101]. Nitration could happen due to an increase of ROS that could derive from mitochondrial malfunction or an inflammatory response. Studies on PD patients presenting LBs, suggested that nitrated α-syn could increase the capacity of this protein to aggregate [84, 85, 102]. However, other studies showed that nitrated α-syn is more prone to form stable and soluble oligomers and to decrease its ability to bind lipid membranes [103-105]. Interestingly, α-syn oxidation of methionine 1, 5, 116, and 127 also induces the formation of stable oligomers [106-108]. These observations could suggest a physiological role of α-syn PTMs generated by ROS species.

As already mentioned, trunc-119 α-syn has been described ubiquitously in all LBs, while truncations at 115, 122, 133, and 135 are more variable [83]. Different studies suggested that these species induced α-syn aggregation and observed trunc-119 in the LBs core [109-111]. Daher and colleagues tried to mimic the effects mediated by truncation and created a conditional animal model expressing trunc-119 α-syn. The authors observed a reduced striatal dopamine release but no spontaneous LBs pathology or dopaminergic neurodegeneration [112].

α-Synuclein spreading

In 2008, two independent studies showed that fetal dopaminergic neurons transplanted in PD patients presented LBs pathologies 11-16 years after transplantation, suggesting host-to-graph disease propagation [113, 114]. Several authors speculated that LBs pathology observed in the graft derived from the transmission of misfolded α-syn from host PD-affected neurons in a prion-like manner [115-117]. Subsequently, several studies confirmed α-syn ability to be transmitted. When α-syn PFFs are added to cell cultures, they can be phagocyted and act as a seed for new aggregates formation if the recipient cells overexpress α-syn. Several studies injected α-syn PFFs in transgenic animal models overexpressing α-syn, showing that the number of cells that develop aggregates increases in different brain regions in a time-dependent manner and confirming that α-syn pathology can propagate also *in vivo* [63, 118].
The same results were obtained by injecting human brain homogenates from patients affected by synucleinopathies. Interestingly, homogenates from MSA patients seem to be more toxic and have a greater ability to spread than homogenates from PD and DLB patients [116, 119]. These finding indicate that the α-syn processed in the oligodendrocytes intracellular environment could present peculiar PTMs that confer to this protein a higher ability to spread and to be toxic. Moreover, α-syn from human homogenates presents different structures and induced different effects compared to α-syn PFFs [120, 121]. The researchers still did not identify how the pathological α-syn species can be transported between cell-to-cell, but several mechanisms have been suggested as vesicle transport, nanotubules, simple diffusion, and others.

Staging hypothesis and their validity

The idea that LBs pathology could propagate from cell to cell and between different regions suggested that these synucleinopathies might have a specific origin and then propagate following ordered neuronal patterns. Based on this concept, Braak and McKeith defined pathological stages in PD and DLB established on LBs and LNs pathology distribution within several brain regions [122-124]. Braak's hypothesis suggested six different pathological stages that define the course of PD pathology. According to this hypothesis, LBs pathology in sporadic PD originates in the anterior olfactory nucleus and the dorsal motor nucleus of the glossopharyngeal and vagal nerves. Then, it propagates following an ascending course involving different grey nuclei and cortical regions [122] (Fig 3). McKeith defined some criteria to identify the pathology course for DLB, with seven stages mainly involving cortical regions [123, 124].
Many researchers around the world follow these systems currently. However, although this is a fascinating hypothesis, it received various criticism that should be

considered [125-127]. Two robust studies tried to assess the accuracy of Braak and McKeith stages, taking into consideration 904 and 1720 human brains and performing a retrospective clinical assessment. These studies showed low correlation between Braak and McKeith staging system and the clinical picture [128, 129]. These discrepancies underlie the heterogeneity of these pathologies and suggest that different pathological sub-types with distinct origins and courses might be present. Furthermore, LBs pathologies could be influenced by other neurological conditions or by other alterations related to aging.

Another interesting observation from these two works was that 30 - 43% of the cases that presented α-syn pathology did not show any neurological impairments. The lack of clinical correlation was also observed in brains with widespread LBs pathology in cortical regions that are supposed to be at the V-VI stages of Braak's hypothesis [128, 129]. A possible explanation could be that these cases represent pre-clinical stages of DLB or PD that still did not manifest symptoms. In the field is known that almost 30% of dopaminergic degeneration and 50-70% of axonal denervation must be present before observing the onset of motor symptoms [130-132]. Another hypothesis is that the toxic species of α-syn could be soluble and LBs formation represent a defence mechanism of the cells seizing α-syn pathological species. In the end, another hypothesis is that α-syn alone cannot entirely explain synucleinopathies and something else needs to be present.

A considerable contribution in understanding LBs pathology progression concerning clinical aspects could arrive from positron emission tomography (PET) when a tracer for LBs will be developed.

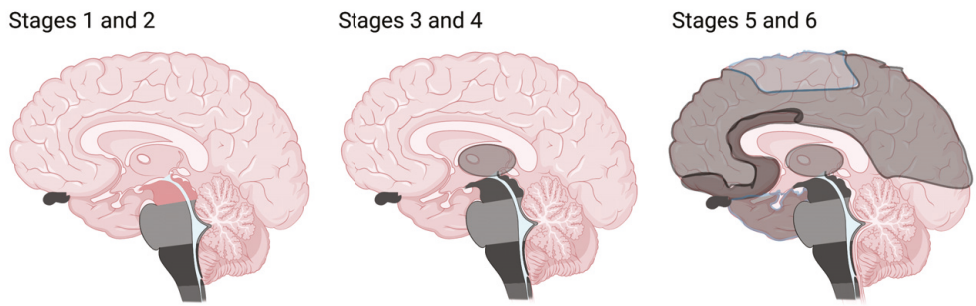

Figure 8. Schematic representation of Braack´s Stages. Brain regions affected in several stages in dark color. Figure created with https://biorender.com/

Neuroinflammation

Neuroinflammation is a common characteristic observed in synucleinopathies and, as well, in almost all neurodegenerative diseases [133-141]. The inflammatory system could be involved in these pathologies for different reasons. It could happen by the presence of pathogens or toxic molecules but also by tissue damage. This broad neuroinflammatory presence in different pathologies probably explains why this system has been underestimated for a long time.
The inflammatory system consists of different cells within the CNS, such as microglia and astrocytes. In the presence of a neuroinflammatory event, immune cells from the peripheric system can also be involved, which migrates inside the brain parenchyma through the BBB. Evidence showed that a robust or a chronic inflammatory response could be deleterious for the surrounding tissue and interesting observations tightly link this system to synucleinopathies.

Microglia

Microglia cells represent the macrophage population of the brain and are widely distributed in all the CNS. During development, these cells originate from the yolk sac and migrate within the brain before the BBB is completely formed [142]. Here, these cells continuously explore the surrounding tissue and participate in maintaining its homeostasis. In the presence of pathogens or toxic agents, microglia and other inflammatory cells act to remove them and re-establish the homeostatic conditions [142]. However, a robust and/or chronic inflammatory response could harm the surrounding tissues. This dangerous effect could be related to the release by inflammatory cells of ROS or mediators that could trigger programmed cell death.
Microglial cells can present pro-inflammatory or protective phenotypes. For this reason, many authors have started using binominal criteria and defined them as M1 and M2 phenotypes. However, evidence showed that there is variability in microglia populations, and different intermediary phenotypes could be present [143]. Although microglia cells are ubiquitously distributed within the brain, their density, morphology, and transcriptomes differ in spatiotemporal dimensions. Lawson and colleagues described different microglia morphologies and densities in several brain regions [31]. For example, clear differences in microglia morphology and density between substantia nigra pars reticulata (SNpr), SNpc and VTA can be observed. De Biasi and collaborators conducted a whole transcriptome RNA sequencing data analysis. They revealed that microglial populations between SN, VTA, Nucleus Accumbens (NAc), and cortex share just 48% of their gene expression [32]. Other studies showed a higher expression of essential inflammatory factors such as the major histocompatibility complex (MHC) I and II and the toll-like receptors 4 (TLR4) in the midbrain compared with the cortex, hippocampus, and striatum [144].

Other investigations also suggested a different expression of crucial inflammatory cytokines such as the tumor necrosis factor-alpha (TNFα) and interleukin 1-beta (IL1β) under inflammatory conditions [144, 145]. Interestingly, after microglia depletion via colony-stimulating factor 1 receptor (CSF1r) inhibition, these cells can repopulate the different brain regions maintaining the original differences [32]. Although many studies focused on studying microglial heterogeneity in resting conditions, it is still unclear whether and how this could lead to different inflammatory responses.
Other studies focused on microglia changing in relation to aging, showing that the morphology and transcriptome of these cells can change throughout all life, becoming more susceptible to getting activated during aging [146].
An increase of evidence showed that microglia are well integrated with the other cells of the CNS and carry out critical physiological functions not correlated with their inflammatory role. These cells can actively interact with neurons and probably have a role in modulating their synapses. This function seems particularly important during the early stage of development when they are crucial to remove the synapses' excess in a process known as pruning [147]. The lack of this process was observed in CX3CR1 total ablated mice, which induced aberrant neuronal circuits and consequent cognitive deficits [147, 148]. Interestingly, rare genetic variants were linked between this receptor and increased risk of developing schizophrenia and autism spectrum disorders [149]. Moreover, inducing microglial depletion in the early stages of mouse brain development caused ventricle enlargement, increased neuronal and astrocytic density, and decreased oligodendrocytes population [150]. Different observations were made when microglial cells were depleted in adult mice, showing no evident alterations. However, studies showed that in the adult mouse brain, microglial cells could modulate neuronal activity, eliminate synapses, stimulate synaptogenesis, and model the extracellular matrix for new synapses [151-157]. These observations suggest that, although microglial cells can modulate neuronal synapses and circuitry at several ages, this role seem less extended and essential in adult mice than in young ones.
Additionally, other interesting functions have been found, such as microglia's ability in iron retention and their possible role in metabolic physiology in the hypothalamus [158-160].

Astrocytes

Astrocytes are another glial cell often involved during a neuroinflammatory event [161, 162]. This cell population is distinct from microglial cells and other immune cells. These cells derive from the primary neuroepithelium and are already present at the early stage of brain development. Here, they are known as glial radial cells and are essential for brain development, driving neurons to their final location [163]. In adult tissue, astrocytes distribute ubiquitously within all CNS maintaining contact through a complex network of gap junctions [164].

Similar to microglial cells, astrocytes present a high level of heterogeneity between different brain regions [165, 166]. These cells represent one of the most versatile cell types within the brain, performing many different functions. They have crucial roles in tissue scaffolding, formation and modulation of BBB, maintaining homeostasis, synaptogenesis, synaptic regulation, neurotransmitter inactivation, and supporting neurons with lactate for their energy demand [165-169]. In the last twenty years, increasing evidence showed that astrocytes carry out crucial functions during inflammation [161, 162, 170-173]. They can express TLR2 and 4 and crucial cytokines such as TNFα and IL1β [161, 174-176]. Some authors suggested their role as sentinel cells due to their strategic position between the BBB and brain parenchyma [171, 177, 178]. Other studies indicated that they might act as antigen-presenting cells, while others showed that these cells could adopt a toxic phenotype and be directly harmful to the neighboring neuronal cells [170, 171, 179].

Neuroinflammation in synucleinopathies

Although inflammatory responses were detected in many neurodegenerative diseases, some studies suggest that the link with PD and related disorders is stronger than previously imagined. Activated microglial and astrocytes cells have been described together with infiltrated lymphocytes in post-mortem examinations of patients affected by synucleinopathies [171, 172, 180, 181]. A significant contribution in the field comes from PET imaging studies that revealed an early and chronic involvement of the neuroinflammatory system in patients affected by these pathologies [182-187]. Studying the human post-mortem brain of PD patients that received human embryonic dopaminergic neuronal implant into the striatum after 18 months, 4 and 16 years, Olanow and colleagues observed that microglia activation precedes LBs formation. Microglia were active 18 months after implant, while LBs pathology appeared later [188]. These findings are in line with the work of George and colleagues, who simulated these human studies by grafting dopaminergic embryonic cells in mice either microglia-depleted or inflamed via lipopolysaccharide (LPS). This study showed that activated microglia could increase α-syn transfer in the host-graft direction [189].
Other interesting correlations were obtained in humans via PET imaging. Using a tracer for microglial activation and one for dopamine transporter, Ouchi and colleagues observed a decrease in dopamine transporter and an increase of microglia signal in PD patents [182]. Another study observed a correlation between inflammation and iron accumulation in SNpc, suggesting a link between these two pathological features [190]. Moreover, neuroinflammation was observed to give an essential contribution to the pathological changes observed in most of the PD animal models, and its inhibition seems to prevent eventual detrimental effects.

Neuroinflammation in experimental models based on α-synuclein

The investigation of how α-syn species could activate the neuroinflammatory system, revealed α-syn interaction with different inflammatory receptors such as TLR2 and 4, cluster of differentiation (CD) 11β (CD11β) , and others [174, 191-198]. Microglia activation was observed *in vitro* after exposure to α-syn oligomers or PFFs, but not with monomers [199].

Studies in mice overexpressing WT or mutated α-syn found microglial activation preceding α-syn inclusions and neurodegeneration [200-202]. Watson and colleagues observed this activation in the striatum and SN (1-5 months) but not in the cerebral cortex, indicating a different α-syn expression or a different inflammatory susceptibility to α-syn in different brain regions [200]. Inflammation was described in the absence of dopaminergic degeneration in wild-type animals five months after α-syn PFFs injection [203]. Moreover, it seems to precede neurodegeneration in models where this was observed, suggesting its involvement in the neurodegenerative process itself [74, 204]. Interestingly, intranasal administration of α-syn PFFs also induced microglia iron deposition [205].

Several studies underlie the crucial impact that also peripheric immune system could have in synucleinopathies. Infiltrated immune cells were observed prior to dopaminergic inflammation in an animal model injected with α-syn PFF, and blocking this cell infiltration was protective [206, 207]. As mentioned, chronic or intense inflammation can be harmful to the surrounding tissue via ROS species or other factors. Several anti-inflammatory treatments seem beneficial for these models [174, 208]. Gordon and colleagues, after inhibiting the neuroinflammasome-3 (NLRP3), observed a reduced pS129 and nitrated α-syn five months after PFFs injection [208].

Several studies observed astrocytes to be particularly vulnerable and sensitive in synucleinopathies [209, 210]. La Vitola and colleagues observed microglial and astrocyte activation after intra-ventricular injection of α-syn oligomers. They showed that astrocyte activation precedes microglia, and it is characterized by IL1β production [174]. These findings suggest a possible sentinel role for these cells. Lee and colleagues indicate that α-syn can directly trigger astrocytes' pro-inflammatory phenotype [209]. Interestingly, blocking astrocytes' pro-inflammatory conversion seems neuroprotective in a transgenic model overexpressing α-syn (A53T) injected with α-syn PFFs [211]. Additionally, an interesting study showed that the expression of α-syn (A53T and A30P) in astrocytes induces endoplasmic reticulum stress and Golgi apparatus fragmentation [212].

Comparing α-syn PFFs uptake and clearance capacity between neurons, microglia, and astrocytes, Lee and colleagues observed that astrocytes and microglia uptake a more significant amount of α-syn PFFs than neurons and that microglia cells present the highest clearance ability. However, the clearance capacity decreases when LPS

activates microglial cells [213]. Another study showed a microglial age-dependent decrease in capacity to uptake α-syn oligomers [214].
Several authors suggested the involvement of microglial cells in α-syn spreading. Xia and colleagues showed that microglia cells can uptake plasma exosomes derived from PD patients and be triggered by them both *in vitro* and *in vivo*. Furthermore, they described that microglial-like cell lines (BV2) presented dysregulated autophagy after exosome administration, inducing α-syn accumulation and accelerated α-syn secretion into extracellular space [215]. In the same year, Guo and colleagues treated microglial cells with humanized α-syn PFFs and confirmed that these cells secrete exosomes containing α-syn. Moreover, they observed that these exosomes could induce α-syn aggregation in neuronal cultures over-expressing α-syn and neurodegeneration in the nigrostriatal pathway *in vivo* [216]. Interestingly, Dutta and colleagues showed that inhibition of the TLR2 pathway decreases inflammation and α-syn spreading both *in vitro* and *in vivo* [217].

Neuroinflammation in experimental models based on toxins and LPS

Several studies investigated the role of inflammation in toxin-based PD models. Although the first hypothesis about the toxin's mode of action was associated with mitochondrial dysfunction and dopamine oxidation, several treatments directed against inflammatory targets had a neuroprotective effect [218-232]. These observations indicate a fundamental role of the neuroinflammatory system also in toxin-based models of PD.
Interesting and useful models to study inflammation are the ones obtained through administration of LPS, a pro-inflammatory component of the extracellular membrane of gram-negative bacteria [233].
Intra nigral or striatal LPS injections trigger progressive and specific SNpc dopaminergic neurodegeneration in rodents [234-237]. Some of these works indicated that ROS species produced during inflammation are the main detrimental factor in these models. In fact, inducible nitric oxide synthase (iNOs) or NADPH-oxidase inhibition partially rescues the neurodegeneration observed in these animals [235-237]. However, Castaño and colleagues did not find the same protective effect when inhibiting iNOs and suggested that other mechanisms might be involved[234].
When LPS is injected intraperitoneally (i.p.), it can induce a systemic inflammatory response that can activate microglial and astrocyte cells in the brain via TNFα signalling. The neuroinflammatory response was absent in mice depleted for TNFα receptors, indicating that this mediator is crucial for the glial activation observed in the brain [238]. Other studies showed that this acute inflammation could be converted to a chronic one, which induces progressive dopaminergic neurodegeneration [238-240]. Recently, Zhao and colleagues showed that chronic inflammation could depend on IL1β local expression since mice knocked out for this receptor did not develop chronic effects [241]. Other studies found that IL1β

expression after systemic LPS injection differs between brain regions [144, 145], suggesting that chronic inflammation could be differentially present in several brain regions.
La Vitola and colleagues found that transgenic mice for α-syn (A53T), but not C57BL6 mice, present dopaminergic neurodegeneration after systemic LPS exposure. Moreover, they observed different chronic responses between microglia and astrocytes in transgenic mice treated with LPS. While microglia presented a pro-inflammatory phenotype, astrocytes atrophied [242]. The same observation was done using another double hit model obtained through i.p. LPS injection coupled with intra-ventricular injection of α-syn oligomers [174].
Other studies observed other neuroinflammatory characteristics interesting for synucleinopathies. For example, chronic inflammation increases iron concentration and ferritin expression in microglial cells [243-246]. Ferritin is a chelator for iron, and its expression is under IRE that, as we mentioned before, is typical of a few other proteins, α-syn included [75, 80]. These data indicate that inflammation per se can induce an increase in iron levels in the brain but that these cells also have a role in the iron seizure, probably with homeostatic function. Moreover, Liu and colleagues identified significant gender differences, with female mice being more resistant to dopaminergic degeneration when injected systemically with LPS than male mice [239]. It seems that female mice could depress inflammation via estrogens inhibiting the Kir2.1 inward-rectifier potassium channel [247]. This channel is usually expressed in activated microglial cells, except in SNpr where it is also expressed in control condition [32]. Another study showed that when 16 months old mice were systematically treated with LPS, they presented higher neurodegeneration than those treated at 3 months old, indicating that inflammatory responses become stronger with aging [240]. Additionally, nicotine attenuates the neuroinflammatory response induced by LPS or other pro-inflammatory agents [248, 249]. All these features strongly link inflammation to Parkinson's disease and related disorders.

α-Synuclein PTMs induced by neuroinflammation

Several α-syn PTMs were linked with inflammation. Gao and colleagues found insoluble α-syn aggregates and nitrated α-syn in transgenic mice overexpressing (A53T) α-syn 5 months after systemic LPS injection. These insoluble α-syn aggregates and nitrated α-syn depended on inducible nitric oxide synthases (iNOs) activity [250]. Reimer and colleagues showed that inflammation-associated serine-threonine kinase (PKR, EIF2AK2) could phosphorylate α-syn at S129 *in vitro* and *in vivo* [251].
An increased interest is growing regarding the involvement of caspase-1 in α-syn processing [252-255]. It seems that it can induce α-syn truncation at 121 a.a., which consequently increase α-syn aggregation and cytotoxicity [252, 253]. Both the

α-syn truncation and caspase-1 were found in the core of LBs in human brains, suggesting their role in the early stages of LBs formation [252]. Caspase-1 is a critical NLRP3 component responsible for pro-IL1β cleavage to generate mature IL1β. Caspase-1 activation has been associated to the age-dependent α-syn aggregation in the gut-brain axis [256]. Reducing C-terminal truncation mediated by this caspase mitigates LBs pathology and neurodegeneration in a model of MSA [255]. These observations are in line with what we mentioned before about other PTMs. The inhibition of NLRP3 in animal models based on α-syn PFFs prevented nitration and pS129 α-syn [208].

An interesting study compared mice overexpressing human α-syn mutations with mice knocked out for α-syn after LPS intra-nigral injection. Mice ablated for α-syn were the only that did not present any dopaminergic neurodegeneration [257]. Taken together, these results suggest the presence of a vicious cycle between α-syn and inflammation, where each of these components is able to trigger and modulate the activity of the other. This could represent the pathological driving force for sustaining synucleinopathies over time.

Aim of the thesis

Neuroinflammation seems to be crucial for PD and related disorders. Several α-syn PTMs were found to be partially dependent by neuroinflammation, and may other exist. Moreover, it is still unclear whether and how inflammation have the same impact in all brain regions.
This thesis aimed to investigate the role of neuroinflammation in synucleinopathies in relation to microglial ability to process α-syn and the inflammatory system heterogeneity.

1. The first project focused on generating a microglial-like cell model that stably over-express α-syn (WT and mutated). We aimed to study α-syn PTMs generated in the intracellular environment of these cells and the following consequences in terms of aggregation and toxicity.

2. The second study aimed to establish a high-throughput screening system to investigate the mechanism involved in α-syn aggregation in HEK293T cells. We used this system to identify new pharmacological targets and explore their molecular mechanisms.

3. The third project aimed to explore whether and how microglial and astrocyte heterogeneity could lead to different inflammatory responses across brain regions. Moreover, we evaluated acute and chronic inflammatory effects in dopaminergic neurons in SNpc and investigated the CX3C axis as a possible pharmacological target.

4. The fourth study focused on whether LBs pathology and α-syn conformations differ within several brain regions of human post-mortem brains from patients affected by PD, DLB, and MSA.

Summary of key results

Paper I: Generation and characterization of α-synuclein expressing BV2 cells for studying α-synuclein aggregation and neuroinflammatory responses

The presence of chronic neuroinflammation since the early stages of PD and related disorders suggest that it can partially influence the course of these pathologies [182-187]. Several findings indicate that chronic inflammation has not only an effect on the surrounding neuronal populations but also on α-syn pathology. In fact, several PTMs identified seem partially depended on inflammation, and other may exist [252-255, 257]. In this project, we generated a microglial-like cell model that stably overexpresses α-syn to investigate these cells' ability to form PTMs and aggregates, and to understand whether an inflammatory condition can modulate this ability.

Generation and characterization of BV2 cells expressing α-syn

Through lentiviral transduction and FACS sorting, we generated several monoclonal BV2 cell lines that stably overexpress α-syn under the eukaryotic translation initiation factor 1 (eIF1α) promoter. We obtained several clones expressing various α-syn mutations (WT, A30P, G51D, A53T) with and without green fluorescent protein (GFP). To determine the more suitable clones for future examinations, we performed an initial characterization. We defined α-syn expression levels in each clone (Fig. 9A and B), and we examined whether α-syn overexpression could modify the inflammatory conditions (Fig. 9C and D). From these analyses, we found significantly Iba1 intensity changes only in 7 clones of 41 in total, and in most cases, they showed a decrease in this parameter. These observations suggested that α-syn expression in BV2 cells *per se* does not trigger a prominent inflammatory reaction.

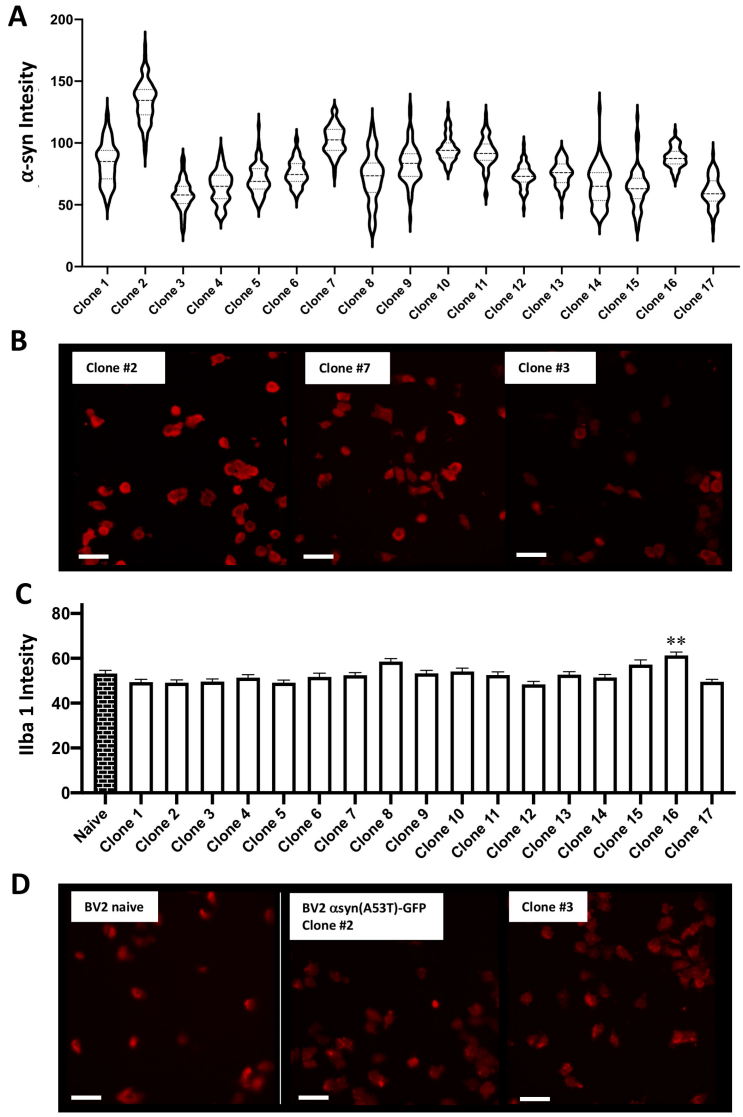

Figure 9. α-Syn (A53T)-GFP expression in BV2 cells does not alter the inflammatory baseline. A) α-Syn expression levels in α-syn A53T-GFP clones. One-way ANOVA with Tukey´s correction. F = 143,8; P value < 0,0001. Multiple comparisons are reported in supplementary statistical tables. **B)** Qualitative images, scale bars = 50 um. **C)** Iba1 quantification in same clones. One-way ANOVA with Tukey´s correction. F = 6,374; P value < 0,0001. Significance (*) respect naive BV2 cells. **D)** Qualitative images of Iba1 in BV2 cells. Scale bars = 50 um

Examination of α-syn aggregation in BV2 cells caused by α-syn PFFs and LPS administration

We aimed to investigate whether BV2 clones could develop aggregates when treated with α-syn PFFs and if the simultaneous exposure with LPS could modulate this process.

We treated BV2 clones expressing α-syn-A53T-GFP and GFP alone with several concentrations of α-syn PFFs (1, 5, 10, and 20 nM) with and without LPS (10 ug/ml) for 48 hours. We observed α-syn aggregates in BV2 cells expressing α-syn-A53T-GFP (up to 10% with 5, 10, and 20nM of α-syn PFFs; Fig. 10A and B). We did not detected differences in α-syn aggregation induced by the presence of LPS (Fig. 10A and B). However, this effect could be due to the presence of GFP that could prevent some PTMs, such as truncation in C-terminal. More experiments need to be performed with clones without GFP.

Then, we verified whether the aggregates observed in BV2 clones were positive for pS129 α-syn. We immune-stained cells with an antibody specifically against this PTM, and found that some pS129 α-syn profiles co-localized with the α-syn GFP signal (arrowheads) (Fig. 11A and C). We also found pS129 α-syn positive signal a surrounded by the GFP one, suggesting that some of the endogenous α-syn may be truncated between S129 and the C-terminal (Fig. 11C). Moreover, α-syn-GFP and pS129 α-syn positive signals also appeared extracellularly. This observation suggested that BV2 cells release these α-syn aggregates or that the aggregates induced BV2 cell death (Fig. 11B and C).

Assessing cell density, we found a significantly lower density in all BV2 clones in all the conditions investigated compared to relative vehicles treated cells (Fig. 11D). Moreover, the combination of α-syn PFFs and LPS induced a significant decrease in BV2 density compared to those treated with α-syn PFFs alone (Fig. 11D). Comparing BV2 expressing αsyn-A53T-GFP and GFP alone, we did not find any differences, suggesting that both clones were sensitive to α-syn PFFs and LPS (Fig. 11D).

Performing live imaging with identical conditions, we found that the formation of intracellular inclusions α-syn-GFP positive induced BV2 cell death (Fig. 12A).

To increase the efficiency of the aggregation, we performed liposome transfection with α-syn PFFs. By doing so, we facilitated α-syn PFFs entrance within the cells, skipping the internalization step, and synchronized the development of intracellular α-syn inclusions in BV2 cells. Twenty-four hours after treatments, we observed a significant number of cells (up to 60% of the total cells) containing α-syn-GFP inclusions at 2,5 nM, 5 nM, and 10nM α-syn PFFs, while 10% of BV2 cells with 1nM (Fig. 12B and E). Moreover, a significantly lower cell density was present between BV2 clones expressing α-syn-GFP administered with lipofectamine and α-syn PFFs (2,5 nM, 5 nM, and 10nM) and compared with the relative control (only lipofectamine) (Fig. 12C). In the end, comparing both BV2 clones, we observed significantly lower changes in BV2 expressing only GFP than those expressing α-syn-A53T-GFP (Fig. 12D).

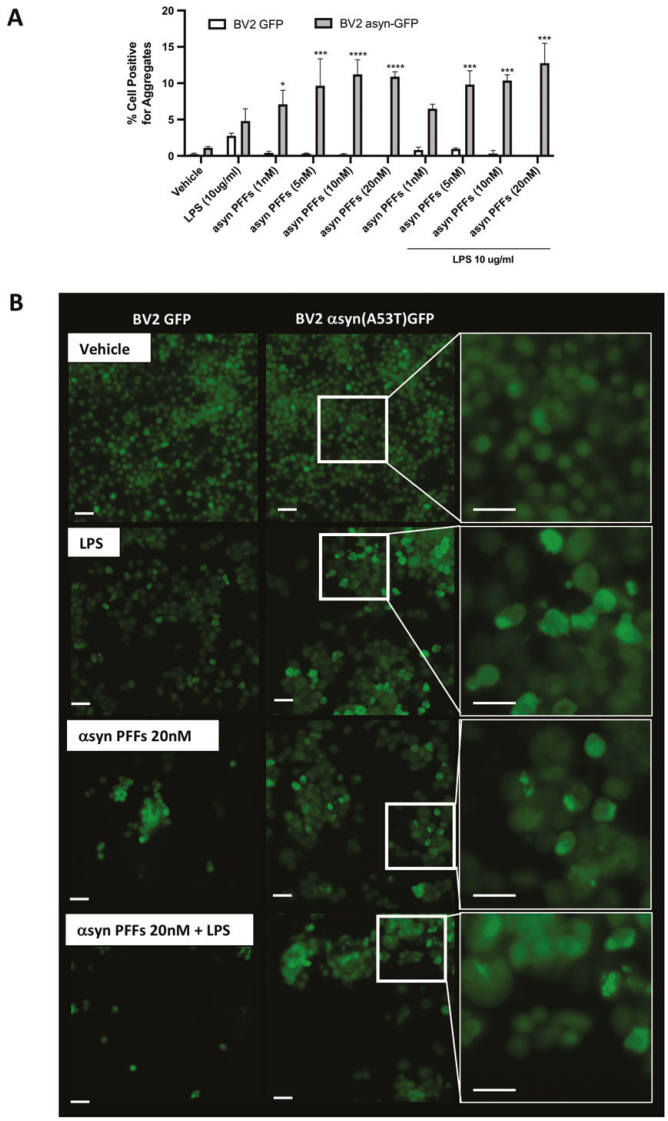

Figure 10. BV2 clones generate intracellular aggregates when exposed to α-syn PFFs. A) Intracellular inclusion in BV2 cells 48 hours after α-syn PFFs administrations in presence or absence of LPS. Statistic performed via two-way ANOVA $F_{treatments}$ (9, 20) =5,691, $p < 0{,}0006$. $F_{\alpha\text{-genotypes}}$ (1, 20) = 324,8, $p < 0{,}0001$. $F_{interactions}$ (9, 20) = 8,267, $p < 0{,}0001$. Significance (*) compared to respective vehicle. **B)** Representative images of BV2 clones administered with vehicle, LPS, and α-syn PFFs 20nM and with or without LPS after 48 hours. Scale bars = 50 um

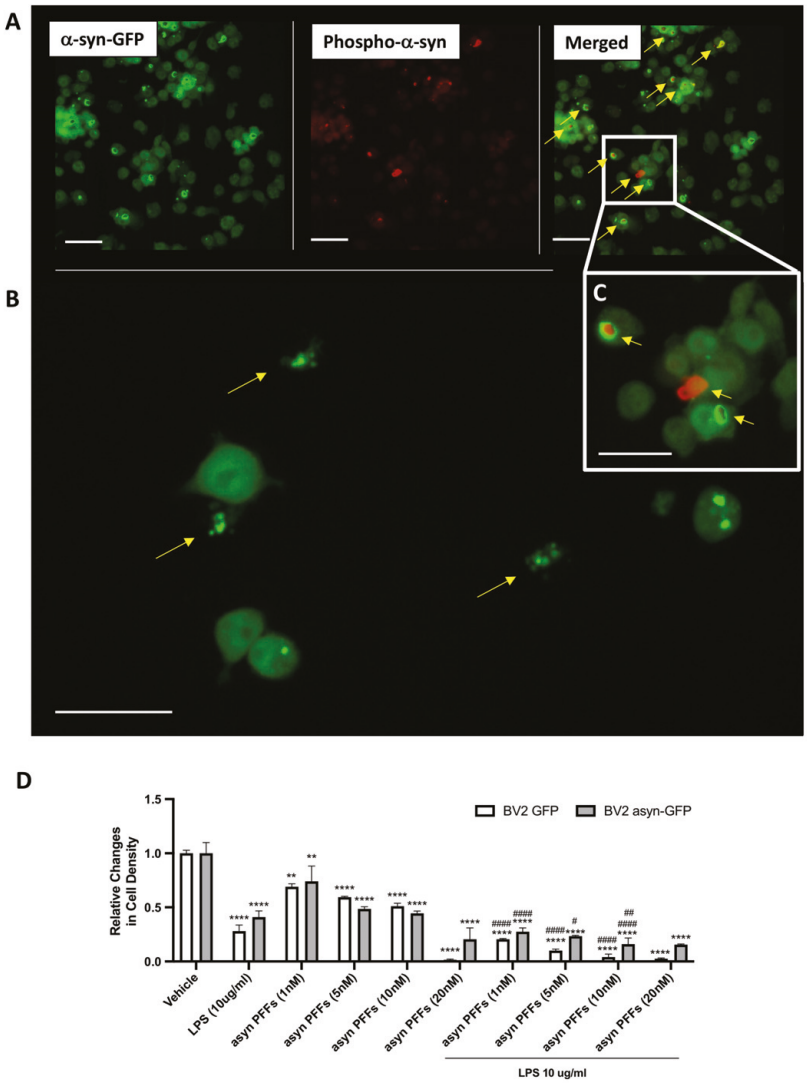

Figure 11. BV2 clones generate pS129 positive inclusion and release aggregates extracellularly. A) Representative images of BV2 cells expressing α-syn-A53T-GFP 48 hours post α -syn PFFs 10 nM administration. α-Syn-A53T-GFP (in green) and pS1299 α-syn (in red). Scale bars = 50 um **B and C)** Representative images of extracellular aggregates GFP-positive (yellow arrow) in the same previous conditions. Scale bars = 50 um **D)** Relative cell density changes 48 hours post α-syn PFFs administrations in presence or absence of LPS. Statistic performed using a two-way ANOVA $F_{treatments}(9, 20) = 131{,}1$, $p < 0{,}0001$. $F_{Genotypes}(1, 20) = 14{,}96$, $p < 0{,}0010$. $F_{Interactions}(9, 20) = 3{,}304$, $p < 0{,}0125$. Significance (*) respect relative control**,** (#) in presence or absence of LPS.

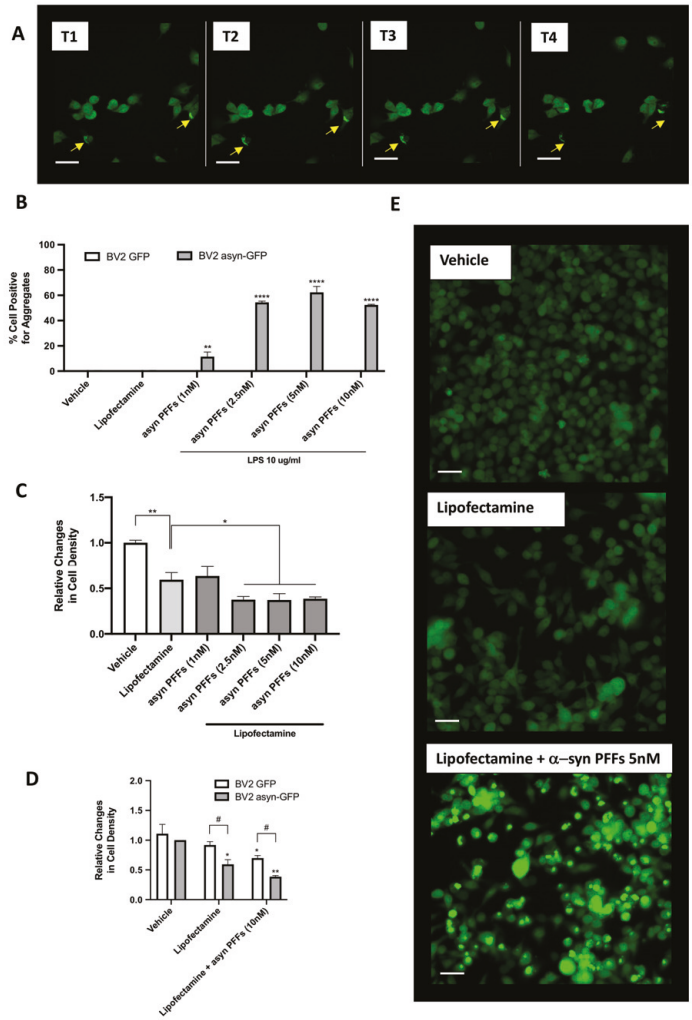

Figure 12. Intracellular aggregates toxicity and α-syn PFFs via lipofectamine transfection. A) Qualitative images extracted from live-imaging acquisitions of BV2 clones overexpressing α-syn-A53T-GFP and administered with α-syn PFFs 20nM. Every image shows the same frame at four sequential times (15 min between each frame). BV2 clones developed α-syn inclusion intracellularly and died subsequently, releasing extracellularly GFP-aggregates. Scale bars = 50 um **B)** Analyses of intracellular aggregates in BV2 clones 24 hours after lipo-transfection in presence or absence of α-syn PFFs (1, 2,5, 5, 10 nM). Statistic performed using a two-way ANOVA $F_{treatments}$ (5, 12) =275,5, $p < 0,0001$. $F_{genotypes}$ (1, 12) = 1773, $p < 0,0001$. $F_{Interactions}$ (5, 12) =275,5, $p < 0,0001$. Significance (*) respect relative control**. C)** Relative changes in cell density 24 hours post lipo- transfection in presence or absence of α-syn PFFs (1, 2,5, 5, 10 nM). Statistic performed using a one-

way ANOVA $F_{treatments}$ (5, 6) =29,17, p < 0,0004. Significance (*) respect BV2 overexpressing α-syn-A53T-GFP administered with lipofectamine**. D)** Relative changes in BV2 clone density 24 hours after lipo-transfection in presence or absence of α-syn PFFs (10 nM). Statistic performed using a two-way ANOVA $F_{treatments}$ (2, 6) = 44,53, p < 0,0003. $F_{genotypes}$ (1, 6) = 31,51, p < 0,0014. $F_{Interactions}$ (5, 12) = 2,475, p < 0,1645. Significance (*) respect relative control, (#) between BV2 cells overexpressing α-syn-A53T-GFP or GFP with the identical treatments. **E)** Qualitative images of BV2 cells administered with the vehicle, lipofectamine 0,5 ul/well, and the combination between lipofectamine and α-syn PFFs 5nM for 24 hours. Scale bars = 50 um

BV2 cells expressing α-syn-GFP release and uptake vesicles

Another interesting feature regarding microglial cells is the release and uptake of vesicles and their possible role in α-syn spreading. We conducted live-imaging acquisitions of BV2 α-syn-A53T-GFP clones in control conditions along 24 hours. We detected vesicles moving in the extracellular media and released/taken up by BV2 cells (Fig. 13A). This finding indicate that these vesicles can carry α-syn protein, since they were positive for GFP signal.

To evaluate whether BV2 vesicles can be exchanged between different kind of cells, we conducted a co-culture between BV2 α-syn-A53T-GFP and HEK α-syn-A53T-mCherry cells. We found that the vesicles could easily be exchanged between them (Fig. 13B). Further investigations have to be executed to assure that these vesicles can carry α-syn and to detect possible aggregates species.

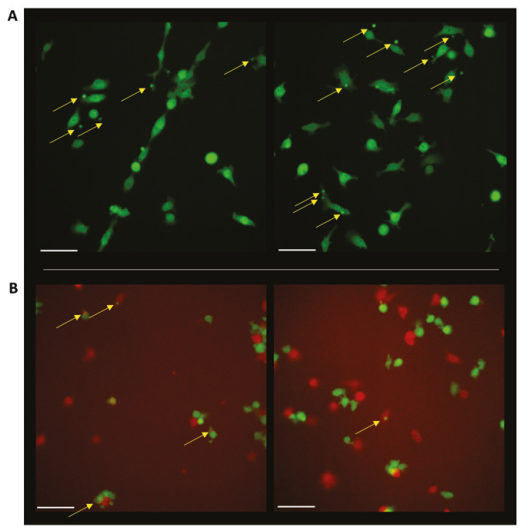

Figure 13. BV2 clones release and uptake vesicles.

A) Representative images of BV2 clone vesicles extrapolated from live-cell imaging. Vesicles are indicated by the. Scale bars = 50 um **B)** Co-cultures between BV2 cells overexpressing α-syn-A53T-GFP with HEK cells overexpressing α-syn-A53T-mCherry. Scale bars = 50 um

Paper II: FRET-based screening identifies p38 MAPK and PKC inhibition as targets for the prevention of seeded α-synuclein aggregation.

Although there has been considerable progress in knowledge regarding α-syn aggregation, much is still unknown regarding key molecular events. The identification of molecular mediators could form the basis for new therapeutic interventions. A possible way to identify new targets can be obtained through high-throughput screening (HTS) of annotated compound libraries.

Generation and validation of FRET-based reporter and kinases inhibitor library screening.

In this work, we developed a fluorescent resonance energy transfer (FRET)-based cellular reporter in HEK293T cells. FRET is suitable for HTS due to the specificity of the signal and the ease of automatization using flow cytometry [258]. Our system showed concentration-dependent sensitivity down to 90 ng/ml and 300 ng/ml, respectively, for liposome-mediated transfection and direct addiction to α-syn PFFs (Fig. 14A and B). These intracellular aggregates were confirmed by pS129 positivity, the presence of detergent-insoluble α-syn, and cross beta-sheet-structures stained with congo red (Fig. 14C - G).

Using this model, we explored possible molecular targets affecting α-syn aggregation. We screened small molecule kinases inhibitors and found three inhibitors (GF; SB80; SB90) of 81 tested, which prevented induced α-syn aggregation (Fig. 15A and B). Two of these molecules were linked to p38 mitogen-activated protein kinase (p38 MAPK) and the last to protein kinase C (PKC).

Then, we investigate their potential as pharmacological targets. We benchmarked our lead compounds with two compounds (Enza and Vx) which were previously involved in clinical trials for other conditions and had an overlapping target with our lead compounds. We found all three of our molecules and Enza exhibited preventative effects on the induced α-syn aggregation as assessed by microscopy and flow cytometry (Fig. 15C and D). Interestingly, Vx showed a comparable aggregation with the control condition (Fig. 15C and D).

Effects of hit compounds on phospho-proteome

Mass spectrometry (MS)-based phospho-proteomics is an interesting methodology for investigating kinases activity and signaling. Aiming to explore the signaling involved in our selected inhibitors, we found a discrete and unique phosphor proteome profile for each. However, comparing the global phosphor-proteome, similarities among inhibitors with the same target were evident according to the inter-sample Pearson's correlation coefficient (PCC) (Fig.16A and B).

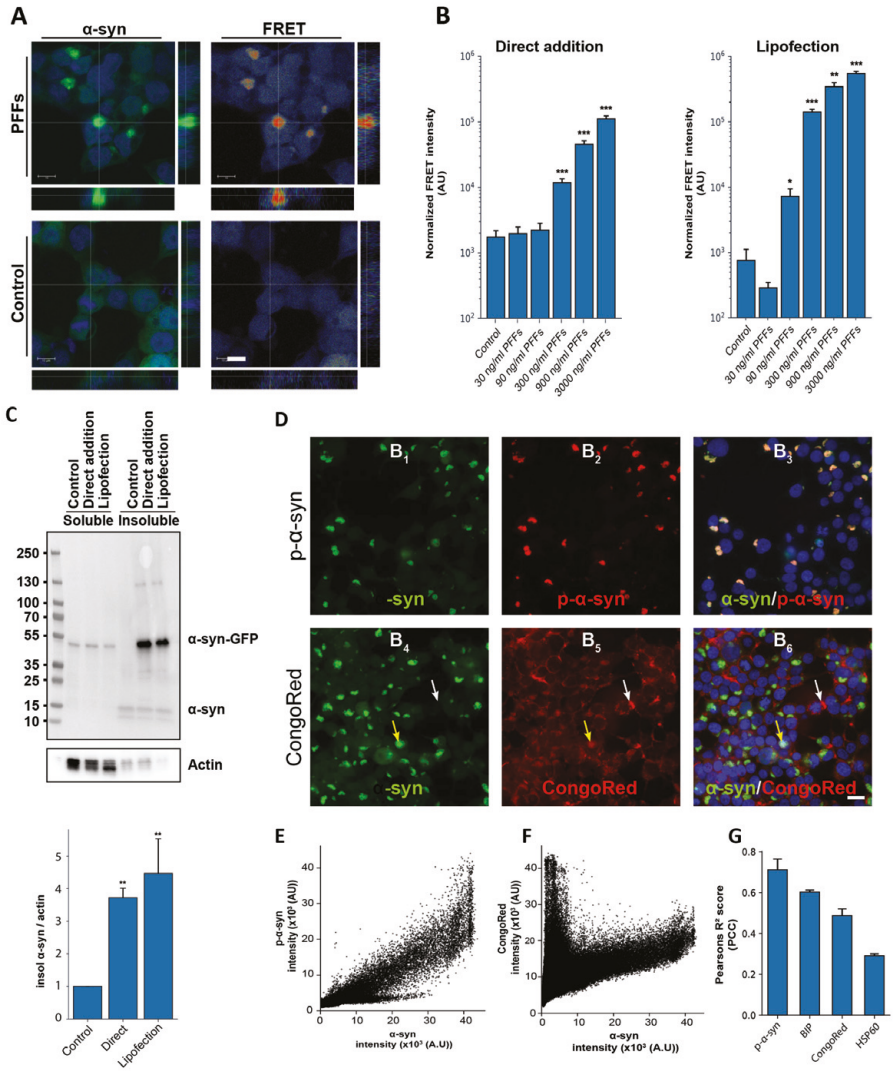

Figure 14. Validation of a FRET-based cell reporter for α-syn aggregation.

A) FRET signal validation for inducing aggregation in the cell line. Cells with aggregates showed a strong co-localized FRET signal. **B)** Assessment of biosensor sensitivity after α-syn PFFs treatment. **C)** Both treatment with PFFs directly and by lipofection leads to α-syn aggregates as seen by α-synuclein detection in the insoluble phase. **D)** Co-localization analysis of generated α-synuclein aggregates. GFP positive aggregates co-stain for pS129 α-syn and the cross-β specific dye CongoRed. (scale bar = 20 μm) **E)** Scatterplot for co-localization between α-syn-GFP and pS129 α-syn. F) Scatterplot for co-localization between α-syn-GFP and CongoRed. **G)** PCC correlation between α-syn-GFP and the relative

markers. Bar chart show mean ± SD, *p < 0.05, **p < 0.005, ***p < 0.001. One-way ANOVA for multiple comparisons to a control group.

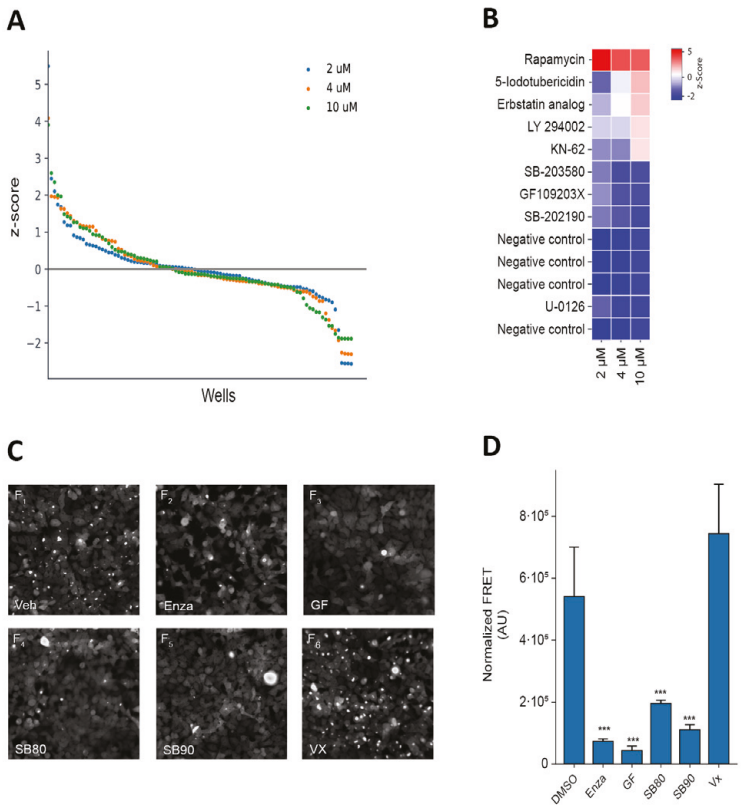

Figure 15. Kinase inhibitor libary screening for the ability to interfere with α-syn aggregation. A) Results from screening a kinase inhibitor library. Z-scores were calculated for each sample, and the resulting output follows a waterfall distribution with similar shapes across concentrations. **B)** Sample´s heatmap with Z-scores >1.5 or <-1.5. **C)** Representative images of cell clones treated with inhibitors and α-synuclein PFFs. (Scale bar = 20 µm) **D)** Inhibitor effects quantification by flow cytometry. Bar charts show mean ± SD, ***p < 0.001. One-way ANOVA with Dunnett's T3 post hoc test for multiple comparisons to a control group.

Further in-depth analyses allowed us to find pathways regulated by our inhibitor treatment. We found the main enrichment/depletion signatures among RNA transport and spliceosome pathways by comparing the annotated KEGG pathway database (Fig. 16C) [259]. These changes suggest that the effects caused by the inhibitors may lie at the translational level.

We also performed proteomic analysis to examine if any changes were present at the protein level. We assessed protein abundance after compound treatment. As we observed for the phospho-proteomic analyses, we found distinct profiles and grouped compounds of similar targets (Fig. 17A and B). Conducting KEGG pathway analyses with the proteome data, we found a depletion of protein related to neurodegeneration pathways, such as the one involved in PD, Alzheimer's disease, and Huntington's disease. This depletion depends mainly on a decrease in mitochondrial proteins such as CYC, NDUF, and COX, which are shared among the annotated pathways (Fig.17C).

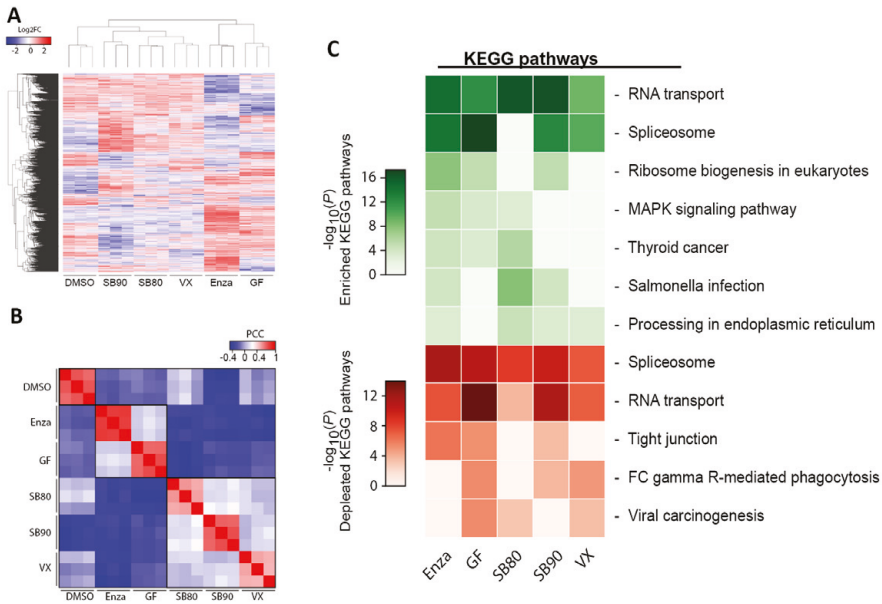

Figure 16. Phopho-proteome analyses for the kinase inhibitors identified.
A) Distinct patterns for each inhibitor are revealed through unsupervised clustering of the significantly regulated phosphor-proteome. **B)** Pearson's correlation matrix reveals sample similarity among replicates and inhibitors with the same target. **C)** Pathway analysis indicated that spliceosome and RNA transport is the most enriched and depleted pathways in terms of phosphor-epitopes.

<u>Examination of mechanisms implicated in prevention of induced α-syn aggregation.</u>
The depletion in genes mapping these pathways contributed to the prevention of aggregation, except for SB80, despite its anti-aggregation effects. Moreover, we observed an enrichment in lysosomal-related proteins for all our compounds, except for Vx.
Lysosomes are membrane-bound cell organelles containing digestive enzymes able to break down cellular components and preserve homeostasis. Our analyses detected

several lysosome-related proteins. Therefore, we quantified the relative abundance of lysosomes via live-cell microscopy and flow cytometry using Lyso Tracker. We

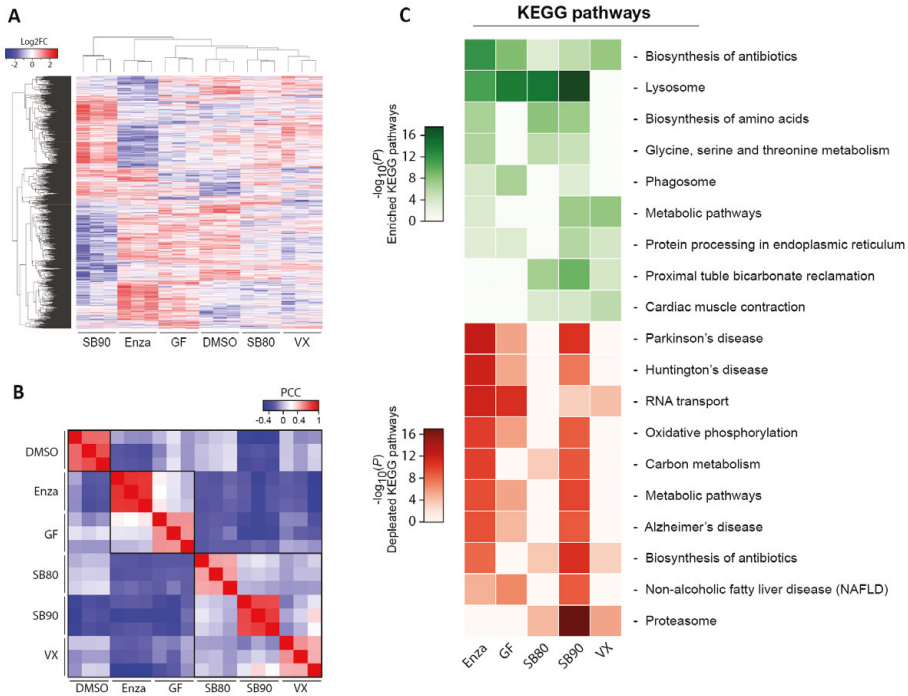

Figure 17. Proteome analyses for the kinase inhibitors identified.
A) Distinct patterns for each inhibitor are revealed through unsupervised clustering of the significantly regulated phosphor-proteome. **B)** Pearson's correlation matrix indicates sample similarity among replicates and inhibitors with the same target. **C)** KEGG pathway analysis exhibits an enrichment in lysosome-related proteins.

found that lysosomal abundance increased following GF, SB90, and Enza treatment but not after SB80 and Vx (Fig. 18A and B). However, further quantification of transcription factor EB (TFEB) [260], the master regulator of lysosomal biogenesis, showed no significant difference for all inhibitors tested (Fig. 18C and D). The lack of TFEB translocation within the nucleus indicated that the increased lysosomes observed did not depend on a new expression of these organelles but derived from other steps of lysosomal maturation.
FITC-dextran was used to investigate the rate of endocytic uptake [261]. Using this tool, we observed a significant decrease in FITC-dextran internalization for GF, SB80, and Vx but not for SB90 and Enza (Fig. 18E and F). The decrease induced by Vx without any protective effects on α-syn aggregation suggested that the

decrease in endocytoses would not explain the protection observed by our hit compounds.
Subsequently, we explored the effects on vesicular permeabilization using a galectin-3 reporter cell line [261]. We observed a significant reduction for all inhibitors, except for Vx, indicating a lower vesicular permeabilization (Fig.18G).

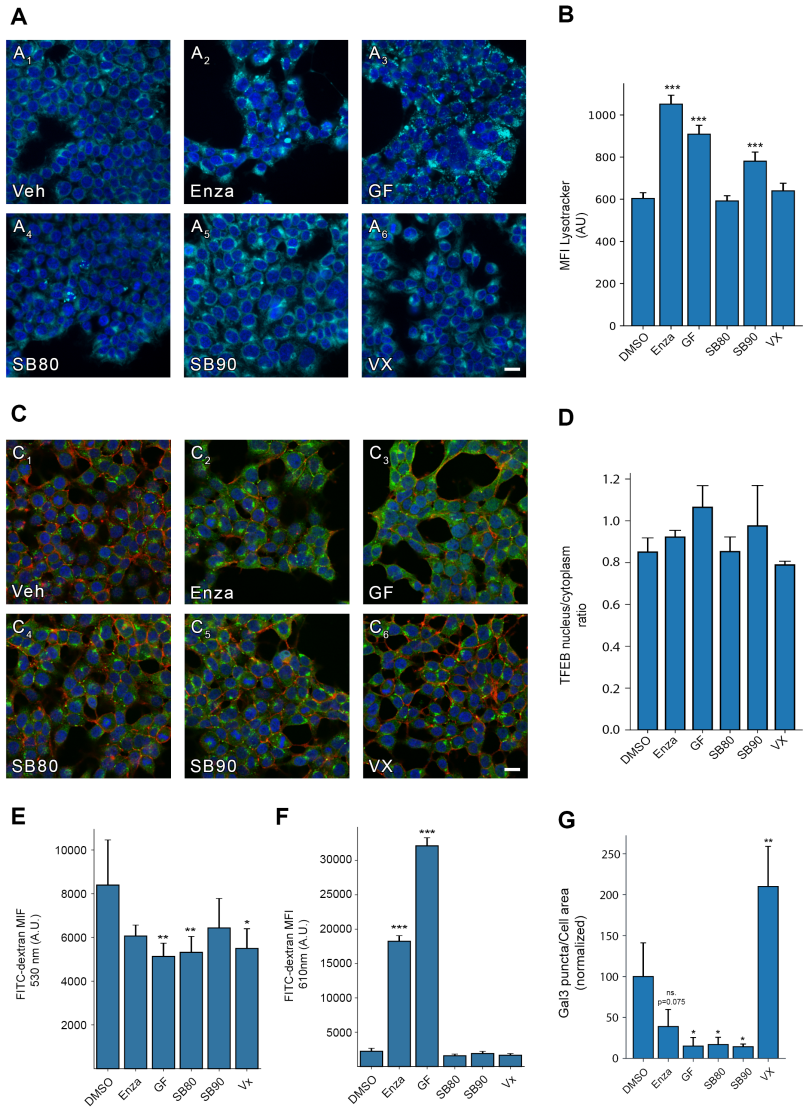

Figure 18. Investigation of mechanisms involved in the inhibition of α-syn aggregation observed by kinase inhibitors A) Representative images of lysotracker in samples treated with inhibitors. **B)** Flow cytometry quantification of lysotracker staining. **C)**

Representative images of nuclear translocation of Transcription Factor EB (TFEB). **D)** Quantification of nuclear translocation of TFEB. **E and F)** Intracellular FITC-dextran quantification by flow cytometry. **E)** at 530 nm; **D)** at 610nm. **G)** Quantification of vesicular permeabilization using a Gal3-GFP model. Bar chart values show MFI ± SD, *$p < 0.05$, **$p < 0.005$, ***$p < 0.001$. One-way ANOVA for multiple comparisons to a control group. (Scale bar = 20 μm).

Paper III**:** Brain region-specific microglial and astrocytic activation in response to systemic LPS exposure

Several studies indicate that microglial and astrocyte populations are heterogeneous among different brain regions in their density, morphology, and transcriptomes [31, 32, 144, 146]. However, whether and how these differences could lead to distinct inflammatory responses is not clear. Microglial or astrocyte phenotypes and responses could potentially direct the course of several neurodegenerative diseases, including synucleinopathies.
In this study, we conducted a topographic study quantifying microglia and astrocyte alterations in 16 brain regions through immunohistochemical examination and computational image analysis. To have a uniform and simultaneous stimulation, we used a systemic LPS mouse model obtained by a single i.p injection. We investigated microglial and astrocytic responses, the impact on the dopaminergic neuronal population in SN, and the possible pharmacological role of the CX3C axis.

Microglia heterogeneity in control C57BL6 mice.
We began evaluating microglia cells in C57BL6 control mice. SNpr appeared as the brain region having the most elevated marked area by Iba1 compared to other brain regions (Fig. 19A and C). On the contrary, the VTA, SNpc, hypothalamus, thalamus, cerebellum, and corpus callosum were the lowest. The other regions presented a similar microglia-marked areas. We found a similar condition when we analysed the cell density (Fig. 19B and C).

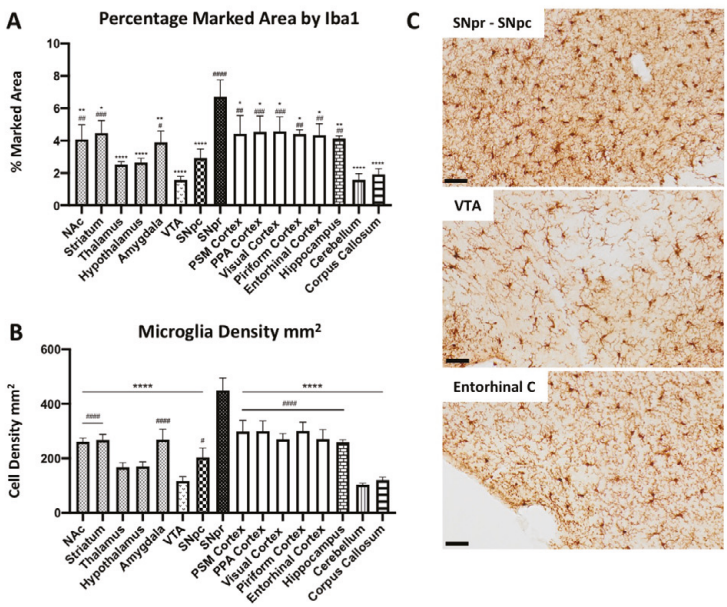

Figure 19. Microglia heterogeneity in control C57BL6 mice.

A) Quantification of the marked area by microglial cells in vehicles C57BL6N mice. Statistic performed using One-way ANOVA: $F_{BrainRegions}$ (15, 32) = 12.06, $p < 0.0001$. n = 3 mice per region. Significance: (*) respect SNpr; (#) respect VTA. Other significances are summarized in Supplementary Methods. **B)** Quantification of microglial cell density per mm^2. Statistic performed using One-way ANOVA: $F_{BrainRegions}$ (15, 32) = 29.35, $p < 0.0001$. n = 3 mice per region. Significance: (*) respect SNpr; (#) respect VTA. Other significances are summarized in Supplementary Methods. **C)** Qualitative images of Iba 1 staining. Scale bar = 50 um.

Brain region-specific microglia responses to systemic LPS administration.

To explore whether microglia populations in different brain regions could present differential inflammatory responses, we first compared microglia activation in mice administrated systematically with either 5 mg/kg LPS or vehicle (PBS).

We found a significant increase in the marked area by the Iba1 and cell density in all brain regions upon LPS exposure (Fig. 20A, B and E). Microglial population in SNpr and entorhinal cortex revealed the most robust Iba1 increase, while in the VTA, cerebellum, and corpus callosum showed the lowest. Investigating the fold changes between LPS-treated and vehicle group, we detected a 2-3-fold increase in microglia marked area and comparable changes in microglia density (Fig. 20C, D and E). Microglial cells in VTA showed the most robust increase in the marked area, while the lowest were in the PSM cortex. Regarding fold changes in microglia density, the most significant changes were observed in the entorhinal cortex, VTA, and SNpc, while the least altered were in the PSM cortex and SNpr.

Lastly, we conducted a semi-quantitative analysis of CD68 changes under LPS exposure. We detected a general increase in all regions. However, the most pronounced change occurred in the SNpr (data not showed). These findings suggest the presence of different microglial responses to systemic LPS administration among several brain regions.

Brain regional specific microglia inflammation induced by several LPS doses.

To investigate whether microglia heterogeneity also influences the sensitivity to a pro-inflammatory agent, we conducted a dose-dependent injection of LPS (from 0.005, 0.05, 0.5 to 5 mg/kg) and PBS as the vehicle control. Microglia changes were examined 24 hours after LPS administration.

We observed that the area marked by microglial cells and cell density significantly increased at 5 mg/kg LPS in most brain regions (such as the thalamus, striatum, VTA, PSM cortex, PPA cortex, hippocampus, and corpus callosum) . In the SNpr, entorhinal cortex, NAc, and hypothalamus, Iba1 area marked and cell density increased from 0,05 mg/kg LPS dose, while the other regions at 0,5 mg/kg LPS dose **(Fig. 21A, B and E)**. Considering the relative changes, microglia populations in the hypothalamus, entorhinal cortex, VTA, and cerebellum presented significant alterations in the marked area and cell density at low doses **(Fig. 21C, D and**

E). Then, we semi-quantitatively compared the CD68 modifications in the hypothalamus, SNpr, and entorhinal cortex. We detected evident changes in the SNpr at 0.05 mg/kg dose (Fig. 22A, B and C)**.**

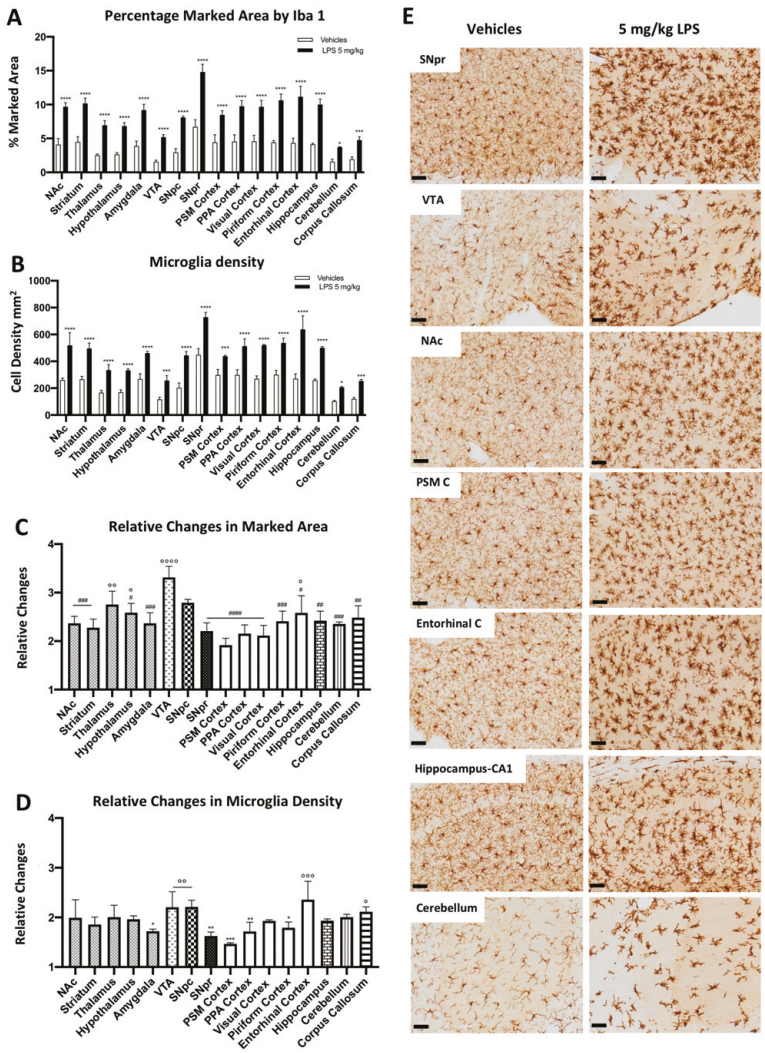

Figure 20. Heterogeneous inflammatory response after systemic injection of 5mg/kg LPS. A) Quantification of the percentage of the marked area by microglial cells in vehicles (white columns) and LPS-treated mice (black columns). Statistic performed using a two-way ANOVA $F_{BrainRegions}$ (15, 64) = 46.13, $p < 0.0001$. $F_{Treatment}$ (1, 64) = 1127, $p < 0.0001$. $F_{Interaction}$ (15, 64) = 6.081, $p < 0.0001$. n = 3 mice per region. Significance: (*) respect relative vehicles. **B)** Quantification of microglial cell density per mm^2 in vehicles (white columns) and LPS-treated mice (black columns). Statistic performed using a two-way ANOVA $F_{BrainRegions}$ (15, 64) = 56.84, $p < 0.0001$. $F_{Treatment}$ (15, 64) = 786.7, $p < 0.0001$. $F_{Interaction}$ (15,

64) = 5.138, $p < 0.0001$. n = 3 mice per region. Significance: (*) respect relative vehicles. **C)** Fold changes in the percentage of the marked area by microglial cells between LPS-treated and vehicle-treated mice. Statistic performed using a one-way ANOVA $F_{BrainRegions}$ (15, 32) = 7.453, $p < 0.0001$. n = 3 mice per region. Significance: (#) respect VTA; (◦) respect PSM cortex. Other significances are summarized in the supplementary results. **D)** Fold changes in cell density between LPS-treated and vehicle-treated mice. Statistic performed using a one-way ANOVA $F_{BrainRegions}$ (15, 32) = 4.890, $p < 0.0001$. n = 3 mice per region. Significance: (*) respect the Entorhinal cortex; (◦) respect the PSM cortex. Other significances are summarized in supplementary results. **E)** Qualitative Iba 1 staining images in SNpr, VTA, NAc, PSM cortex, entorhinal cortex, hippocampus (CA1), and cerebellum. Scale bar = 50 um.

In the end, we examined the vessel distribution to verify that the difference in sensitivity was independent of TNFα / LPS diffusion within the brain. We found more vessels in the thalamus, cerebellum, PSM, PPA, and visual cortices, indicating that our data does not depend by different TNFα / LPS diffusion (Fig. 22D and E).

Brain region-specific chronic inflammation 30 days after LPS treatment.

Another interesting feature of inflammation is the ability to maintain a pro-inflammatory phenotype chronically. However, whether chronic neuroinflammation is distributed uniformly within the brain is still unclear.

To investigate this, we systematically administered mice with 5 mg/kg LPS and vehicle and sacrificed them 30 days after treatment. We detect a slight increase in the microglial density and area marked in some brain regions, such as the amygdala, SNpr, PSM cortex, and the piriform cortex (Fig. 23A, B and C). These data suggest sustainable microglia activation in selected brain regions one month after LPS administration.

Specific and transient synaptic alterations due to neuroinflammation in SNpr.

The peculiar microglial histology in SNpr, together with our data, brought us to examine the consequences of neuronal profiles in this specific region. We conducted a double immune-labeling for tyrosine hydroxylase (TH), the key enzyme for dopamine synthesis, and Iba1. We found that the dopaminergic dendrites from the SNpc are intermingled with microglial branches in SNpr, indicating possible interactions (Fig. 24A and B). Quantitative confocal examinations revealed the density of the dopaminergic dendrites decreased significantly in medial SNpr in mice treated with 5 mg/kg LPS compared to the vehicle mice 24 hours post injection (Fig. 24C and E). Interestingly, this decrease was no more evident 30 days post LPS administration (data not showed). Quantitative analyses of gephyrin, a marker for GABAergic synapses, indicated no alteration in all conditions examined (Fig. 24D). These findings suggest that the acute inflammatory response generated by LPS leads to specific and reversible alterations of dopaminergic dendrites in SNpr.

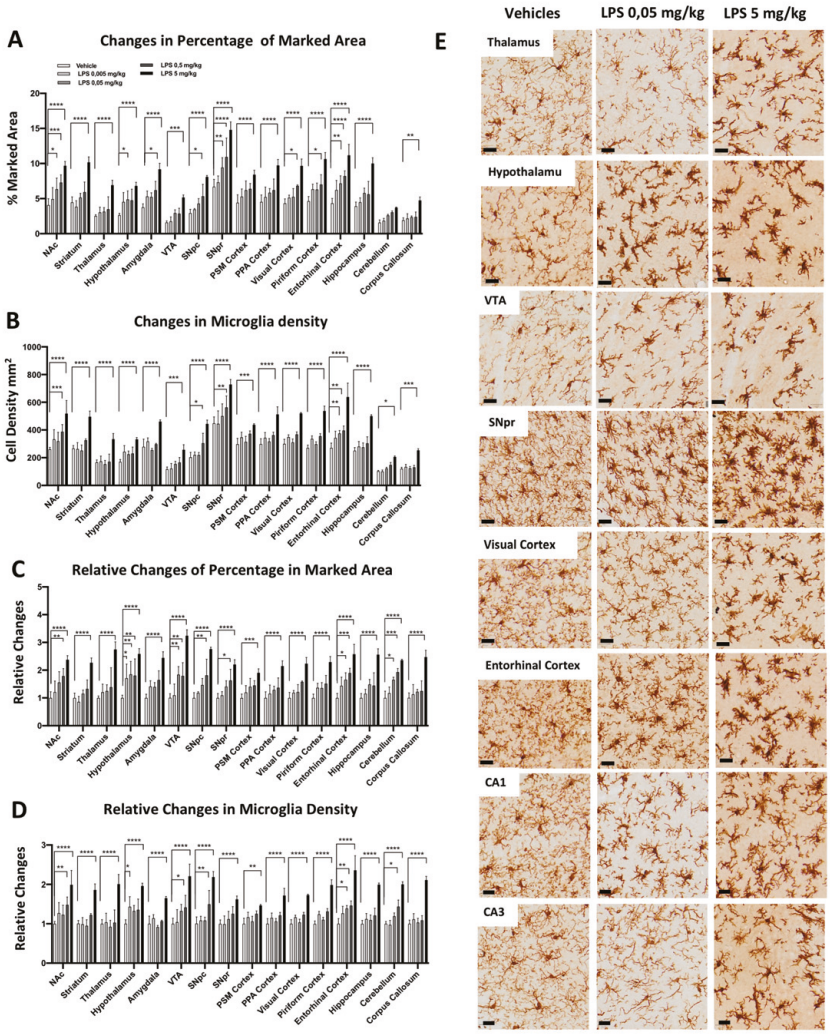

Figure 21. Region-specific inflammatory susceptibility to different LPS doses.

A) Quantification of percentage of the marked area by microglial cells in vehicles (white columns), LPS treated mice with 0.005 mg/kg (clear gray columns), 0.05 mg/kg (medium gray columns), 0.5 mg/kg (dark gray columns), 5 mg/kg (black columns). Statistics were performed using a two-way ANOVA with Tukey correction. $F_{BrainRegions}$ (15, 160) = 57.94, $p < 0.0001$. $F_{Treatment}$ (4, 160) = 188.3, $p < 0.0001$. $F_{Interaction}$ (60, 160) = 1.599, $p < 0.0110$. n = 3 mice per region. Significances are respecting relative vehicles. **B)** Quantification of cell density mm^2. Same column color as panel (A). Statistics were performed using a two-way ANOVA with Tukey correction. $F_{BrainRegions}$ (15, 160) = 112.7, $p < 0.0001$. $F_{Treatment}$ (4, 160) = 222.1, $p < 0.0001$. $F_{Interaction}$ (60, 160) = 2.039, $p < 0.0002$. n = 3 mice per region. Significance: (*) Significance is respecting relative vehicles. **C)** Fold changes in the percentage of the area marked by microglial cells. Same column color as panel (A). Statistic

performed using a two-way ANOVA with Tukey correction. $F_{BrainRegions}$ (15, 160) = 4.169, $p < 0.0001$. $F_{Treatment}$ (4, 160) = 202.4, $p < 0.0001$. $F_{Interaction}$ (60, 160) = 1.259, $p < 0.1304$. n = 3 mice per region. Significance: (*) respect relative vehicles. **D)** Fold changes in cell density. Same column color as panel (A). Statistics were performed using a two-way ANOVA with Tukey correction. $F_{BrainRegions}$ (15, 160) = 5.660, $p < 0.0001$. $F_{Treatment}$ (4, 160) = 247.6, $p < 0.0001$. $F_{Interaction}$ (60, 160) = 1.848, $p < 0.0013$. n = 3 mice per region. Significance: (*) respect relative vehicles. **E)** Qualitative images of Iba 1 staining in Veh, 0.05, and 5 mg/kg LPS doses. Scale bars = 50 um.

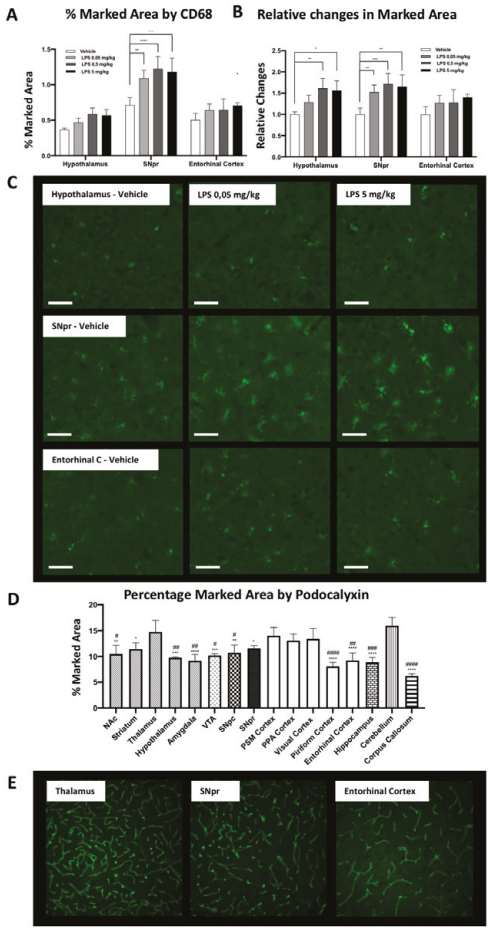

Figure 22. Region-specific CD68 alterations and vessel distribution.
A) Quantification of the percentage marked area by CD68 immunoreactivity in vehicles (white columns), LPS treated mice with 0,05 mg/kg (medium grey columns), 0,5 mg/kg (dark grey columns), 5 mg/kg (black columns). Statistics were performed using a two-way ANOVA with Tukey correction. $F_{Brain\ Regions}$ (2, 24) = 79,43, $p < 0,0001$. $F_{Treatment}$ (3, 24) = 13,26, $p < 0,0001$. $F_{Interaction}$ (6, 24) =1,787, $p < 0,1443$. n=3 mice per region. Significances are respecting relative vehicles. B) Fold changes in CD68 marked areas between the vehicle-

and different doses of LPS (0.05-5mg/kg) treatments in different brain regions. The same column color as graph A). Statistics were performed using a two-way ANOVA with Tukey correction. $F_{Brain\ Regions}$ (2, 24) =4,131, p < 0,0001. $F_{Treatment}$ (3, 24) =14,11, p < 0,0287. $F_{Interaction}$ (6, 24) = 0,8165, p < 0,5678. n=3 mice per region. Significance: (*) respect relative vehicles. **C)** Qualitative images of CD68 staining in the dose-dependent treatment. Scale bars = 20 um **D)** Quantification of the percentage of the marked area by podocalyxin in vehicles C57BL6N mice. Statistic performed using a one-way ANOVA $F_{Brain\ Regions}$ (15, 32) =11,69, p < 0,0001. n=3 mice per region. Significance: (*) respect the cerebellum; (#) respect the thalamus. Other significances are summarized in supplementary results. **E)** Representative images of podocalyxin staining.

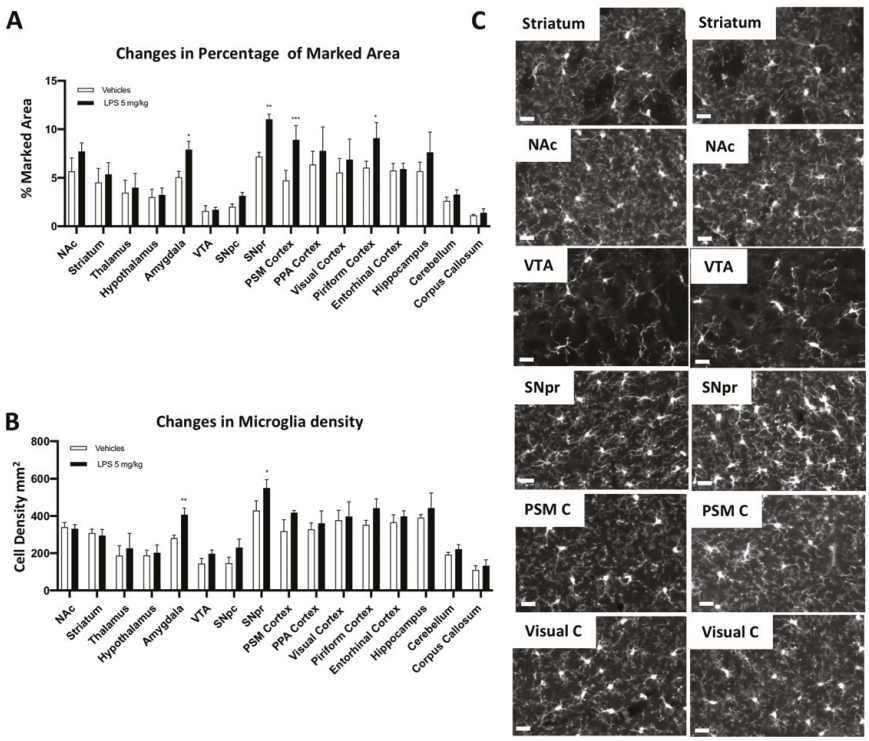

Figure 23. Brain regional chronic inflammatory response 30 day after LPS administration. A) Quantification of the percentage of the marked area by microglial cells in vehicles (white columns) and LPS-treated mice (black columns) 30 days post-administration. Statistic performed using a two-way ANOVA $F_{BrainRegions}$ (15, 64) = 25.33, p < 0.0001; $F_{Treatment}$ (1, 64) = 44.38, p < 0.0001. $F_{Interaction}$ (15, 64) = 2.069, p < 0.0233; n = 3 mice per region. Significance: (*) respect relative vehicles. **B)** Quantification of cell density mm^2 in vehicles (white columns) and LPS-treated mice 30 days post-administration (black columns). Satistic performed using a two-way ANOVA $F_{BrainRegions}$ (15, 64) = 37.93, p < 0.0001; $F_{Treatment}$ (1, 64) = 32.59, p < 0.0001; $F_{Interaction}$ (15, 64) = 1.517, p < 0.1259; n = 3 mice per region. Significance: (*) respect relative vehicles. (C) Qualitative images of Iba 1 staining. Scalebar = 50 um.

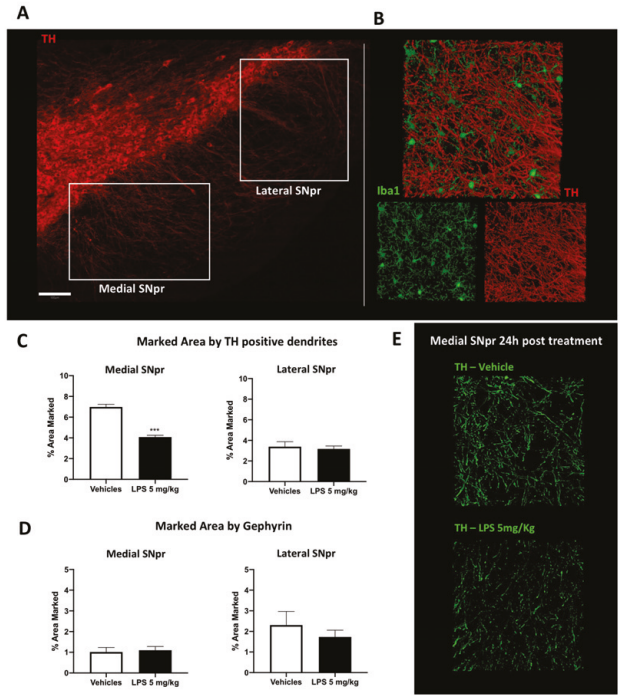

Figure 24. Dopaminergic dendritic loss in medial SNpr 24 hours after 5mg/kg LPS administration. A) Representative images of TH staining in the SNpc. Scale bar = 100 um **B)** Qualitative confocal images of dopaminergic (TH^+) dendrites (red) and microglial cells in SNpr (green). **C)** Quantification of the percentage of the marked area by TH dendrites in medial and lateral SNpr 24 h after 5 mg/kg LPS or vehicle administration. Statistics were performed using an Unpaired t-test: Medial SNpr: $F_{Treatment}$ 2.250, $p < 0.0007$. Lateral SNpr: $F_{Treatment}$ 2.842, $p < 0.7245$. **D)** Quantification of the percentage of the marked area by Gephyrin in medial and lateral SNpr 24 h after 5 mg/kg LPS or vehicle administration. Statistics were performed using an Unpaired t-test. Medial SNpr: $F_{Treatment}$ 1.469, $p < 0.7793$. Lateral SNpr: $F_{Treatment}$ 4.027, $p < 0.4810$. E) Representative confocal images of TH+ dendrites in medial SNpr 24 h after treatment.

<u>CX3CR1 partial ablation decreased microglia inflammation and prevented the chronic one.</u>

CX3C axis was widely studied in various models of neurodegenerative diseases, and it seems that an increase of its ligand or a decrease of its receptor could have anti-inflammatory effects. However, contrasting data were obtained regarding the total ablated mice for CX3C receptor 1 and systemic LPS models. Here, we examined microglia changes in CX3CR1 partially ablated mice ($CX3CR1^{+/GFP}$).

We first compared $CX3CR1^{+/GFP}$ with C57BL6 in the control condition. We did not observe any alteration in microglial population (Fig. 25A). Then, comparing relative

changes between 5 mg/kg LPS- and vehicle-treated groups in both mice models, we observed a significant reduction in activation across all regions in mice partially ablated by CX3CR1 compared with C57BL6 (Fig. 25B, C and E). These data indicate that partial ablation of this receptor reduce microglia activation induced by TNFα / LPS .
Recently, a study examined the chronic LPS effects in C57BL6 mice, comparing 1 and 5 mg/kg doses. They showed that only the higher dose presented chronic microglial activation [241]. Here, we examined whether the lower microglia activation detected in CX3CR1$^{+/GFP}$ mice 24 hours post systemic LPS injection can be maintained for a long time. Thirty days post LPS treatment, we did not detect any microglia alteration compared with vehicle-control mice (data not shown). These findings suggest that CX3CR1 partial ablation decreased sensitivity to microglia activation and sustainability in response to systemic LPS administration.

Brain region-specific astrocytes activation in response to systemic LPS administration.

In the end, we also explored astrocytic heterogeneity using the glial fibrillary acid protein (GFAP) as a marker. Although this marker is the most common used in the field, its expression is highly heterogenous between different brain regions. For this reason, we need to be aware that the following analyses could be influenced by this heterogeneity.
We started investigating the marked area by GFAP in C57BL6 mice in the vehicle condition. SNpr, hippocampus, and corpus callosum showed a significantly higher density of GFAP positive cells (Fig. 26A). Moreover, their morphology seemed different among different brain regions. Then, we compared C57BL6 mice treated with 5 mg/kg LPS and relative control. This analysis revealed a heterogeneous increase in GFAP signal between different brain regions. We found a significant astrocyte increase in the hippocampus, SNpc, SNpr (Fig. 26B and C), and corpus callosum, but not in the other areas. Additional alterations were observed qualitatively. GFAP increases in the hypothalamus, but intra-regional differences mitigate this increase. GFAP also increased in other regions, such as the cerebellum and the thalamus. However, the signal was below the threshold considered in the analyses, and this increase was not detected. When we compared GFAP-positive cells between C57BL6 and CX3CR1$^{+/GFP}$ mice, we found a similar GFAP pattern in the naive (non-LPS treated) mice (data not shown). The only exception was a significant increase in GFAP marked area in SNpr in CX3CR1$^{+/GFP}$ mice. Exploring astrocytic activation in CX3CR1$^{+/GFP}$ mice treated with 5 mg/kg of LPS compared to the vehicle-treated mice, we found an increase in GFAP signal only in the hippocampus but not in SNpr (data not shown). These data indicated that astrocytes present a brain regional-specific activation and a lower inflammatory response in CX3CR1 partially ablated mice compared to mice that express the physiological level of this receptor.

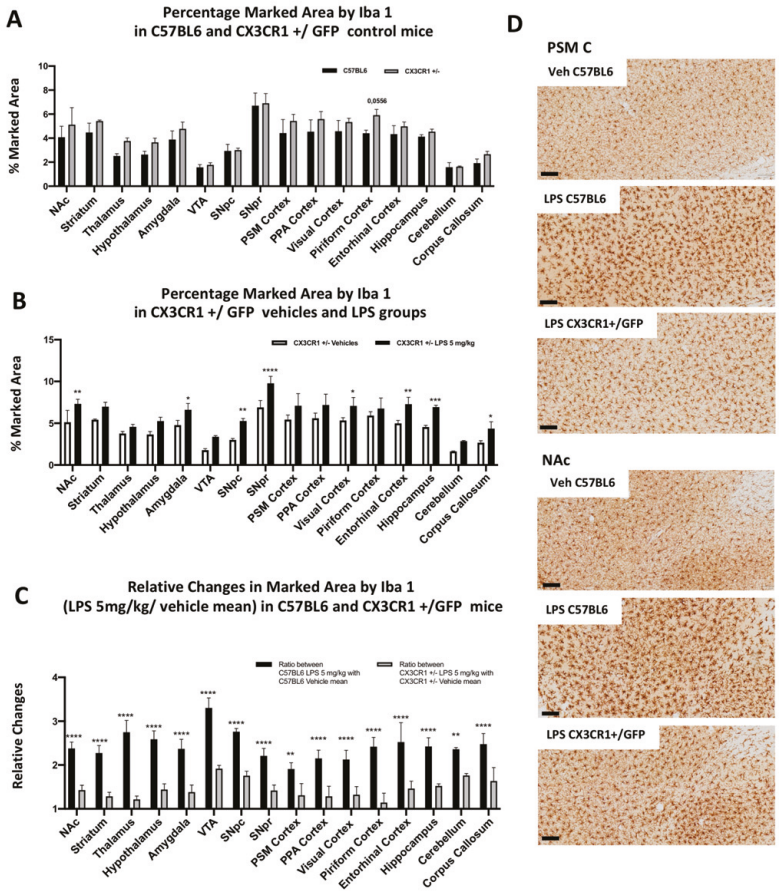

Figure 25. Partial ablation of CX3CR1 decrease the inflammatory response induced by systemic LPS A) Quantification of the percentage of the marked area by microglial cells between C57BL6 (black column) and CX3CR1+/GFP mice (gray columns) in control conditions. Statistics were performed using a two way-ANOVA FBrainRegions (15, 64) = 32.50, $p < 0.0001$. FGenotype (1, 64) = 36.68, $p < 0.0001$. FInteraction (15, 64) = 0.7510, $p < 0.7241$. n = 3 mice per region. Significance: (*) respect the same regions between two genotypes. **B)** Quantification of the percentage of the marked area by microglial cells in CX3CR1+/GFP mice. Vehicles (white columns) and LPS-treated mice (black columns). Statistics were performed using a two-way ANOVA FBrainRegions (15, 64) = 34.78, $p < 0.0001$. FTreatment (1, 64) = 164.9, $p < 0.0001$. FInteraction (15, 64) = 1.327, $p < 0.2129$. n = 3 mice per region. Significance: (*) respect relative vehicles. **C)** Fold changes in the percentage of the marked area by microglial cells between LPS 5 mg/kg and vehicles mice 24 h post treatment in C57BL6 mice (black columns) and CX3CR1+/GFP mice (gray columns). Statistics were performed using a two-way ANOVA FBrainRegions (15, 64) = 10.13, $p < 0.0001$. FTreatment (1, 64) = 687.5, $p < 0.0001$. FInteraction (15, 64) = 2.862, $p < 0.0018$. n = 3 mice per region. Significance: (*) respect relative vehicles. **D)** Qualitative

images of microglial activation n C57BL6 and CX3CR1+/GFP mice treated with 5 mg/kg LPS or vehicles. Scale bar = 100 um.

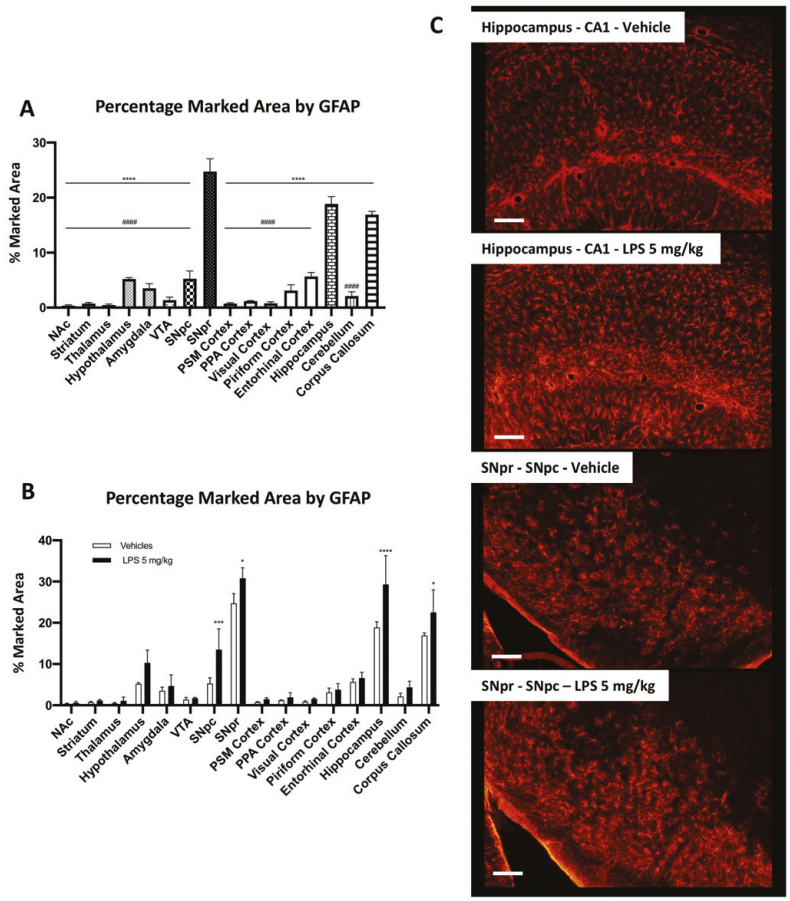

Figure 26. Region-specific astrocytic response to systemin LPS administration. **A)** Quantification of the percentage of the marked area by GFAP positive astrocytes in vehicles C57BL6N mice. Statistics were performed using a one-way ANOVA $F_{BrainRegions}$ (15, 32) = 206.8, $p < 0.0001$. n = 3 mice per region. Significance: (*) respect SNpr; (#) respect hippocampus and corpus callosum. Other significances are summarized in supplementary results. **B)** Quantification of the percentage of the marked area by GFAP positive cells in vehicles (white columns) and LPS-treated mice (black columns). Statistics were performed using a two-way ANOVA $F_{BrainRegions}$ (15, 64) = 100.6, $p < 0.0001$. $F_{Treatment}$ (1, 64) = 39.24, $p < 0.0001$. $F_{Interaction}$ (15, 64) = 3.406, $p < 0.0003$. n = 3 mice per region. Significance: (*) respect relative vehicles. **C)** Qualitative images of GFAP positive astrocytes in hippocampus and SNpr in vehicles and LPS treated mice.

Paper IV: Epitope-specific α-synuclein pathology in different synucleinopathies

Several studies described different α-syn PTMs, such as phosphorylation, nitration, oxidation, methylation, glycation, and truncations [83-85]. Each of these PTMs can induce alterations in α-syn conformation and influence its ability to aggregate [103-111]. Moreover, other indications suggest that some PTMs are more frequent in LBs than others [41-43]. Furthermore, studies also showed that LBs pathology affects several brain regions differently [122-124]. However, in most cases, few antibodies and α-syn epitopes were considered, and it is not well understood whether we could identify a different distribution of this protein considering its varied conformations. This study aimed to explore whether α-syn presents different epitopes within several brain region in synucleinopathies. We analysed α-syn distribution in six different brain regions of patients affected by PD, DLB, MSA, and age-matched control using several α-syn antibodies able to bind a number of α-syn epitopes.

α-Synuclein presents different structural conformations patterns in different brain regions

Firstly, we observed that all the antibodies used in this study were able to stain our tissues (Fig. 27; Antibodies´ table pag.81). The staining for the epitope 1-20 regularly detected LBs pathology and α-syn in the terminal nerve. The epitope 34-45 showed a particular pattern, presenting robust staining in all regions except in the hippocampus of DLB patients, while it stained primarily white matter pathology in PD and MSA in the same region. pS129 antibody showed consistent and numerous LNs-like structures not detected by other antibodies. This observation could indicate that pS129 α-syn could assume a conformation that hides the other epitopes. Other antibodies detected LNs pathology, but these were different in number and morphology compared to the ones identified by the pS129 antibody. In the end, the 103-108 epitope antibody mostly detected α-syn in the nerve terminals.

Differences in brain region LBs distribution in synucleinopathies

In PD patients, the SNpc region was the most affected by LBs pathology, followed by the amygdala. On the contrary, the frontal cortex and cerebellum were the less affected (Fig. 28). Patients affected by DLB showed more pathology in SNpc, hippocampus, and amygdala than in the other regions (Fig. 28 annd 29). MSA patients presented a wide distribution of intracellular inclusion in almost all regions, particularly in SNpc and putamen. Moreover, as expected, it was the only synucleinopathy where we observed LBs pathology in the cerebellum (Fig. 29).

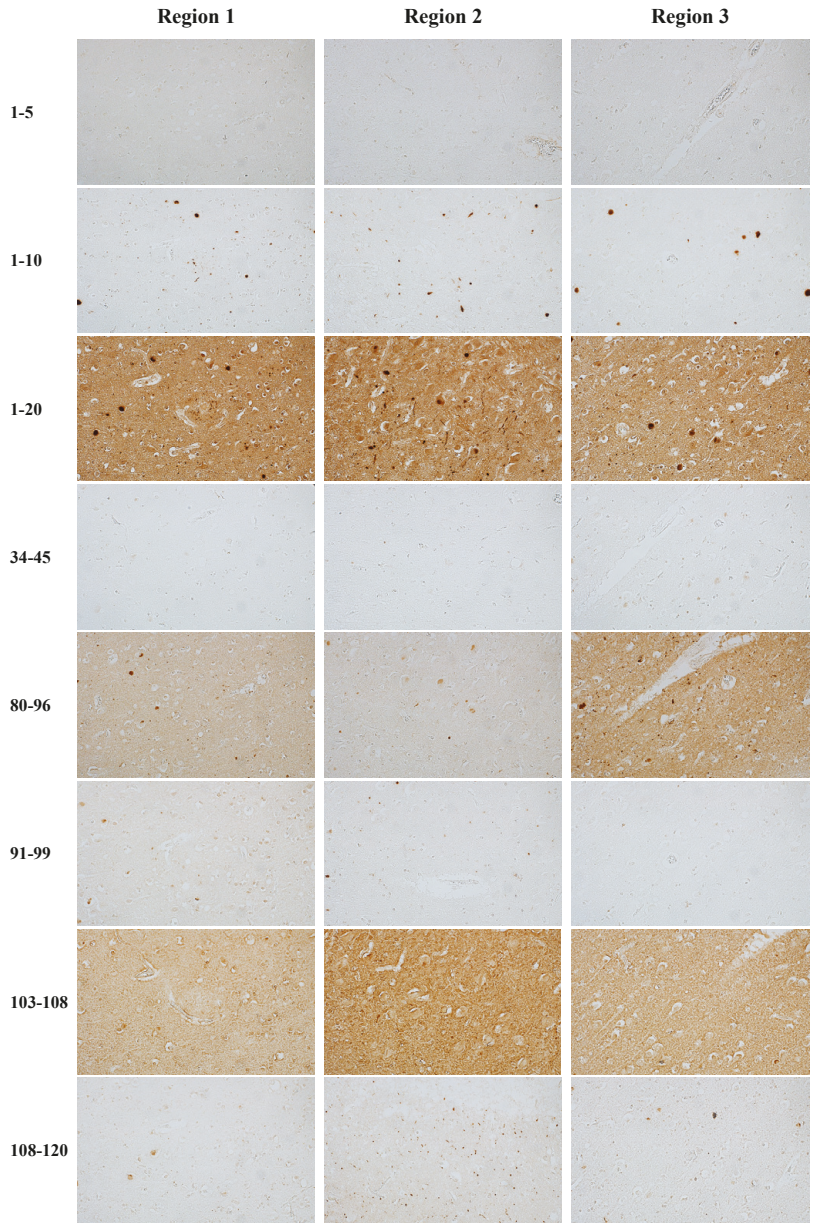

Figure 27. Region-specific α-syn conformations in human post-mortem brains. Representative images of hippocampus sections from a patient with DLB stained with antibodies against different α-syn epitopes. Scale bar = 20 µm

DIAGNOSIS	AGE	SEX	RACE	PMI (H)	BRAIN REGION	α-SYN EPITOPE											
						1-20			80-96			134-138			pS129		
						LB	LN	NT	LB	LN	NT	LB	LN	NT	LB	LN	NT
PD	84	Female	White	23.5	Hippocampus	+	+	++	++	-	+	-	+	-	-	+	-
					Substantia nigra	++	++	-	++	-	+	+	+	-	++	+	-
					Amygdala	+	+	++	+	+	+++	-	-	-	++	+	-
					Putamen	+	+	+	+	+/-	-	-	+	-	+	+	-
					Cortex	+/-	+/-	+	+/-	+/-	+++	-	-	-	-	-	-
					Cerebellum	-	-	+	+/-	+/-	+	-	-	-	-	-	-
PD	82	Female	White	8	Hippocampus	+	+	++	-	-	+	-	+	-	+/-	-	-
					Substantia nigra	++	+	-	+++	+++	+	-	+	-	+	+/-	-
					Amygdala	++	++	+	++	++	+++	-	+	-	+/-	-	-
					Putamen	+	+	++	+	+	+++	-	++	-	+/-	+/-	-
					Cortex	+/-	+/-	++	-	-	+++	-	-	-	+/-	+/-	-
					Cerebellum	-	-	++	-	-	+++	-	-	-	+/-	-	-
PD	84	Male	White	4	Hippocampus	+/-	+/-	++	+/-	-	+++	-	+/-	-	+/-	+/-	-
					Substantia nigra	+++	++	-	++	++	++	++	++	-	+++	+	-
					Amygdala	+	+	++	+	+	+++	++	++	-	+	+	-
					Putamen	+/-	+/-	-	+/-	-	+	-	+	++	+	+/-	-
					Cortex	+/-	+/-	++	+/-	-	+++	-	-	++	+	+/-	++
					Cerebellum	+/-	+/-	++	+/-	-	++	-	-	-	+/-	+/-	++
DLBD	87	Female	White	4	Hippocampus	+++	++	++	+++	+++	+++	++	++	++	++	+	+
					Substantia nigra	+++	++	-	+	++	+	++	++	-	+	+	+
					Amygdala	+	+	+++	++	+++	+++	++	++	++	++	+	+
					Putamen	+	+	++	+	++	++	-	+	+	-	+/-	+/-
					Cortex	+	+	++	+/-	+/-	+++	-	+	-	-	-	++
					Cerebellum	-	-	++	+/-	+/-	++	-	+	-	-	-	++

Figure 28. Different α-syn epitopes and distribution within several brain regions and different synucleinopathies. LBs and LNs assessment in several brain regions of patients with various synucleinopathies utilizing antibodies for several α-syn epitopes.

DIAGNOSIS	AGE	SEX	RACE	PMI (H)	BRAIN REGION	α-SYN EPITOPE											
						1-20			80-96			134-138			pS129		
						LB	LN	NT	LB	LN	NT	LB	LN	NT	LB	LN	NT
DLBD	77	Male	White	8.25	Hippocampus	+++	++	++	+++	+++	++	+	++	+	++	+	-
					Substantia nigra	++	+	-	+++	+++	++	++	++	-	++	+	-
					Amygdala	+++	++	++	-	++	+++	++	+++	+	+	+	-
					Putamen	+	+	++	-	++	+++	+	++	++	-	+/-	-
					Cortex	+	+	++	-	++	+++	+	+	++	-	+	-
					Cerebellum	-	-	++	-	-	+++	-	-	++	+	-	-
DLBD	86	Female	Black	18	Hippocampus	+	+	+	+	+	-	++	++	-	+	+	-
					Substantia nigra	+	+	-	+	+	+/-	+	+	-	+	+	-
					Amygdala	++	++	-	+	+++	++	+	+	-	+	+	-
					Putamen	+	+	++	+	+	-	+/-	+/-	-	+/-	+	-
					Cortex	+/-	+/-	++	-	-	++	+/-	+/-	-	+/-	+/-	-
					Cerebellum	-	-	++	-	-	++	+/-	-	-	+/-	+/-	-
MSA	69	Female	Asian	4.5	Hippocampus	+	+	++	++	-	++++	++	-	+	++	+/-	+
					Substantia nigra	++	+	+	++++	+	++	++	+/-	++	++	+	-
					Amygdala	+	+	++	+	-	+++	++	+/-	++	+	+	-
					Putamen	++	+/-	-	++++	+	++	++	+/-	++	++	+	-
					Cortex	+	+/-	++	++++	+/-	++	++++	+/-	+	++	+	-
					Cerebellum	++	+	++	++++	-	+++	++++	+/-	+	+++	+	-
MSA	69	Male	White	3	Hippocampus	+++	++	+	++++	+	++	++++	+/-	++	+++	+++	+
					Substantia nigra	+++	++	+/-	++++	+	++	++	+	-	++	+	+/-
					Amygdala	++	++	+	++++	+	++	++++	++	++	+	+	-
					Putamen	+++	++	+	++++	+	++	+++	++	++	+++	++	+
					Cortex	++	+	++	++	+	++	++	+	++	+	+	-
					Cerebellum	+	-	++	++	-	++	+	+	+	+	-	-

Figure 29. Different α-syn epitopes and distribution within several brain regions and different synucleinopathies. LBs and LNs assessment in several brain regions of patients with various synucleinopathies utilizing antibodies for several α-syn epitopes.

C-terminal truncation is more frequent in PD than in DLB and MSA

Subsequently, we systematically evaluated whether we could identify diseases or brain signatures of α-syn pathology. We stained consecutive sections of each region and pathology considered in the study (Fig. 30).

Interestingly, we observed varied patterns among different regions and pathologies concerning C-terminal α-syn staining. Although the C-terminal antibody (134-138) was detected in some LBs in PD brains, NAC 80-96 and pS129 antibodies were more frequently observed, indicating the presence of a truncation between amino acids 129 and C-terminal α-syn. This difference was not present in DLB and MSA. To confirm this observation, we performed double-labeling using NAC 80-96 and C-terminal 134-138 antibodies. Through this staining, we confirmed that in PD patients, most LBs were marked by NAC 80-96 but not C-terminal 134-138 antibodies, while both antibodies were co-labeled in MSA and DLB.

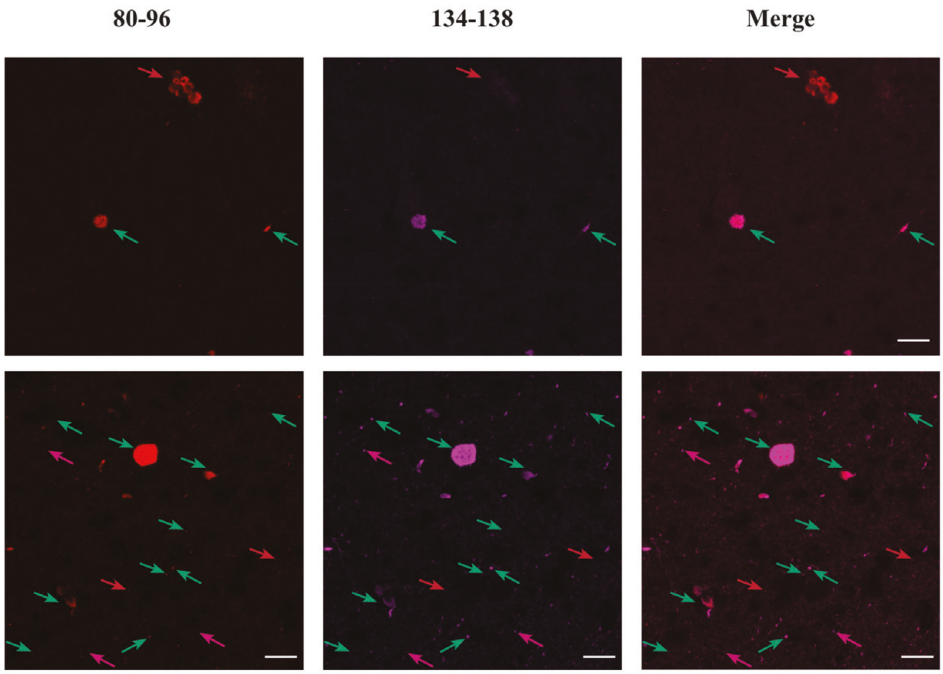

Figure 30. α-syn C-terminal truncation is more common in PD patients than MSA and DLB. Representative images of SN from PD patient and corpus callosum from MSA patient. Double-labelling with antibodies targeting α-syn epitopes 80-96 and 134-138 of -syn. Scale bar = 20 μm.

Discussion and future perspective

Synucleinopathies are a group of neurodegenerative disorders characterized by intracellular inclusions, neurodegeneration, neuroinflammation, and iron accumulation. This thesis aimed to better understand the neuroinflammatory involvement in these pathologies. The classic hypothesis supports the idea that oligomeric and fibrillar α-syn species can trigger microglia and astrocyte pro-inflammatory phenotypes that, in turn, could participate in the synaptic loss and neurodegeneration observed [174, 199-202, 211]. However, several other studies suggest that the inflammatory system might have a more critical role in PD and related disorders [234-240].
The involvement of neuroinflammation seems to be present since the early stage of these pathologies, as shown by PET imaging studies [182-187]. This chronic inflammation could be able to induce a progressive dopaminergic neurodegeneration in SNpc [238-240]. Moreover, investigating the dopaminergic grafts in PD patients have showed that microglial activation precedes the formation of LB pathology, suggesting that inflammation could facilitate α-syn spreading from the host to grafts or create the conditions favourable for α-syn aggregation [188, 189].
Inflammation could induce α-syn PTMs directly in neurons by activating neuronal inflammasome NLRP3 and caspase-1 [208, 255, 256]. As we mention, this caspase can form trunc-121 α-syn, which seems to increase the α-syn capacity to form aggregates [252, 253]. Other PTMs that could partially be derived from pro-inflammatory conditions have been described, such as pS129 and nitrated α-syn [208, 250, 251], and may others need to be discovered. Moreover, microglia and astrocytes can internalize α-syn, contribute to its clearance, induce PTMs within their intracellular environment, and may contribute to α-syn spreading [215, 217]. These findings suggest a vicious cycle between α-syn and inflammatory cells that could sustain the pathology progression.

Our first manuscript explored the consequence of a high amount of α-syn within the microglial intracellular environment. We generated microglial-like cell clones overexpressing a set of α-syn mutations. In the control condition, we observed neither pro-inflammatory alterations induced by α-syn over-expression nor the formation of spontaneous aggregates. Inducing the aggregation via α-syn PFFs, we observed that microglial-like cells can develop aggregates and some positive pS129

α-syn. Interestingly, we also observed that some pS129 α-syn was not co-localizing with GFP, indicating the presence of truncated α-syn between S129 and the C-terminal.
Stimulating BV2 clones expressing α-syn-GFP with LPS, we did not observe any aggregates. We also did not detect evident alterations of the aggregation process when LPS was combined with α-syn PFFs. These findings were in contrast with the studies previously mentioned [208, 252, 253]. However, GFP could prevent some PTMs and hide consequent alterations. Further investigations need to be performed to systematically explore the presence of α-syn PTMs and soluble species in control conditions and investigate alteration in α-syn aggregation using LPS with or without α-syn PFFs in BV2 cells expressing α-syn without GFP.
Another intriguing aspect of our experiments was the susceptibility observed in BV2 cells to α-syn PFFs internalization and subsequent α-syn aggregation process. Both BV2 expressing α-syn-GFP and GFP suffered from α-syn PFFs and LPS treatment after 48 hours, implying that this cell line is probably susceptible to conditions used in our work. However, our live-imaging recording also indicated toxicity induced during the formation of intracellular aggregates, suggesting that also the aggregates developed intra-cellularly were toxic.
Furthermore, we observed exchanges of α-syn loaded vesicles between BV2 cells, indicating that these models could be helpful for studying the role of these vesicles in α-syn propagation.

A useful tool to investigate the mechanisms behind α-syn aggregation is represented by a high-throughput screening system. Our study used a FRET-based reporter system in HEK293T to follow the α-syn aggregation process and to screen a kinases library. We identified three compounds linked with PKC and p38 MAPK, and further analyses indicate a compromised lysosomal system.
A similar approach can be used to explore α-syn PTMs formation and aggregation in our BV2 clones. For example, this system could be useful to identify the molecular pathway responsible for the truncation observed between S129 and C-terminal α-syn or to find a target to against the toxicity observed.

Recently, several studies showed that microglial and astrocyte populations are heterogeneous within the brain in many aspects [31, 32, 144]. Considering the peculiar histology regarding microglia and astrocyte cells in SNpr compared to all other regions [31, 32], we speculated this characteristic could highly affect the dopaminergic neuronal population in SNpc. To examine the uniqueness of this brain region, we choose to compare it with other 15 brain areas. Using a mouse model based on systemic LPS administration, we showed that the inflammatory response within the brain differs in intensity, sensitivity, and ability to persist one month after injection. Moreover, we showed that the microglial population in SNpr seemed to induce one of the most robust inflammatory responses, to be one of the most

sensitive populations to systemic TNFα and/or LPS, and to be altered chronically. We also observed a peculiar activation of lysosome-associated protein CD68 in the microglial population exclusively in SNpr, indicating that this microglial population possess a peculiar lysosomal system.
Additionally, we also observed that the acute inflammatory response in this region induced a transitory dopaminergic dendritic loss, which recovered one month after treatment. This transitory effect is not in agreement with other studies that showed dopaminergic neurodegeneration followed by chronic inflammation. However, we did not investigate neurodegeneration in SNpc and other forms of compensative mechanisms could re-establish the average dendritic density, such as an increase of TH activity [262]. Moreover, the molecular mechanisms driving the acute effects may not coincide with the ones driving neurodegeneration chronically.
The classic hypothesis of dopaminergic neurodegeneration observed in SNpc was initially linked to ROS and mitochondrial damage. However, this explanation does not justify why this neurodegenerative process almost spares the same neuronal population in VTA. Subsequently, to explain this aspect, studies focused more on the neuronal networks involved in these pathologies and α-syn propagations. Here, we suggest that the peculiar histological characteristics together with our observation in SNpr could highly affect the dopaminergic neurons in SNpc. This characteristic could represent the main differential factor between SNpc and VTA, explaining the differential neurodegeneration observed in PD and related disorders.

In nature, the "structure" has always a link with its functions. However, the reasons and functions behind the peculiar histology observed in SNpr are entirely unknown. The presence of high density in glial cells and fibers, opposed to the low neuronal density, suggests that these two components could interact. SNpr is one of the main outputs of BG nuclei, and it receives projections from the striatonigral bundle which make synapses with local neurons and dendrites from dopaminergic neurons in SNpc [33]. These dendrites appear to be intermingled with microglial cells which, as we mentioned before, can modulate neuronal synapses. On the other way around, these dendrites could release dopamine in SNpr, which could modulate the microglial cells [35-38, 263-267]. This microglial population presents a higher amount of TLR4 receptors, is particularly sensitive to systemic TNFa and/or LPS, and shows other characteristics that indicate a fast-reacting phenotype [32, 144]. However, the same population in SNpr is the only one compared to the cortex, striatum, and hippocampus that expresses anti-inflammatory cytokines TGFβ and IL-10 48 hours after systemic LPS injection in mice [144]. This finding indicates the presence of negative feedback that could be essential to preserve the surrounding tissue and suggest that these cells could be finely modulated.
All these characteristics taken together brought us to speculate that SNpr could represent the "bridge" between the systemic immune system.and the BG circuitry. According to this hypothesis, the microglial population in SNpr could perceive the systemic immune condition and convert this message altering the neuronal circuitry.

The result of this could be a modulation of motor behaviour depending on organism conditions, decreasing unnecessary movement and allowing healing in case of some pathology.

Shifting our attention to other pathologies, we also observed a peculiar microglial or astrocytic activation in regions more affected in Alzheimer's disease, such as the entorhinal cortex, hippocampus, piriform cortex, NAc, amygdala, and corpus callosum. Moreover, our data on chronic inflammation induced by systemic inflammation could also suggest the role of neuroinflammation in cognitive symptoms observed in long-Covid19 cases. Similar to LPS, Covid-19 also causes an increase of systemic TNFα that can pass the BBB and trigger chronic neuroinflammation [268-271].

The presence of region-specific inflammatory responses could significantly influence the course of neurodegenerative diseases and the characteristics observed in post-mortem tissues. In the last work, we set the preliminary conditions to study the neuroinflammatory influence on α-syn conformations and pathology.
Studying the human post-mortem brains of patients affected by PD, DLB, and MSA, we found differential α-syn epitopes and pathology distribution in several brain regions and between synucleinopathies. Our findings also highlight the presence of a truncation between S129 and C-terminal α-syn in PD patients but not in DLB and MSA. Whether this truncation could be related to the one observed in our first manuscript is not clear, but this redundancy needed to be mentioned.
Using the same human samples, we already stained for Iba1, GFAP, and NeuN, aiming to assess possible correlations between inflammation and α-syn PTMs.

Currently, different clinical trials are using anti-inflammatory treatment in PD and related disorders. Studies indicate a beneficial effect of ibuprofen and other drugs [272-275]. In our third project, we explored the role of the CX3C axis in the neuroinflammatory response induced by systemic TNFα and/or LPS. Our data showed that partial ablation of CX3C receptor 1 generally decreases the acute inflammatory response and prevents the chronic one. Our data agree with many other studies in different animal models and suggest the CX3C axis as a potential pharmacological target [276-278].

Materials and Methods

Experimental models

Cell cultures

We used BV2 and HEK 293T cell lines in the first two projects. These cells were cultured at 37 °C, 95% humidity, and 5% CO_2. Cells were kept in DMEM supplemented with 10% FBS and 1% penicillin-streptomycin. For the experimental procedure, HEK 293T cells were plated in a coated plate (Collagen-PBS 1:20), while no coating was used for BV2 cells.
At the end of the experiments, cells were fixed with 4% paraformaldehyde (PFA) for 20 min, followed by 3 gentle washes with PBS at room temperature.

Mouse models

For the third project, adult male 6-months-old C57BL6 and CX3CR1$^{+/GFP}$ were used. C57BL6 were bought by Janvier labs (Saint Berthevin Cedex, France), while CX3CR1$^{+/GFP}$ mice were bred *in loco*. Mice were housed in an environment with a temperature of 21°C, controlled humidity, 12 hours light/dark cycle, an environment enriched by *stimuli*, and fed *ad libitum* with a rodent pellet diet and water. Experiments involved three mice in each group and were conducted on the same day. Mice were sacrificed 1 or 30 days post-administration.
Mice were deeply anesthetized using pentobarbital and perfused with 4% PFA. Brains were collected and post-fixed O/N in the same fixative and submerged in 30% sucrose in PBS until their use.
All animals and the procedures were conducted according to the Malmö/Lund Animal Ethical Committee (Dnr 5.8.18-09454/2021).

Human post-mortem brains

Human samples used in the fourth study were obtained from the Division of Oncology and Pathology of Lund University Hospital and the Brain Bank at Mount Sinai. These patients were affected by PD, DLB, and MSA and compared with age-

matched controls. Six different regions were analyzed for each subject: midbrain, putamen, amygdala, hippocampus, frontal cortex, and cerebellum.

Molecular biology

Cloning

The principal method for construct generation used in our cell works was the Gibson cloning due to its scarless DNA assembly, ease of planning, high efficiency, and low background.
Clonings were planned using the online tool New England Biolabs, NEBuilder, for all Gibson assemblies performed.
To linearize the vector backbone, we used restriction digestion and subsequently isolated it using Zymo Gel DNA recovery kits.
Inserts were generated by PCR amplification utilizing guides designed with NEBuilder and Phusion Hotstart II DNA polymerase 2x Master Mix. PCR reactions were composed of 25 µl Phusion Hotstart II 2x Master Mix, 5 ng template DNA, 1 µl forward primer (10 µM), 1 µl reverse primer (10 µM), and water till 50 µl total reaction volume. Thermo cycling was performed by standard protocol: Subsequently, the PCR product was purified on an agarose gel and recovered by a Zymo Gel DNA recovery kit. Purified vector backbone (50 ng) and insert (2x molar excess) were then used in an isothermal Gibson reaction (New England Biolabs) at 50 °C for 1 hour. The consequent ligation mix was then transformed into Shure2 competent cells to determine positive colonies.

Lentivirus production and titration

Production of lentivirus was performed by PEI-based transfection in HEK 293T cells. On the day preceding virus production, $14x10^6$ (for the first project) and $12.5x10^6$ (for the second project) HEK 293T cells were seeded in a T175 flask to reach 85-90% confluence the next day. The following day, the culture medium was replaced 1-2 hours before transfection. DNA was prepared by diluting 5.1µg pMD2G, 7.1 µg pMDL, and 4 µg pRsvRev along with 18 µg lentiviral vector plasmid in 1.7 ml OPTI-MEM and mixed by the vortex.
Liposomes were made by adding 102.6 µg PEI to diluted DNA, vortexed, and incubated for 15 min at RT before adding it to cells for transfection. Lentiviruses were collected with the supernatant 48 hours after transfection, spun at 800xg for 10 min to eliminate cell debris, and filtered through a 0.45 µm syringe filter. The supernatant was further concentrated by ultracentrifugation for 1.5 hours, 107000xg

at 4 °C. Then, the pellet with lentivirus was resuspended 0/N at 4 °C in PBS to produce the final lentivirus preparation.
Aiming to assess the lentiviral titer, we established a reference batch of lentivirus with GFP-driven by eIF1α. The reference batch titer was functionally assessed by flow cytometry. Lentiviral preparations were subsequently compared by qPCR based on WPRE integrations to the reference batch to select titers. HEK 293T cells were seeded at 100.000 cells in each well in a 6-well plate and incubated at 37 °C to permit sedimentation and adherence. These cells were then transduced with 0.3 µl, 1 µl, or 3 µl virus preparation. 72 hours after incubation, we extracted the genomic DNA using Qiagen DNeasy Blood & Tissue kit. Viral integration was quantified by qPCR utilizing self-quenching FAM probes for WPRE and albumin.

Generation of monoclonal cell lines

Cells were harvested 6 days after lentiviral transfection and resuspended in PBS supplemented with 2% FBS. Subsequently, these suspensions were sorted as single cells on a FACS Aria III equipped with a 100 µM nozzle into a 96 well plate. These sorted cells were then expanded till the formation of stable cell lines.

Treatments

α-synuclein PFFs

α-syn PFFs were obtained from α-syn monomers in Tris buffer (10 mM Tris, 150 mM NaCl, pH 7.5) at a concentration of 0.5 µg/µl incubated for 14 days at 37 °C under 1000 rpm shaking utilizing a 3 mm magnetic stir-bar. Fibrillation was followed by individual readings of Thioflavin T fluorescence in control well to confirm that a plateau was reached. PFFs generated were collected, aliquoted, and stored at -80 °C until their use.
α-syn PFFs administration was preceded by sonication. This step was performed using a cup-horn sonicator at 100% amplitude 1 sec on/off cycles for 6 minutes (for the first project) or 60% amplitude in 3 sec on/off cycles for 15 sec (for the second project).
Lipo-transfection was conducted utilizing lipofectamine 2000 (Thermo Fisher Scientific, Cat. 11668019) and diluted with Opti-MEM (Thermo Fisher Scientific, Cat. 31985070) at 1 ul every 10 ul total solution. Subsequently, Opti-MEM with lipofectamine was combined with 10ul Opti-MEM in the presence or absence of α-syn PFFs.

Lipopolysaccharides

Freeze-dried LPS (clone O55:B5, Sigma Aldrich) was resuspended in distilled water with a concentration of 1 mg/ml and frozen at minus 20°C for subsequent use.
Before using it for cell cultures, LPS was thawed and diluted in media at final concentrations (10 ug/ml).
For mice treatments, we diluted LPS in PBS at final concentrations.
We performed a single intraperitoneal injection (i.p.) of LPS (5 mg/kg, 0,5mg/kg, 0,05 mg/kg, 0,005 mg/kg doses) or vehicle alone.

Immunochemistry

Cells samples

Fixed cells were immuno-stained for α-syn 211 (Cat. sc-12767, Santa Cruz Biotechnology), phosphorylated-129 α-syn (Cat. AB51253, Abcam), Iba 1 (1:1000, Nordic Cat. #019-19741, Biolabs, Wako Chemicals), HSP60 (Cat. #4870, Cell signaling), BIP (Cat. #AB21685, Abcam), TFEB (Cat. #A303-673A, Thermo Fisher), and DAPI. Primary antibodies were diluted in PBS with the serum (5-10%) and 0,1% Tween or Triton-X 100.

Animal samples

Perfused brains were sectioned at 25 μm thickness using a microtome (Leica SM2010R) and preserved at -20°C in an anti-frozen solution in the presence of sodium azide. Slices were immune-stained for Iba 1 (Cat. #019-19741, Nordic Biolabs, Wako Chemicals), TH (Cat. #AB152 and #MAB358, Chemicon, Millipore), Gephyrin (Synaptic Systems, Cat. #147011C3). The primary antibody was diluted in PBS with the serum (5-10%) and 0,3% Triton-X 100.

Human samples

Formalin-fixed paraffin-embedded samples were sectioned at 5 μm thickness utilizing a paraffin microtome (Galileo AUTO) and mounted onto Thermofrost glass slides.
Before immunostainings, the sections were dried at 60°C for 1 hour. Subsequently, they were deparaffinated with xylene and ethanol baths. Subsequently, sections were immersed in 80% formic acid for 10 minutes and washed in distilled water. Subsequently, we performed a heat-mediated antigen retrieval in 0.01M Citrate buffer (pH 6.0) for 40 minutes at 95°C. Samples were washed and cooled in PBS.

Quenching was conducted using a 3% H_2O_2 in PBS solution for 15 minutes at RT. Primary antibodies were diluted in PBS with the serum (5-10%) and 0,3% Triton-X 100.

Antibody	Epitope	Source	Host animal	Dilution used
EGT 403	α-syn residues 1-5	EPFL	Mouse	1:200
EGT 410	α-syn residues 1-10	EPFL	Mouse	1:500
BL-LASH-N-Term	α-syn residues 1-20	EPFL	Rabbit	1:2000
BL-LASH-34-45	α-syn residues 34-45	EPFL also available at Biolegend (849101)	Mouse	1:500
BL-LASH-80-96	α-syn residues 80-96	EPFL also available at Biolegend (848301)	Mouse	1:2000
Syn-1	α-syn residues 91-99	BD Biosciences (BD610787)	Mouse	1:500
4B12	α-syn residues 103-108	Biolegend (807804)	Mouse	1:500
EGT 406	α-syn residues 108-120	EPFL	Mouse	1:500
EGT 408	α-syn residues 107-140	EPFL	Mouse	1:500
Far C-terminal	α-syn residues 134-138	Abcam (ab131508)	Rabbit	1:2000
pS129	α-syn phosphorylated at Serine 129	Abcam (ab51253)	Rabbit	1:1000
Biotinylated anti-mouse	Mouse IgG (H+L)	Vector Laboratories (BA2001)	Horse	1:500
Biotinylated anti-rabbit	Rabbit IgG (H+L)	Vector Laboratories (BA1000)	Goat	1:500
Cy3-anti-mouse	Mouse IgG (H+L)	Jackson Immuno Research (715-165-150)	Donkey	1:400
Cy5-anti-rabbit	Rabbit IgG (H+L)	Jackson Immuno Research (711-175-152)	Donkey	1:400

Imaging

Microscopes

Cells were acquired using a Nikon Eclipse Ti microscope. The same microscope was used for live-imaging acquisition, where cells were maintained in standard conditions (at 37 °C, 95% humidity, and 5% CO_2**).**

Mice and human samples were acquired using the Olympus BX53 microscope, the scanner microscope Olympus Virtual Stage 120 with an extended focus imaging setting (EFI), and LEICA Stellaris 8 Dive for confocal images.

FRET-based flow cytometry

To perform the FRET analyses, cells were fixed in suspension at the endpoint. Cells were transferred to DMEM +10%FBS +1% P/S and centrifuged at 800g for 10 min to pellet. The pellet was resuspended in PBS 2% PFA. Fixed cells were washed three times in PBS before analysis on a BD LSRFortessa. To detect the FRET signal, a scatterplot of CFP vs. FRET was set up by exciting with the 405 nm laser, and emission was collected at a detector equipped with a 405/50 nm and 525/50 nm filter, respectively. We calculated the normalized FRET score (% FRET+ x FRET mean fluorescence intensity) to quantify FRET intensity.

Acknowledgement

It is difficult to find the words to say thanks to all the people that I met in the past five years. Each of them had a role for me to achieve these results and to survive to five cold winter in Sweden.
I would like to start from my supervisor Jia Yi. I mostly judge a person for how they behave with other people. I should say that I always saw a person extremely polite with everyone and that took care of his students during Covid-19 time as no other PI did here in Lund University. Furthermore, I also would say thanks for the freedom that I had to develop my projects. It was difficult but more satisfying.
I would like to dedicate a warm thanks to two wonderful people and colleagues, Alex and Laura. Both of you are special person and were essential for me during these years.
I would like to say thanks also to others lab members, as Di, Wen, and Caroline, and also to Susanne and Catarina for their help in the lab.
Thanks a lot also to Martino and Matilde (Negrini) for the daily support along all these years and for their hospitality in recent period. You were super kind and gentle.
I would like to thanks all A10 people, Carolina, Filip, Kajsa, Elna, Andreas, Jana, Lautaro, Osama, Abderahim, Robert, and also old A10 members as Janita, Tiberio, Andy, and Marcus. It was a pleasure to work and spend time with all of you.
Thanks a lot also to BMC people, Silvia, Sara, Sertan, Frank, Edoardo, Rosalia, and to all (ex or almost ex) Ph.D. students as Fabio, Julie, Roberta, Elinska, Andreas, Laura, Isak, Lluís and all others. It was fun and a pleasure to meet all of you.
“Really thanks” to my Italian family here in Sweden. Michael, Miriana, Matilde (Forni), Per, Paul, Valeria, Alessandro, Paola, Valentina, and Mattia. You made me feel at home. I will bring all of you in my heart and I am sure that we will meet still many times.
A warm thanks goes also to my dear friend Yasir for all carefree time spent together and for his support in many occasions.
Furthermore, I would like to say thanks to my historical friends Gigio, Luca, Paolo, Rocco, Pasquale, Ciccio, Nicola, Riccardo, Antonio. Thanks to be always there in the important moment.
Then, I would like to say thanks to my family, for their support and their constant love. I missed you all this time.
Lastly, I would like to say thanks to my guardian angel Sonny. I promise you that I will never leave you alone, I brought you around all Europe, and I will continue.
Thanks to everybody, I wish you the best.

References

1. Erkkinen, M.G., M.O. Kim, and M.D. Geschwind, *Clinical Neurology and Epidemiology of the Major Neurodegenerative Diseases.* Cold Spring Harb Perspect Biol, 2018. **10**(4).
2. de Lau, L.M. and M.M. Breteler, *Epidemiology of Parkinson's disease.* Lancet Neurol, 2006. **5**(6): p. 525-35.
3. Hou, Y., et al., *Ageing as a risk factor for neurodegenerative disease.* Nat Rev Neurol, 2019. **15**(10): p. 565-581.
4. Savica, R., et al., *Incidence and pathology of synucleinopathies and tauopathies related to parkinsonism.* JAMA Neurol, 2013. **70**(7): p. 859-66.
5. Ascherio, A. and M.A. Schwarzschild, *The epidemiology of Parkinson's disease: risk factors and prevention.* Lancet Neurol, 2016. **15**(12): p. 1257-1272.
6. Tolosa, E., G. Wenning, and W. Poewe, *The diagnosis of Parkinson's disease.* Lancet Neurol, 2006. **5**(1): p. 75-86.
7. Wolters, E., *Variability in the clinical expression of Parkinson's disease.* J Neurol Sci, 2008. **266**(1-2): p. 197-203.
8. Berg, D., et al., *Prodromal Parkinson disease subtypes - key to understanding heterogeneity.* Nat Rev Neurol, 2021. **17**(6): p. 349-361.
9. Halliday, G.M., et al., *Neuropathology underlying clinical variability in patients with synucleinopathies.* Acta Neuropathol, 2011. **122**(2): p. 187-204.
10. Jankovic, J., *Parkinson's disease: clinical features and diagnosis.* J Neurol Neurosurg Psychiatry, 2008. **79**(4): p. 368-76.
11. Schapira, A.H.V., K.R. Chaudhuri, and P. Jenner, *Non-motor features of Parkinson disease.* Nat Rev Neurosci, 2017. **18**(7): p. 435-450.
12. Gomperts, S.N., *Lewy Body Dementias: Dementia With Lewy Bodies and Parkinson Disease Dementia.* Continuum (Minneap Minn), 2016. **22**(2 Dementia): p. 435-63.

13. Fanciulli, A., et al., *Multiple system atrophy.* Int Rev Neurobiol, 2019. **149**: p. 137-192.
14. Palma, J.A., L. Norcliffe-Kaufmann, and H. Kaufmann, *Diagnosis of multiple system atrophy.* Auton Neurosci, 2018. **211**: p. 15-25.
15. Langston, J.W., et al., *Chronic Parkinsonism in humans due to a product of meperidine-analog synthesis.* Science, 1983. **219**(4587): p. 979-80.
16. Davis, G.C., et al., *Chronic Parkinsonism secondary to intravenous injection of meperidine analogues.* Psychiatry Res, 1979. **1**(3): p. 249-54.
17. Tanner, C.M., et al., *Rotenone, paraquat, and Parkinson's disease.* Environ Health Perspect, 2011. **119**(6): p. 866-72.
18. Perese, D.A., et al., *A 6-hydroxydopamine-induced selective parkinsonian rat model.* Brain Res, 1989. **494**(2): p. 285-93.
19. Hatcher, J.M., K.D. Pennell, and G.W. Miller, *Parkinson's disease and pesticides: a toxicological perspective.* Trends Pharmacol Sci, 2008. **29**(6): p. 322-9.
20. Bove, J., et al., *Toxin-induced models of Parkinson's disease.* NeuroRx, 2005. **2**(3): p. 484-94.
21. Martinez, T.N. and J.T. Greenamyre, *Toxin models of mitochondrial dysfunction in Parkinson's disease.* Antioxid Redox Signal, 2012. **16**(9): p. 920-34.
22. Betarbet, R., et al., *Chronic systemic pesticide exposure reproduces features of Parkinson's disease.* Nat Neurosci, 2000. **3**(12): p. 1301-6.
23. Pan-Montojo, F., et al., *Progression of Parkinson's disease pathology is reproduced by intragastric administration of rotenone in mice.* PLoS One, 2010. **5**(1): p. e8762.
24. Pan-Montojo, F., et al., *Environmental toxins trigger PD-like progression via increased alpha-synuclein release from enteric neurons in mice.* Sci Rep, 2012. **2**: p. 898.
25. Zhang, J., et al., *Comparison of the effect of rotenone and 1methyl4phenyl1,2,3,6tetrahydropyridine on inducing chronic Parkinson's disease in mouse models.* Mol Med Rep, 2022. **25**(3).
26. Forno, L.S., et al., *An electron microscopic study of MPTP-induced inclusion bodies in an old monkey.* Brain Res, 1988. **448**(1): p. 150-7.
27. Kowall, N.W., et al., *MPTP induces alpha-synuclein aggregation in the substantia nigra of baboons.* Neuroreport, 2000. **11**(1): p. 211-3.

28. Huang, B., et al., *Phosphorylated alpha-Synuclein Accumulations and Lewy Body-like Pathology Distributed in Parkinson's Disease-Related Brain Areas of Aged Rhesus Monkeys Treated with MPTP.* Neuroscience, 2018. **379**: p. 302-315.
29. Fornai, F., et al., *Parkinson-like syndrome induced by continuous MPTP infusion: convergent roles of the ubiquitin-proteasome system and alpha-synuclein.* Proc Natl Acad Sci U S A, 2005. **102**(9): p. 3413-8.
30. Dias, V., E. Junn, and M.M. Mouradian, *The role of oxidative stress in Parkinson's disease.* J Parkinsons Dis, 2013. **3**(4): p. 461-91.
31. Lawson, L.J., et al., *Heterogeneity in the distribution and morphology of microglia in the normal adult mouse brain.* Neuroscience, 1990. **39**(1): p. 151-70.
32. De Biase, L.M., et al., *Local Cues Establish and Maintain Region-Specific Phenotypes of Basal Ganglia Microglia.* Neuron, 2017. **95**(2): p. 341-356 e6.
33. Lanciego, J.L., N. Luquin, and J.A. Obeso, *Functional neuroanatomy of the basal ganglia.* Cold Spring Harb Perspect Med, 2012. **2**(12): p. a009621.
34. Zhou, F.M. and C.R. Lee, *Intrinsic and integrative properties of substantia nigra pars reticulata neurons.* Neuroscience, 2011. **198**: p. 69-94.
35. Bjorklund, A. and O. Lindvall, *Dopamine in dendrites of substantia nigra neurons: suggestions for a role in dendritic terminals.* Brain Res, 1975. **83**(3): p. 531-7.
36. Mercer, L., M. del Fiacco, and A.C. Cuello, *The smooth endoplasmic reticulum as a possible storage site for dendritic dopamine in substantia nigra neurones.* Experientia, 1979. **35**(1): p. 101-3.
37. Geffen, L.B., et al., *Release of dopamine from dendrites in rat substantia nigra.* Nature, 1976. **260**(5548): p. 258-60.
38. Cheramy, A., V. Leviel, and J. Glowinski, *Dendritic release of dopamine in the substantia nigra.* Nature, 1981. **289**(5798): p. 537-42.
39. Spillantini, M.G., et al., *Alpha-synuclein in Lewy bodies.* Nature, 1997. **388**(6645): p. 839-40.
40. Wakabayashi, K., et al., *The Lewy body in Parkinson's disease and related neurodegenerative disorders.* Mol Neurobiol, 2013. **47**(2): p. 495-508.

41. Leverenz, J.B., et al., *Proteomic identification of novel proteins in cortical lewy bodies.* Brain Pathol, 2007. **17**(2): p. 139-45.
42. Polymeropoulos, M.H., et al., *Mutation in the alpha-synuclein gene identified in families with Parkinson's disease.* Science, 1997. **276**(5321): p. 2045-7.
43. Shahmoradian, S.H., et al., *Lewy pathology in Parkinson's disease consists of crowded organelles and lipid membranes.* Nat Neurosci, 2019. **22**(7): p. 1099-1109.
44. Emamzadeh, F.N., *Alpha-synuclein structure, functions, and interactions.* J Res Med Sci, 2016. **21**: p. 29.
45. Ulmer, T.S., et al., *Structure and dynamics of micelle-bound human alpha-synuclein.* J Biol Chem, 2005. **280**(10): p. 9595-603.
46. Fortin, D.L., et al., *Lipid rafts mediate the synaptic localization of alpha-synuclein.* J Neurosci, 2004. **24**(30): p. 6715-23.
47. Middleton, E.R. and E. Rhoades, *Effects of curvature and composition on alpha-synuclein binding to lipid vesicles.* Biophys J, 2010. **99**(7): p. 2279-88.
48. Kjaer, L., et al., *The influence of vesicle size and composition on alpha-synuclein structure and stability.* Biophys J, 2009. **96**(7): p. 2857-70.
49. Kamp, F. and K. Beyer, *Binding of alpha-synuclein affects the lipid packing in bilayers of small vesicles.* J Biol Chem, 2006. **281**(14): p. 9251-9.
50. Chandra, S., et al., *Alpha-synuclein cooperates with CSPalpha in preventing neurodegeneration.* Cell, 2005. **123**(3): p. 383-96.
51. Burre, J., et al., *Alpha-synuclein promotes SNARE-complex assembly in vivo and in vitro.* Science, 2010. **329**(5999): p. 1663-7.
52. Burre, J., M. Sharma, and T.C. Sudhof, *alpha-Synuclein assembles into higher-order multimers upon membrane binding to promote SNARE complex formation.* Proc Natl Acad Sci U S A, 2014. **111**(40): p. E4274-83.
53. Hawk, B.J.D., R. Khounlo, and Y.K. Shin, *Alpha-Synuclein Continues to Enhance SNARE-Dependent Vesicle Docking at Exorbitant Concentrations.* Front Neurosci, 2019. **13**: p. 216.
54. Garcia-Reitbock, P., et al., *SNARE protein redistribution and synaptic failure in a transgenic mouse model of Parkinson's disease.* Brain, 2010. **133**(Pt 7): p. 2032-44.
55. Liu, G., et al., *alpha-Synuclein is differentially expressed in mitochondria from different rat brain regions and dose-dependently*

down-regulates complex I activity. Neurosci Lett, 2009. **454**(3): p. 187-92.
56. Kim, T.D., et al., *Alpha-synuclein has structural and functional similarities to small heat shock proteins.* Biochem Biophys Res Commun, 2004. **324**(4): p. 1352-9.
57. Chandra, S., et al., *Double-knockout mice for alpha- and beta-synucleins: effect on synaptic functions.* Proc Natl Acad Sci U S A, 2004. **101**(41): p. 14966-71.
58. Klivenyi, P., et al., *Mice lacking alpha-synuclein are resistant to mitochondrial toxins.* Neurobiol Dis, 2006. **21**(3): p. 541-8.
59. Thomas, B., et al., *Resistance to MPTP-neurotoxicity in alpha-synuclein knockout mice is complemented by human alpha-synuclein and associated with increased beta-synuclein and Akt activation.* PLoS One, 2011. **6**(1): p. e16706.
60. Patterson, J.R., et al., *Generation of Alpha-Synuclein Preformed Fibrils from Monomers and Use In Vivo.* J Vis Exp, 2019(148).
61. Polinski, N.K., et al., *Best Practices for Generating and Using Alpha-Synuclein Pre-Formed Fibrils to Model Parkinson's Disease in Rodents.* J Parkinsons Dis, 2018. **8**(2): p. 303-322.
62. Luk, K.C., et al., *Exogenous alpha-synuclein fibrils seed the formation of Lewy body-like intracellular inclusions in cultured cells.* Proc Natl Acad Sci U S A, 2009. **106**(47): p. 20051-6.
63. Rahayel, S., et al., *Differentially targeted seeding reveals unique pathological alpha-synuclein propagation patterns.* Brain, 2022. **145**(5): p. 1743-1756.
64. Paumier, K.L., et al., *Intrastriatal injection of pre-formed mouse alpha-synuclein fibrils into rats triggers alpha-synuclein pathology and bilateral nigrostriatal degeneration.* Neurobiol Dis, 2015. **82**: p. 185-199.
65. Wu, Q., et al., *alpha-Synuclein (alphaSyn) Preformed Fibrils Induce Endogenous alphaSyn Aggregation, Compromise Synaptic Activity and Enhance Synapse Loss in Cultured Excitatory Hippocampal Neurons.* J Neurosci, 2019. **39**(26): p. 5080-5094.
66. Thomsen, M.B., et al., *PET imaging reveals early and progressive dopaminergic deficits after intra-striatal injection of preformed alpha-synuclein fibrils in rats.* Neurobiol Dis, 2021. **149**: p. 105229.
67. Tapias, V., et al., *Synthetic alpha-synuclein fibrils cause mitochondrial impairment and selective dopamine*

neurodegeneration in part via iNOS-mediated nitric oxide production. Cell Mol Life Sci, 2017. **74**(15): p. 2851-2874.
68. Luk, K.C., et al., *Pathological alpha-synuclein transmission initiates Parkinson-like neurodegeneration in nontransgenic mice.* Science, 2012. **338**(6109): p. 949-53.
69. Guan, Y., et al., *Pathogenic Mutations Differentially Regulate Cell-to-Cell Transmission of alpha-Synuclein.* Front Cell Neurosci, 2020. **14**: p. 159.
70. Lazaro, D.F., et al., *Systematic comparison of the effects of alpha-synuclein mutations on its oligomerization and aggregation.* PLoS Genet, 2014. **10**(11): p. e1004741.
71. Neumann, M., et al., *Misfolded proteinase K-resistant hyperphosphorylated alpha-synuclein in aged transgenic mice with locomotor deterioration and in human alpha-synucleinopathies.* J Clin Invest, 2002. **110**(10): p. 1429-39.
72. Masliah, E., et al., *Dopaminergic loss and inclusion body formation in alpha-synuclein mice: implications for neurodegenerative disorders.* Science, 2000. **287**(5456): p. 1265-9.
73. Gentzel, R.C., et al., *Intracranial administration of alpha-synuclein fibrils in A30P-synuclein transgenic mice causes robust synucleinopathy and microglial induction.* Neurobiol Aging, 2021. **106**: p. 12-25.
74. Negrini, M., et al., *Sequential or Simultaneous Injection of Preformed Fibrils and AAV Overexpression of Alpha-Synuclein Are Equipotent in Producing Relevant Pathology and Behavioral Deficits.* J Parkinsons Dis, 2022. **12**(4): p. 1133-1153.
75. Lingor, P., E. Carboni, and J.C. Koch, *Alpha-synuclein and iron: two keys unlocking Parkinson's disease.* J Neural Transm (Vienna), 2017. **124**(8): p. 973-981.
76. Binolfi, A., et al., *Interaction of alpha-synuclein with divalent metal ions reveals key differences: a link between structure, binding specificity and fibrillation enhancement.* J Am Chem Soc, 2006. **128**(30): p. 9893-901.
77. Rasia, R.M., et al., *Structural characterization of copper(II) binding to alpha-synuclein: Insights into the bioinorganic chemistry of Parkinson's disease.* Proc Natl Acad Sci U S A, 2005. **102**(12): p. 4294-9.

78. Kostka, M., et al., *Single particle characterization of iron-induced pore-forming alpha-synuclein oligomers.* J Biol Chem, 2008. **283**(16): p. 10992-1003.
79. Uversky, V.N., J. Li, and A.L. Fink, *Metal-triggered structural transformations, aggregation, and fibrillation of human alpha-synuclein. A possible molecular NK between Parkinson's disease and heavy metal exposure.* J Biol Chem, 2001. **276**(47): p. 44284-96.
80. Anderson, C.P., et al., *Mammalian iron metabolism and its control by iron regulatory proteins.* Biochim Biophys Acta, 2012. **1823**(9): p. 1468-83.
81. Davies, P., D. Moualla, and D.R. Brown, *Alpha-synuclein is a cellular ferrireductase.* PLoS One, 2011. **6**(1): p. e15814.
82. Mezzaroba, L., et al., *The role of zinc, copper, manganese and iron in neurodegenerative diseases.* Neurotoxicology, 2019. **74**: p. 230-241.
83. Anderson, J.P., et al., *Phosphorylation of Ser-129 is the dominant pathological modification of alpha-synuclein in familial and sporadic Lewy body disease.* J Biol Chem, 2006. **281**(40): p. 29739-52.
84. Giasson, B.I., et al., *Oxidative damage linked to neurodegeneration by selective alpha-synuclein nitration in synucleinopathy lesions.* Science, 2000. **290**(5493): p. 985-9.
85. Duda, J.E., et al., *Widespread nitration of pathological inclusions in neurodegenerative synucleinopathies.* Am J Pathol, 2000. **157**(5): p. 1439-45.
86. Muntane, G., I. Ferrer, and M. Martinez-Vicente, *alpha-synuclein phosphorylation and truncation are normal events in the adult human brain.* Neuroscience, 2012. **200**: p. 106-19.
87. Fujiwara, H., et al., *alpha-Synuclein is phosphorylated in synucleinopathy lesions.* Nat Cell Biol, 2002. **4**(2): p. 160-4.
88. Takahashi, M., et al., *Phosphorylation of alpha-synuclein characteristic of synucleinopathy lesions is recapitulated in alpha-synuclein transgenic Drosophila.* Neurosci Lett, 2003. **336**(3): p. 155-8.
89. Oueslati, A., M. Fournier, and H.A. Lashuel, *Role of post-translational modifications in modulating the structure, function and toxicity of alpha-synuclein: implications for Parkinson's disease pathogenesis and therapies.* Prog Brain Res, 2010. **183**: p. 115-45.

90. Azeredo da Silveira, S., et al., *Phosphorylation does not prompt, nor prevent, the formation of alpha-synuclein toxic species in a rat model of Parkinson's disease.* Hum Mol Genet, 2009. **18**(5): p. 872-87.
91. McFarland, N.R., et al., *Alpha-synuclein S129 phosphorylation mutants do not alter nigrostriatal toxicity in a rat model of Parkinson disease.* J Neuropathol Exp Neurol, 2009. **68**(5): p. 515-24.
92. Febbraro, F., et al., *Ser129D mutant alpha-synuclein induces earlier motor dysfunction while S129A results in distinctive pathology in a rat model of Parkinson's disease.* Neurobiol Dis, 2013. **56**: p. 47-58.
93. Chau, K.Y., et al., *Relationship between alpha synuclein phosphorylation, proteasomal inhibition and cell death: relevance to Parkinson's disease pathogenesis.* J Neurochem, 2009. **110**(3): p. 1005-13.
94. Machiya, Y., et al., *Phosphorylated alpha-synuclein at Ser-129 is targeted to the proteasome pathway in a ubiquitin-independent manner.* J Biol Chem, 2010. **285**(52): p. 40732-44.
95. Lu, Y., et al., *Phosphorylation of alpha-Synuclein at Y125 and S129 alters its metal binding properties: implications for understanding the role of alpha-Synuclein in the pathogenesis of Parkinson's Disease and related disorders.* ACS Chem Neurosci, 2011. **2**(11): p. 667-75.
96. Nubling, G.S., et al., *Modelling Ser129 phosphorylation inhibits membrane binding of pore-forming alpha-synuclein oligomers.* PLoS One, 2014. **9**(6): p. e98906.
97. Huang, Z., et al., *Determining nuclear localization of alpha-synuclein in mouse brains.* Neuroscience, 2011. **199**: p. 318-32.
98. Yu, S., et al., *Extensive nuclear localization of alpha-synuclein in normal rat brain neurons revealed by a novel monoclonal antibody.* Neuroscience, 2007. **145**(2): p. 539-55.
99. Goers, J., et al., *Nuclear localization of alpha-synuclein and its interaction with histones.* Biochemistry, 2003. **42**(28): p. 8465-71.
100. McFarland, M.A., et al., *Proteomics analysis identifies phosphorylation-dependent alpha-synuclein protein interactions.* Mol Cell Proteomics, 2008. **7**(11): p. 2123-37.
101. McCormack, A.L., S.K. Mak, and D.A. Di Monte, *Increased alpha-synuclein phosphorylation and nitration in the aging primate substantia nigra.* Cell Death Dis, 2012. **3**: p. e315.
102. Paxinou, E., et al., *Induction of alpha-synuclein aggregation by intracellular nitrative insult.* J Neurosci, 2001. **21**(20): p. 8053-61.

103. Hodara, R., et al., *Functional consequences of alpha-synuclein tyrosine nitration: diminished binding to lipid vesicles and increased fibril formation.* J Biol Chem, 2004. **279**(46): p. 47746-53.
104. Burai, R., et al., *Elucidating the Role of Site-Specific Nitration of alpha-Synuclein in the Pathogenesis of Parkinson's Disease via Protein Semisynthesis and Mutagenesis.* J Am Chem Soc, 2015. **137**(15): p. 5041-52.
105. Yamin, G., V.N. Uversky, and A.L. Fink, *Nitration inhibits fibrillation of human alpha-synuclein in vitro by formation of soluble oligomers.* FEBS Lett, 2003. **542**(1-3): p. 147-52.
106. Glaser, C.B., et al., *Methionine oxidation, alpha-synuclein and Parkinson's disease.* Biochim Biophys Acta, 2005. **1703**(2): p. 157-69.
107. Zhou, W., et al., *Methionine oxidation stabilizes non-toxic oligomers of alpha-synuclein through strengthening the auto-inhibitory intra-molecular long-range interactions.* Biochim Biophys Acta, 2010. **1802**(3): p. 322-30.
108. Leong, S.L., et al., *Formation of dopamine-mediated alpha-synuclein-soluble oligomers requires methionine oxidation.* Free Radic Biol Med, 2009. **46**(10): p. 1328-37.
109. Prasad, K., et al., *Critical role of truncated alpha-synuclein and aggregates in Parkinson's disease and incidental Lewy body disease.* Brain Pathol, 2012. **22**(6): p. 811-25.
110. Al-Hilaly, Y.K., et al., *The involvement of dityrosine crosslinking in alpha-synuclein assembly and deposition in Lewy Bodies in Parkinson's disease.* Sci Rep, 2016. **6**: p. 39171.
111. Sorrentino, Z.A., et al., *Physiological C-terminal truncation of alpha-synuclein potentiates the prion-like formation of pathological inclusions.* J Biol Chem, 2018. **293**(49): p. 18914-18932.
112. Daher, J.P., et al., *Conditional transgenic mice expressing C-terminally truncated human alpha-synuclein (alphaSyn119) exhibit reduced striatal dopamine without loss of nigrostriatal pathway dopaminergic neurons.* Mol Neurodegener, 2009. **4**: p. 34.
113. Kordower, J.H., et al., *Lewy body-like pathology in long-term embryonic nigral transplants in Parkinson's disease.* Nat Med, 2008. **14**(5): p. 504-6.
114. Li, J.Y., et al., *Lewy bodies in grafted neurons in subjects with Parkinson's disease suggest host-to-graft disease propagation.* Nat Med, 2008. **14**(5): p. 501-3.

115. Hansen, C. and J.Y. Li, *Beyond alpha-synuclein transfer: pathology propagation in Parkinson's disease.* Trends Mol Med, 2012. **18**(5): p. 248-55.
116. Olanow, C.W. and S.B. Prusiner, *Is Parkinson's disease a prion disorder?* Proc Natl Acad Sci U S A, 2009. **106**(31): p. 12571-2.
117. Olanow, C.W. and P. Brundin, *Parkinson's disease and alpha synuclein: is Parkinson's disease a prion-like disorder?* Mov Disord, 2013. **28**(1): p. 31-40.
118. Kordower, J.H., et al., *Transfer of host-derived alpha synuclein to grafted dopaminergic neurons in rat.* Neurobiol Dis, 2011. **43**(3): p. 552-7.
119. Prusiner, S.B., et al., *Evidence for alpha-synuclein prions causing multiple system atrophy in humans with parkinsonism.* Proc Natl Acad Sci U S A, 2015. **112**(38): p. E5308-17.
120. Marotta, N.P., et al., *Alpha-synuclein from patient Lewy bodies exhibits distinct pathological activity that can be propagated in vitro.* Acta Neuropathol Commun, 2021. **9**(1): p. 188.
121. Dhillon, J.S., et al., *Comparative analyses of the in vivo induction and transmission of alpha-synuclein pathology in transgenic mice by MSA brain lysate and recombinant alpha-synuclein fibrils.* Acta Neuropathol Commun, 2019. **7**(1): p. 80.
122. Braak, H., et al., *Staging of brain pathology related to sporadic Parkinson's disease.* Neurobiol Aging, 2003. **24**(2): p. 197-211.
123. McKeith, I.G., et al., *Diagnosis and management of dementia with Lewy bodies: third report of the DLB Consortium.* Neurology, 2005. **65**(12): p. 1863-72.
124. McKeith, I.G., et al., *Diagnosis and management of dementia with Lewy bodies: Fourth consensus report of the DLB Consortium.* Neurology, 2017. **89**(1): p. 88-100.
125. Kalaitzakis, M.E., et al., *Controversies over the staging of alpha-synuclein pathology in Parkinson's disease.* Acta Neuropathol, 2008. **116**(1): p. 125-8; author reply 129-31.
126. Kalaitzakis, M.E., et al., *Evidence against a reliable staging system of alpha-synuclein pathology in Parkinson's disease.* Neuropathol Appl Neurobiol, 2009. **35**(1): p. 125-6.
127. Jellinger, K.A., *A critical reappraisal of current staging of Lewy-related pathology in human brain.* Acta Neuropathol, 2008. **116**(1): p. 1-16.

128. Parkkinen, L., et al., *Alpha-synuclein pathology does not predict extrapyramidal symptoms or dementia.* Ann Neurol, 2005. **57**(1): p. 82-91.
129. Parkkinen, L., T. Pirttila, and I. Alafuzoff, *Applicability of current staging/categorization of alpha-synuclein pathology and their clinical relevance.* Acta Neuropathol, 2008. **115**(4): p. 399-407.
130. Fearnley, J.M. and A.J. Lees, *Ageing and Parkinson's disease: substantia nigra regional selectivity.* Brain, 1991. **114 (Pt 5)**: p. 2283-301.
131. Greffard, S., et al., *Motor score of the Unified Parkinson Disease Rating Scale as a good predictor of Lewy body-associated neuronal loss in the substantia nigra.* Arch Neurol, 2006. **63**(4): p. 584-8.
132. Ma, S.Y., et al., *Correlation between neuromorphometry in the substantia nigra and clinical features in Parkinson's disease using disector counts.* J Neurol Sci, 1997. **151**(1): p. 83-7.
133. Leng, F. and P. Edison, *Neuroinflammation and microglial activation in Alzheimer disease: where do we go from here?* Nat Rev Neurol, 2021. **17**(3): p. 157-172.
134. Kam, T.I., et al., *Microglia and astrocyte dysfunction in parkinson's disease.* Neurobiol Dis, 2020. **144**: p. 105028.
135. Vezzani, A., S. Balosso, and T. Ravizza, *Neuroinflammatory pathways as treatment targets and biomarkers in epilepsy.* Nat Rev Neurol, 2019. **15**(8): p. 459-472.
136. Maida, C.D., et al., *Neuroinflammatory Mechanisms in Ischemic Stroke: Focus on Cardioembolic Stroke, Background, and Therapeutic Approaches.* Int J Mol Sci, 2020. **21**(18).
137. Beers, D.R. and S.H. Appel, *Immune dysregulation in amyotrophic lateral sclerosis: mechanisms and emerging therapies.* Lancet Neurol, 2019. **18**(2): p. 211-220.
138. Bjelobaba, I., D. Savic, and I. Lavrnja, *Multiple Sclerosis and Neuroinflammation: The Overview of Current and Prospective Therapies.* Curr Pharm Des, 2017. **23**(5): p. 693-730.
139. Saba, J., et al., *Neuroinflammation in Huntington's Disease: A Starring Role for Astrocyte and Microglia.* Curr Neuropharmacol, 2022. **20**(6): p. 1116-1143.
140. Vieira, B.D., et al., *Neuroinflammation in Multiple System Atrophy: Response to and Cause of alpha-Synuclein Aggregation.* Front Cell Neurosci, 2015. **9**: p. 437.

141. Surendranathan, A., J.B. Rowe, and J.T. O'Brien, *Neuroinflammation in Lewy body dementia.* Parkinsonism Relat Disord, 2015. **21**(12): p. 1398-406.
142. Ginhoux, F., et al., *Origin and differentiation of microglia.* Front Cell Neurosci, 2013. **7**: p. 45.
143. Ransohoff, R.M., *A polarizing question: do M1 and M2 microglia exist?* Nat Neurosci, 2016. **19**(8): p. 987-91.
144. Abellanas, M.A., et al., *Midbrain microglia mediate a specific immunosuppressive response under inflammatory conditions.* J Neuroinflammation, 2019. **16**(1): p. 233.
145. Silverman, H.A., et al., *Brain region-specific alterations in the gene expression of cytokines, immune cell markers and cholinergic system components during peripheral endotoxin-induced inflammation.* Mol Med, 2015. **20**: p. 601-11.
146. Silvin, A. and F. Ginhoux, *Microglia heterogeneity along a spatio-temporal axis: More questions than answers.* Glia, 2018. **66**(10): p. 2045-2057.
147. Paolicelli, R.C., et al., *Synaptic pruning by microglia is necessary for normal brain development.* Science, 2011. **333**(6048): p. 1456-8.
148. Zhan, Y., et al., *Deficient neuron-microglia signaling results in impaired functional brain connectivity and social behavior.* Nat Neurosci, 2014. **17**(3): p. 400-6.
149. Ishizuka, K., et al., *Rare genetic variants in CX3CR1 and their contribution to the increased risk of schizophrenia and autism spectrum disorders.* Transl Psychiatry, 2017. **7**(8): p. e1184.
150. Erblich, B., et al., *Absence of colony stimulation factor-1 receptor results in loss of microglia, disrupted brain development and olfactory deficits.* PLoS One, 2011. **6**(10): p. e26317.
151. Parkhurst, C.N., et al., *Microglia promote learning-dependent synapse formation through brain-derived neurotrophic factor.* Cell, 2013. **155**(7): p. 1596-609.
152. Badimon, A., et al., *Negative feedback control of neuronal activity by microglia.* Nature, 2020. **586**(7829): p. 417-423.
153. Basilico, B., et al., *Microglia shape presynaptic properties at developing glutamatergic synapses.* Glia, 2019. **67**(1): p. 53-67.
154. Crapser, J.D., et al., *Microglia as hackers of the matrix: sculpting synapses and the extracellular space.* Cell Mol Immunol, 2021. **18**(11): p. 2472-2488.

155. Raghuraman, R., et al., *Activation of microglia in acute hippocampal slices affects activity-dependent long-term potentiation and synaptic tagging and capture in area CA1.* Neurobiol Learn Mem, 2019. **163**: p. 107039.
156. Sun, H., et al., *The CD200/CD200R signaling pathway contributes to spontaneous functional recovery by enhancing synaptic plasticity after stroke.* J Neuroinflammation, 2020. **17**(1): p. 171.
157. Saw, G., et al., *Epigenetic regulation of microglial phosphatidylinositol 3-kinase pathway involved in long-term potentiation and synaptic plasticity in rats.* Glia, 2020. **68**(3): p. 656-669.
158. Puy, V., et al., *Predominant role of microglia in brain iron retention in Sanfilippo syndrome, a pediatric neurodegenerative disease.* Glia, 2018. **66**(8): p. 1709-1723.
159. Valdearcos, M., M.G. Myers, Jr., and S.K. Koliwad, *Hypothalamic microglia as potential regulators of metabolic physiology.* Nat Metab, 2019. **1**(3): p. 314-320.
160. Rosin, J.M. and D.M. Kurrasch, *Emerging roles for hypothalamic microglia as regulators of physiological homeostasis.* Front Neuroendocrinol, 2019. **54**: p. 100748.
161. Linnerbauer, M., M.A. Wheeler, and F.J. Quintana, *Astrocyte Crosstalk in CNS Inflammation.* Neuron, 2020. **108**(4): p. 608-622.
162. Liddelow, S.A. and B.A. Barres, *Reactive Astrocytes: Production, Function, and Therapeutic Potential.* Immunity, 2017. **46**(6): p. 957-967.
163. Mori, T., A. Buffo, and M. Gotz, *The novel roles of glial cells revisited: the contribution of radial glia and astrocytes to neurogenesis.* Curr Top Dev Biol, 2005. **69**: p. 67-99.
164. Kielian, T., *Glial connexins and gap junctions in CNS inflammation and disease.* J Neurochem, 2008. **106**(3): p. 1000-16.
165. Zhou, B., Y.X. Zuo, and R.T. Jiang, *Astrocyte morphology: Diversity, plasticity, and role in neurological diseases.* CNS Neurosci Ther, 2019. **25**(6): p. 665-673.
166. Matias, I., J. Morgado, and F.C.A. Gomes, *Astrocyte Heterogeneity: Impact to Brain Aging and Disease.* Front Aging Neurosci, 2019. **11**: p. 59.
167. Pellerin, L., et al., *Evidence supporting the existence of an activity-dependent astrocyte-neuron lactate shuttle.* Dev Neurosci, 1998. **20**(4-5): p. 291-9.

168. Abbott, N.J., et al., *Structure and function of the blood-brain barrier.* Neurobiol Dis, 2010. **37**(1): p. 13-25.
169. Perea, G., M. Navarrete, and A. Araque, *Tripartite synapses: astrocytes process and control synaptic information.* Trends Neurosci, 2009. **32**(8): p. 421-31.
170. Sobue, A., et al., *Astroglial major histocompatibility complex class I following immune activation leads to behavioral and neuropathological changes.* Glia, 2018. **66**(5): p. 1034-1052.
171. Rostami, J., et al., *Astrocytes have the capacity to act as antigen-presenting cells in the Parkinson's disease brain.* J Neuroinflammation, 2020. **17**(1): p. 119.
172. Imamura, K., et al., *Distribution of major histocompatibility complex class II-positive microglia and cytokine profile of Parkinson's disease brains.* Acta Neuropathol, 2003. **106**(6): p. 518-26.
173. King, E. and A. Thomas, *Systemic Inflammation in Lewy Body Diseases: A Systematic Review.* Alzheimer Dis Assoc Disord, 2017. **31**(4): p. 346-356.
174. La Vitola, P., et al., *Alpha-synuclein oligomers impair memory through glial cell activation and via Toll-like receptor 2.* Brain Behav Immun, 2018. **69**: p. 591-602.
175. Phulwani, N.K., et al., *TLR2 expression in astrocytes is induced by TNF-alpha- and NF-kappa B-dependent pathways.* J Immunol, 2008. **181**(6): p. 3841-9.
176. Gorina, R., et al., *Astrocyte TLR4 activation induces a proinflammatory environment through the interplay between MyD88-dependent NFkappaB signaling, MAPK, and Jak1/Stat1 pathways.* Glia, 2011. **59**(2): p. 242-55.
177. Mossner, R., et al., *Astrocytes as antigen presenting cells for primary and secondary T cell responses: effect of astrocyte infection by murine hepatitis virus.* Adv Exp Med Biol, 1990. **276**: p. 647-54.
178. Cornet, A., et al., *Role of astrocytes in antigen presentation and naive T-cell activation.* J Neuroimmunol, 2000. **106**(1-2): p. 69-77.
179. Liddelow, S.A., et al., *Neurotoxic reactive astrocytes are induced by activated microglia.* Nature, 2017. **541**(7638): p. 481-487.
180. Doorn, K.J., et al., *Microglial phenotypes and toll-like receptor 2 in the substantia nigra and hippocampus of incidental Lewy body disease cases and Parkinson's disease patients.* Acta Neuropathol Commun, 2014. **2**: p. 90.

181. Amin, J., et al., *Neuroinflammation in dementia with Lewy bodies: a human post-mortem study.* Transl Psychiatry, 2020. **10**(1): p. 267.
182. Ouchi, Y., et al., *Microglial activation and dopamine terminal loss in early Parkinson's disease.* Ann Neurol, 2005. **57**(2): p. 168-75.
183. Iannaccone, S., et al., *In vivo microglia activation in very early dementia with Lewy bodies, comparison with Parkinson's disease.* Parkinsonism Relat Disord, 2013. **19**(1): p. 47-52.
184. Lavisse, S., et al., *Increased microglial activation in patients with Parkinson disease using [(18)F]-DPA714 TSPO PET imaging.* Parkinsonism Relat Disord, 2021. **82**: p. 29-36.
185. Terada, T., et al., *Extrastriatal spreading of microglial activation in Parkinson's disease: a positron emission tomography study.* Ann Nucl Med, 2016. **30**(8): p. 579-87.
186. Kobylecki, C., et al., *Diffusion-weighted imaging and its relationship to microglial activation in parkinsonian syndromes.* Parkinsonism Relat Disord, 2013. **19**(5): p. 527-32.
187. Gerhard, A., et al., *In vivo imaging of microglial activation with [11C](R)-PK11195 PET in idiopathic Parkinson's disease.* Neurobiol Dis, 2006. **21**(2): p. 404-12.
188. Olanow, C.W., et al., *Temporal evolution of microglia and alpha-synuclein accumulation following foetal grafting in Parkinson's disease.* Brain, 2019. **142**(6): p. 1690-1700.
189. George, S., et al., *Microglia affect alpha-synuclein cell-to-cell transfer in a mouse model of Parkinson's disease.* Mol Neurodegener, 2019. **14**(1): p. 34.
190. Martin-Bastida, A., et al., *Iron and inflammation: in vivo and post-mortem studies in Parkinson's disease.* J Neural Transm (Vienna), 2021. **128**(1): p. 15-25.
191. Lee, S.B., et al., *Identification of the amino acid sequence motif of alpha-synuclein responsible for macrophage activation.* Biochem Biophys Res Commun, 2009. **381**(1): p. 39-43.
192. Kim, C., et al., *beta1-integrin-dependent migration of microglia in response to neuron-released alpha-synuclein.* Exp Mol Med, 2014. **46**: p. e91.
193. Panicker, N., et al., *Fyn kinase regulates misfolded alpha-synuclein uptake and NLRP3 inflammasome activation in microglia.* J Exp Med, 2019. **216**(6): p. 1411-1430.
194. Venezia, S., et al., *Toll-like receptor 4 stimulation with monophosphoryl lipid A ameliorates motor deficits and nigral*

neurodegeneration triggered by extraneuronal alpha-synucleinopathy. Mol Neurodegener, 2017. **12**(1): p. 52.
195. Fellner, L., et al., *Toll-like receptor 4 is required for alpha-synuclein dependent activation of microglia and astroglia.* Glia, 2013. **61**(3): p. 349-60.
196. Kim, C., et al., *Neuron-released oligomeric alpha-synuclein is an endogenous agonist of TLR2 for paracrine activation of microglia.* Nat Commun, 2013. **4**: p. 1562.
197. Gustot, A., et al., *Amyloid fibrils are the molecular trigger of inflammation in Parkinson's disease.* Biochem J, 2015. **471**(3): p. 323-33.
198. Codolo, G., et al., *Triggering of inflammasome by aggregated alpha-synuclein, an inflammatory response in synucleinopathies.* PLoS One, 2013. **8**(1): p. e55375.
199. Zhang, W., et al., *Aggregated alpha-synuclein activates microglia: a process leading to disease progression in Parkinson's disease.* FASEB J, 2005. **19**(6): p. 533-42.
200. Watson, M.B., et al., *Regionally-specific microglial activation in young mice over-expressing human wildtype alpha-synuclein.* Exp Neurol, 2012. **237**(2): p. 318-34.
201. Su, X., et al., *Synuclein activates microglia in a model of Parkinson's disease.* Neurobiol Aging, 2008. **29**(11): p. 1690-701.
202. Gomez-Isla, T., et al., *Motor dysfunction and gliosis with preserved dopaminergic markers in human alpha-synuclein A30P transgenic mice.* Neurobiol Aging, 2003. **24**(2): p. 245-58.
203. Earls, R.H., et al., *Intrastriatal injection of preformed alpha-synuclein fibrils alters central and peripheral immune cell profiles in non-transgenic mice.* J Neuroinflammation, 2019. **16**(1): p. 250.
204. Duffy, M.F., et al., *Lewy body-like alpha-synuclein inclusions trigger reactive microgliosis prior to nigral degeneration.* J Neuroinflammation, 2018. **15**(1): p. 129.
205. Guo, J.J., et al., *Intranasal administration of alpha-synuclein preformed fibrils triggers microglial iron deposition in the substantia nigra of Macaca fascicularis.* Cell Death Dis, 2021. **12**(1): p. 81.
206. Harms, A.S., et al., *alpha-Synuclein fibrils recruit peripheral immune cells in the rat brain prior to neurodegeneration.* Acta Neuropathol Commun, 2017. **5**(1): p. 85.

207. Harms, A.S., et al., *Peripheral monocyte entry is required for alpha-Synuclein induced inflammation and Neurodegeneration in a model of Parkinson disease.* Exp Neurol, 2018. **300**: p. 179-187.
208. Gordon, R., et al., *Inflammasome inhibition prevents alpha-synuclein pathology and dopaminergic neurodegeneration in mice.* Sci Transl Med, 2018. **10**(465).
209. Lee, H.J., C. Kim, and S.J. Lee, *Alpha-synuclein stimulation of astrocytes: Potential role for neuroinflammation and neuroprotection.* Oxid Med Cell Longev, 2010. **3**(4): p. 283-7.
210. Sorrentino, Z.A., B.I. Giasson, and P. Chakrabarty, *alpha-Synuclein and astrocytes: tracing the pathways from homeostasis to neurodegeneration in Lewy body disease.* Acta Neuropathol, 2019. **138**(1): p. 1-21.
211. Yun, S.P., et al., *Block of A1 astrocyte conversion by microglia is neuroprotective in models of Parkinson's disease.* Nat Med, 2018. **24**(7): p. 931-938.
212. Liu, M., et al., *alphasynuclein induces apoptosis of astrocytes by causing dysfunction of the endoplasmic reticulumGolgi compartment.* Mol Med Rep, 2018. **18**(1): p. 322-332.
213. Lee, H.J., et al., *Clearance and deposition of extracellular alpha-synuclein aggregates in microglia.* Biochem Biophys Res Commun, 2008. **372**(3): p. 423-8.
214. Bliederhaeuser, C., et al., *Age-dependent defects of alpha-synuclein oligomer uptake in microglia and monocytes.* Acta Neuropathol, 2016. **131**(3): p. 379-91.
215. Xia, Y., et al., *Microglia as modulators of exosomal alpha-synuclein transmission.* Cell Death Dis, 2019. **10**(3): p. 174.
216. Guo, M., et al., *Microglial exosomes facilitate alpha-synuclein transmission in Parkinson's disease.* Brain, 2020. **143**(5): p. 1476-1497.
217. Dutta, D., et al., *Selective targeting of the TLR2/MyD88/NF-kappaB pathway reduces alpha-synuclein spreading in vitro and in vivo.* Nat Commun, 2021. **12**(1): p. 5382.
218. Wu, D.C., et al., *NADPH oxidase mediates oxidative stress in the 1-methyl-4-phenyl-1,2,3,6-tetrahydropyridine model of Parkinson's disease.* Proc Natl Acad Sci U S A, 2003. **100**(10): p. 6145-50.
219. Gao, H.M., et al., *Critical role of microglial NADPH oxidase-derived free radicals in the in vitro MPTP model of Parkinson's disease.* FASEB J, 2003. **17**(13): p. 1954-6.

220. Javed, H., et al., *NLRP3 inflammasome and glia maturation factor coordinately regulate neuroinflammation and neuronal loss in MPTP mouse model of Parkinson's disease.* Int Immunopharmacol, 2020. **83**: p. 106441.
221. Costa, T., et al., *Combined 1-Deoxynojirimycin and Ibuprofen Treatment Decreases Microglial Activation, Phagocytosis and Dopaminergic Degeneration in MPTP-Treated Mice.* J Neuroimmune Pharmacol, 2021. **16**(2): p. 390-402.
222. He, D., et al., *Echinocystic Acid Inhibits Inflammation and Exerts Neuroprotective Effects in MPTP-Induced Parkinson's Disease Model Mice.* Front Pharmacol, 2021. **12**: p. 787771.
223. Lee, S., et al., *Neuroprotective and Anti-Inflammatory Effects of Evernic Acid in an MPTP-Induced Parkinson's Disease Model.* Int J Mol Sci, 2021. **22**(4).
224. Liu, W.W., et al., *BMAL1 regulation of microglia-mediated neuroinflammation in MPTP-induced Parkinson's disease mouse model.* FASEB J, 2020. **34**(5): p. 6570-6581.
225. Benner, E.J., et al., *Nitrated alpha-synuclein immunity accelerates degeneration of nigral dopaminergic neurons.* PLoS One, 2008. **3**(1): p. e1376.
226. Walsh, S., D.P. Finn, and E. Dowd, *Time-course of nigrostriatal neurodegeneration and neuroinflammation in the 6-hydroxydopamine-induced axonal and terminal lesion models of Parkinson's disease in the rat.* Neuroscience, 2011. **175**: p. 251-61.
227. Maia, S., et al., *Longitudinal and parallel monitoring of neuroinflammation and neurodegeneration in a 6-hydroxydopamine rat model of Parkinson's disease.* Synapse, 2012. **66**(7): p. 573-83.
228. Goes, A.T.R., et al., *Protective role of chrysin on 6-hydroxydopamine-induced neurodegeneration a mouse model of Parkinson's disease: Involvement of neuroinflammation and neurotrophins.* Chem Biol Interact, 2018. **279**: p. 111-120.
229. Kubota, M., et al., *Carnosine suppresses neuronal cell death and inflammation induced by 6-hydroxydopamine in an in vitro model of Parkinson's disease.* PLoS One, 2020. **15**(10): p. e0240448.
230. Huang, M., et al., *HMGB1 Mediates Paraquat-Induced Neuroinflammatory Responses via Activating RAGE Signaling Pathway.* Neurotox Res, 2020. **37**(4): p. 913-925.
231. Chen, M., et al., *Paraquat-induced retinal degeneration is exaggerated in CX3CR1-deficient mice and is associated with*

increased retinal inflammation. Invest Ophthalmol Vis Sci, 2013. **54**(1): p. 682-90.
232. Amin, F., et al., *Systemic inflammation and oxidative stress induced by inhaled paraquat in rat improved by carvacrol, possible role of PPARgamma receptors.* Biofactors, 2021. **47**(5): p. 778-787.
233. Rietschel, E.T., et al., *Bacterial endotoxin: molecular relationships of structure to activity and function.* FASEB J, 1994. **8**(2): p. 217-25.
234. Castano, A., et al., *Lipopolysaccharide intranigral injection induces inflammatory reaction and damage in nigrostriatal dopaminergic system.* J Neurochem, 1998. **70**(4): p. 1584-92.
235. Gao, H.M., et al., *Microglial activation-mediated delayed and progressive degeneration of rat nigral dopaminergic neurons: relevance to Parkinson's disease.* J Neurochem, 2002. **81**(6): p. 1285-97.
236. Hunter, R.L., et al., *Intrastriatal lipopolysaccharide injection induces parkinsonism in C57/B6 mice.* J Neurosci Res, 2009. **87**(8): p. 1913-21.
237. Kim, W.G., et al., *Regional difference in susceptibility to lipopolysaccharide-induced neurotoxicity in the rat brain: role of microglia.* J Neurosci, 2000. **20**(16): p. 6309-16.
238. Qin, L., et al., *Systemic LPS causes chronic neuroinflammation and progressive neurodegeneration.* Glia, 2007. **55**(5): p. 453-62.
239. Liu, Y., et al., *Endotoxin induces a delayed loss of TH-IR neurons in substantia nigra and motor behavioral deficits.* Neurotoxicology, 2008. **29**(5): p. 864-70.
240. Zheng, H.F., et al., *Autophagic impairment contributes to systemic inflammation-induced dopaminergic neuron loss in the midbrain.* PLoS One, 2013. **8**(8): p. e70472.
241. Zhao, Z., et al., *A novel role of NLRP3-generated IL-1beta in the acute-chronic transition of peripheral lipopolysaccharide-elicited neuroinflammation: implications for sepsis-associated neurodegeneration.* J Neuroinflammation, 2020. **17**(1): p. 64.
242. La Vitola, P., et al., *Peripheral inflammation exacerbates alpha-synuclein toxicity and neuropathology in Parkinson's models.* Neuropathol Appl Neurobiol, 2021. **47**(1): p. 43-60.
243. Zhang, J., et al., *Intrapallidal lipopolysaccharide injection increases iron and ferritin levels in glia of the rat substantia nigra and induces locomotor deficits.* Neuroscience, 2005. **135**(3): p. 829-38.

244. Thomsen, M.S., et al., *Neurodegeneration with inflammation is accompanied by accumulation of iron and ferritin in microglia and neurons.* Neurobiol Dis, 2015. **81**: p. 108-18.
245. Huo, J., et al., *LPS induces dopamine depletion and iron accumulation in substantia nigra in rat models of Parkinson's disease.* Int J Clin Exp Pathol, 2018. **11**(10): p. 4942-4949.
246. Verina, T., et al., *Manganese exposure induces microglia activation and dystrophy in the substantia nigra of non-human primates.* Neurotoxicology, 2011. **32**(2): p. 215-26.
247. Wu, S.Y., et al., *Estrogen ameliorates microglial activation by inhibiting the Kir2.1 inward-rectifier K(+) channel.* Sci Rep, 2016. **6**: p. 22864.
248. Tyagi, E., et al., *Cholinergic protection via alpha7 nicotinic acetylcholine receptors and PI3K-Akt pathway in LPS-induced neuroinflammation.* Neurochem Int, 2010. **56**(1): p. 135-42.
249. Nizri, E., et al., *Activation of the cholinergic anti-inflammatory system by nicotine attenuates neuroinflammation via suppression of Th1 and Th17 responses.* J Immunol, 2009. **183**(10): p. 6681-8.
250. Gao, H.M., et al., *Neuroinflammation and alpha-synuclein dysfunction potentiate each other, driving chronic progression of neurodegeneration in a mouse model of Parkinson's disease.* Environ Health Perspect, 2011. **119**(6): p. 807-14.
251. Reimer, L., et al., *Inflammation kinase PKR phosphorylates alpha-synuclein and causes alpha-synuclein-dependent cell death.* Neurobiol Dis, 2018. **115**: p. 17-28.
252. Wang, W., et al., *Caspase-1 causes truncation and aggregation of the Parkinson's disease-associated protein alpha-synuclein.* Proc Natl Acad Sci U S A, 2016. **113**(34): p. 9587-92.
253. Ma, L., et al., *C-terminal truncation exacerbates the aggregation and cytotoxicity of alpha-Synuclein: A vicious cycle in Parkinson's disease.* Biochim Biophys Acta Mol Basis Dis, 2018. **1864**(12): p. 3714-3725.
254. Nuber, S. and D.J. Selkoe, *Caspase-1 clipping causes complications for alpha-synuclein.* Proc Natl Acad Sci U S A, 2016. **113**(36): p. 9958-60.
255. Bassil, F., et al., *Reducing C-terminal truncation mitigates synucleinopathy and neurodegeneration in a transgenic model of multiple system atrophy.* Proc Natl Acad Sci U S A, 2016. **113**(34): p. 9593-8.

256. Hu, Q., et al., *Age-dependent aggregation of alpha-synuclein in the nervous system of gut-brain axis is associated with caspase-1 activation.* Metab Brain Dis, 2022. **37**(5): p. 1669-1681.
257. Gao, H.M., et al., *Neuroinflammation and oxidation/nitration of alpha-synuclein linked to dopaminergic neurodegeneration.* J Neurosci, 2008. **28**(30): p. 7687-98.
258. Holmes, B.B., et al., *Proteopathic tau seeding predicts tauopathy in vivo.* Proc Natl Acad Sci U S A, 2014. **111**(41): p. E4376-85.
259. Kanehisa, M. and S. Goto, *KEGG: kyoto encyclopedia of genes and genomes.* Nucleic Acids Res, 2000. **28**(1): p. 27-30.
260. Di Malta, C., L. Cinque, and C. Settembre, *Transcriptional Regulation of Autophagy: Mechanisms and Diseases.* Front Cell Dev Biol, 2019. **7**: p. 114.
261. Freeman, D., et al., *Alpha-synuclein induces lysosomal rupture and cathepsin dependent reactive oxygen species following endocytosis.* PLoS One, 2013. **8**(4): p. e62143.
262. Ong, L.K., et al., *Peripheral inflammation induces long-term changes in tyrosine hydroxylase activation in the substantia nigra.* Neurochem Int, 2021. **146**: p. 105022.
263. Farber, K., U. Pannasch, and H. Kettenmann, *Dopamine and noradrenaline control distinct functions in rodent microglial cells.* Mol Cell Neurosci, 2005. **29**(1): p. 128-38.
264. Yan, Y., et al., *Dopamine controls systemic inflammation through inhibition of NLRP3 inflammasome.* Cell, 2015. **160**(1-2): p. 62-73.
265. Elgueta, D., et al., *Pharmacologic antagonism of dopamine receptor D3 attenuates neurodegeneration and motor impairment in a mouse model of Parkinson's disease.* Neuropharmacology, 2017. **113**(Pt A): p. 110-123.
266. Dominguez-Meijide, A., et al., *Dopamine modulates astroglial and microglial activity via glial renin-angiotensin system in cultures.* Brain Behav Immun, 2017. **62**: p. 277-290.
267. Fan, Y., et al., *Differential Regulation of Adhesion and Phagocytosis of Resting and Activated Microglia by Dopamine.* Front Cell Neurosci, 2018. **12**: p. 309.
268. Robinson, P.C., et al., *The Potential for Repurposing Anti-TNF as a Therapy for the Treatment of COVID-19.* Med (N Y), 2020. **1**(1): p. 90-102.
269. Marshall, M., *COVID and the brain: researchers zero in on how damage occurs.* Nature, 2021. **595**(7868): p. 484-485.

270. Feldmann, M., et al., *Trials of anti-tumour necrosis factor therapy for COVID-19 are urgently needed.* Lancet, 2020. **395**(10234): p. 1407-1409.
271. Del Valle, D.M., et al., *An inflammatory cytokine signature predicts COVID-19 severity and survival.* Nat Med, 2020. **26**(10): p. 1636-1643.
272. Zaminelli, T., et al., *Antidepressant and antioxidative effect of Ibuprofen in the rotenone model of Parkinson's disease.* Neurotox Res, 2014. **26**(4): p. 351-62.
273. Swiatkiewicz, M., et al., *Potential neuroprotective effect of ibuprofen, insights from the mice model of Parkinson's disease.* Pharmacol Rep, 2013. **65**(5): p. 1227-36.
274. Casper, D., et al., *Ibuprofen protects dopaminergic neurons against glutamate toxicity in vitro.* Neurosci Lett, 2000. **289**(3): p. 201-4.
275. Singh, A., P. Tripathi, and S. Singh, *Neuroinflammatory responses in Parkinson's disease: relevance of Ibuprofen in therapeutics.* Inflammopharmacology, 2021. **29**(1): p. 5-14.
276. Fumagalli, S., et al., *CX3CR1 deficiency induces an early protective inflammatory environment in ischemic mice.* Glia, 2013. **61**(6): p. 827-42.
277. Soriano, S.G., et al., *Mice deficient in fractalkine are less susceptible to cerebral ischemia-reperfusion injury.* J Neuroimmunol, 2002. **125**(1-2): p. 59-65.
278. Yeo, S.I., et al., *The roles of fractalkine/CX3CR1 system in neuronal death following pilocarpine-induced status epilepticus.* J Neuroimmunol, 2011. **234**(1-2): p. 93-102.

Printed by Media-Tryck, Lund 2022 NORDIC SWAN ECOLABEL 3041 0903

About the author

Born and raised in Italy, I got my degree in Biology and my master in Neurobiology at Pavia University, the same as Camillo Golgi. Then, I had a short experience at C. Mondino Neurological Institute and another three years at the Pharmacological Institute Mario Negri in Milan. In 2017, I moved to Sweden to start my Ph.D. aiming to investigate the role of neuroinflammation in PD and related disorders. My thesis defense will take place on the 11th of November at 13:30 in Segerfallksalen at BMC, Lund University.

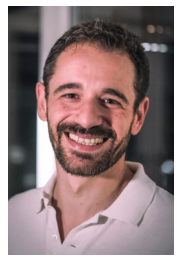

LUND UNIVERSITY

FACULTY OF MEDICINE

Department of Experimental Medical Science

Lund University, Faculty of Medicine
Doctoral Dissertation Series 2022:148
ISBN 978-91-8021-310-3
ISSN 1652-8220